2019

Harnessing The Pro-Apoptotic Function Of Myc To Improve Therapeutic Responses In Chemoresistant B-Cell Lymphoma

Colleen Harrington
University of Pennsylvania

Harnessing The Pro-Apoptotic Function Of Myc To Improve Therapeutic Responses In Chemoresistant B-Cell Lymphoma

Abstract

Therapeutic targeting of initiating oncogenes is the mainstay of precision medicine. Considerable efforts have been expended toward silencing MYC, which drives many human cancers including Burkitt lymphomas (BL). Yet, the effects of MYC silencing on standard-of-care therapies are poorly understood. Here we found that inhibition of MYC transcription renders B-lymphoblastoid cells refractory to chemotherapeutic agents. This suggested that in the context of chemotherapy, stabilization of Myc protein could be more beneficial than its inactivation. We tested this hypothesis by pharmacologically inhibiting glycogen synthase kinase 3 (GSK-3), which normally targets Myc for proteasomal degradation. We discovered that chemorefractory BL cell lines responded better to doxorubicin and other anti-cancer drugs when Myc was thus stabilized. In vivo, GSK3 inhibitors (GSK3i) enhanced doxorubicin-induced apoptosis in BL patient-derived xenografts (BL-PDX) as well as in murine MYC-driven lymphoma allografts. This enhancement was accompanied by and required deregulation of several key genes acting in the extrinsic, death receptor-mediated apoptotic pathway. Consistent with this mechanism of action, GSK3i also facilitated lymphoma cell killing by a death ligand TRAIL and by a death receptor agonist mapatumumab. Thus, GSK3i synergizes with both standard chemotherapeutics and direct engagers of death receptors and could improve outcomes in patients with refractory lymphomas.

Degree Type

Dissertation

Degree Name

Doctor of Philosophy (PhD)

Graduate Group

Cell & Molecular Biology

First Advisor

Andrei . Thomas-Tikhonenko

Subject Categories

Cell Biology | Molecular Biology | Oncology

HARNESSING THE PRO-APOPTOTIC FUNCTION OF MYC TO IMPROVE THERAPEUTIC RESPONSES IN CHEMORESISTANT B-CELL LYMPHOMA

Colleen Theobald Harrington

A DISSERTATION

in

Cell and Molecular Biology

Presented to the Faculties of the University of Pennsylvania

in

Partial Fulfillment of the Requirements for the

Degree of Doctor of Philosophy

2019

Supervisor of Dissertation

_____

Andrei Thomas-Tihhonenko, Ph.D.
Mildred L. Roeckle Endowed Chair in Pathology; Chief, Division of Cancer Pathobiology
Professor of Pathology & Laboratory Medicine and Pediatrics

Graduate Group Chairperson

_____

Daniel S. Kessler, Ph.D.
Associate Professor of Cell and Developmental Biology

Dissertation Committee

Xiaolu Yang, Ph.D. (chair), Professor of Cancer Biology

Chi V. Dang, M.D., Ph.D., Professor, Molecular and Cellular Oncogenesis Program

Michael Hogarty, M.D., Professor of Pediatrics

Peter S. Klein, M.D., Ph.D., Professor of Medicine

HARNESSING THE PRO-APOPTOTIC FUNCTION OF MYC TO IMPROVE THERAPEUTIC RESPONSES IN CHEMORESISTANT B-CELL LYMPHOMA

To my parents and my sister, for their endless love and support.

ACKNOWLEDGMENTS

There are many people that I would like to thank who have contributed to my scientific growth and helped me throughout graduate school.

I would like to thank all of my scientific mentors I have had throughout my life. Firstly, my thesis advisor Andrei for his support, encouragement and guidance throughout the all the phases of my graduate training. I also thank my committee members for their insights and guidance for my thesis project. Thank you to all of my former science teachers and undergraduate research mentors for encouraging my enthusiasm and curiosity for science, particularly my former boss Dr. James Eshleman, whose mentorship and guidance fortified my resolve to go to graduate school.

I need to thank members of the ATT lab, past and present, for their support throughout graduate school. I am grateful for this dysfunctional, crazy family that I called my own for these past few years. I especially need to thank Claudia- thank you for letting me convince you to join the ATT lab, and for being the best lab mate and friend- I couldn't have gotten through this without you.

I want to acknowledge the Cancer Biology CAMB program and all the CAMB coordinators, particularly Kathy and Christina, for all their support of graduate students. Also thank you to the 4th floor of CTRB and the Cancer Pathobiology Department for the support, feedback, and fun lunchtime conversations.

I would like to thank my friends from my graduate program, particularly Steve, Terra, Danielle, Lisa, Kelsey, Devin, Steve, Chris, Meg, Somdutta, Bobby, Christin, and Glendon. I would not have enjoyed graduate school nearly as much without these friendships I made along the way. I'm so glad we made time to do fun things outside of lab, from restaurant week dinners, movie nights, dancing, and frequenting beer gardens in the summer, to beach and hiking trips and even weddings. It's been amazing to have such a great group of people to enjoy my time in Philadelphia with. Also thanks to all my friends from childhood and from college who provided at times much needed distractions from lab, and who listened and tried to understand what I've been researching

all this time. Extra special thanks my oldest and best friend/honorary Harrington daughter #3 Winnie for always making time to talk and stay in touch no matter where we are in our lives.

Lastly, I need to thank those dearest to me. To David- your support and words of encouragement have meant so much to me. All I can say is, thank you for everything.

And finally, to my family- I have been so lucky to have my parents in Philadelphia for my entire time in graduate school and to have my sister here for the tail end. Nothing made me feel better than going to spend time with you all over a home-cooked meal. Thank you Mom and Dad for all of your love and support throughout my entire life and especially in graduate school. You are the most wonderful parents and I am so grateful to have had you so close by. To Goober- thank you for being the most incredible sister anyone could ask for. Nobody I have ever met is as caring, thoughtful, and supportive as you are. You are one of a kind and I am the luckiest person ever to have you on my team as my sister and best friend.

ABSTRACT

HARNESSING THE PRO-APOPTOTIC FUNCTION OF MYC TO IMPROVE THERAPEUTIC RESPONSES IN CHEMORESISTANT B-CELL LYMPHOMA

Colleen Theobald Harrington

Andrei Thomas-Tikhonenko, Ph.D.

Therapeutic targeting of initiating oncogenes is the mainstay of precision medicine. Considerable efforts have been expended toward silencing MYC, which drives many human cancers including Burkitt lymphomas (BL). Yet, the effects of MYC silencing on standard-of-care therapies are poorly understood. Here we found that inhibition of MYC transcription renders B-lymphoblastoid cells refractory to chemotherapeutic agents. This suggested that in the context of chemotherapy, stabilization of Myc protein could be more beneficial than its inactivation. We tested this hypothesis by pharmacologically inhibiting glycogen synthase kinase 3 (GSK-3), which normally targets Myc for proteasomal degradation. We discovered that chemorefractory BL cell lines responded better to doxorubicin and other anti-cancer drugs when Myc was thus stabilized. *In vivo*, GSK3 inhibitors (GSK3i) enhanced doxorubicin-induced apoptosis in BL patient-derived xenografts (BL-PDX) as well as in murine MYC-driven lymphoma allografts. This enhancement was accompanied by and required deregulation of several key genes acting in the extrinsic, death receptor-mediated apoptotic pathway. Consistent with this mechanism of action, GSK3i also facilitated lymphoma cell killing by a death ligand TRAIL and by a death receptor agonist mapatumumab. Thus, GSK3i synergizes with both standard chemotherapeutics and direct engagers of death receptors and could improve outcomes in patients with refractory lymphomas.

TABLE OF CONTENTS

LIST OF ILLUSTRATIONS

LIST OF ILLUSTRATIONS (continued)

CHAPTER 1: Introduction

Introduction to Myc as an Oncogene

Myc is a nuclear transcription factor that belongs to a family that includes N-Myc and L-Myc. Myc controls and regulates cellular processes critical for normal cell growth and proliferation. As such, transcriptional targets of Myc encapsulate cellular functions such as cell cycle control, metabolism, signaling, protein biosynthesis, and apoptosis. MYC is deregulated in over half of all cancers, making it the most frequently altered oncogene [1]. Like many oncogenes, Myc was discovered through studying retroviruses found in animal cancers. In the case of Myc, early studies on chicken tumors caused by retroviruses identified the oncogene *v-myc* [2,3]. Soon after, the human homolog of *v-myc* was identified as *c-myc* [4]. MYC was first identified to function as an oncogene through the observation that the chromosomal region harboring MYC participates in balanced chromosomal rearrangements in Burkitt lymphoma (BL) (Fig. 1) [5,6].

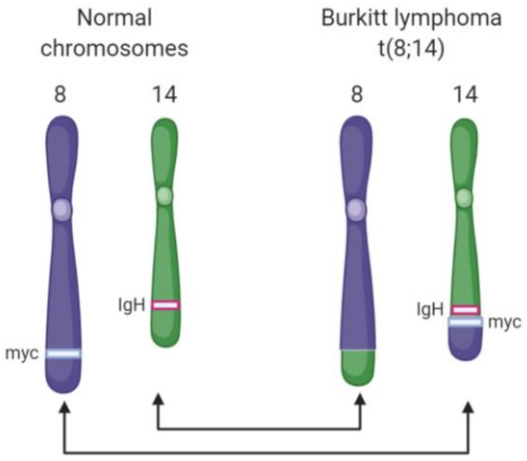

Figure 1. Chromosomal translocation involving MYC found in Burkitt lymphoma.

Transcriptional Function of Myc

The Myc protein structure contains two conserved Myc boxes (I and II) located in the N-terminal transcriptional regulatory domain, followed by boxes III and IV, a nuclear localization signal, and at the C-terminus, a basic HLH-Zip domain. It is this C-terminal domain that is critical for Myc to heterodimerize with its binding partner Max, which allows for association with E-box DNA sequences (CACGTG) and transcription activation [7]. The MYC-MAX heterodimer activates transcription through multiple mechanisms. Firstly, the MBII binding protein TRRAP associates with this complex, and through TRRAP, Myc is able to recruit histone acetyltransferases, such as TIP60, CBP/P300 and GCN5, to chromatin [8,9]. Furthermore, Myc regulates chromatin conformation by interacting with members of the SWI-SNF chromatin remodeling complex such as INI1 [10]. Myc also promotes transcription by recruiting RNA polymerase II and influencing RNA polymerase II C-terminal phosphorylation through recruitment of CDK-9, leading to transcriptional elongation [11,12].

In addition to the well-established role as a transcriptional activator, Myc can function as a transcriptional repressor. One such early piece of evidence was the finding that exogenous Myc is able to repress endogenous MYC, and that the domains required for this repression were the same domains required for oncogenic transformation [13,14]. Further evidence supporting this transcriptional repressor model came from the finding that Myc could repress activity at promoters independently of the E-box Myc binding sites [15]. Identification of direct Myc-repressed target genes aided in understanding Myc's role as a repressor, as did genome-wide analyses that revealed that as many Myc targets are repressed as are activated. Current models of Myc mediated transcriptional repression depict a model where the MYC-MAX heterodimer binds to transcriptional activators bound to DNA, and displaces other co-activators to instead favor recruitment of co-repressors [16,17].

Breakthroughs in deciphering how Myc promotes tumorigenesis came from the identification of Myc target genes and gene networks. Myc targets began being identified using a model where MYC was fused to the estrogen receptor (ER) to allow for controlled regulation of Myc activity [18]. Some of these early targets induced by Myc activity included PMTA and ODC1 [19,20]. MYC null model systems were also utilized to identify some of the first Myc-repressed target genes such as GADD45A [21]. With the advances in genome sequencing technologies and high-throughput chromatin immunoprecipitation techniques, whole genome evaluations of the Myc target gene network could be performed. Myc was found to bind to 10-15% of human genes and regulate both protein-coding and non-coding RNA genes, suggesting that it acts as a global transcriptional regulator [22,23]. A large proportion of the genes that Myc regulates are beneficial for tumor growth and survival. This includes genes that control the cell cycle, cell growth, metabolism, and protein synthesis, as well as genes that block differentiation and promote stem-cell self-renewal. Other processes represented in the network of Myc target genes are cell adhesion and migration, angiogenesis, DNA breaks, chromosomal instability, and cellular transformation. These pathways all contribute to Myc mediated transformation of cells into cancer.

Regulation of MYC Expression

The levels of Myc mRNA and protein are under tight regulatory control in the cell. The half-life of both MYC mRNA and protein are extremely short, averaging around 10 minutes for mRNA and 30 minutes for protein [24,25]. Presumably these short half-lives allow for cells to rapidly respond to external mitogenic stimuli by appropriately adjusting the level of Myc and growth signaling downstream of Myc. MYC mRNA induction and mitogenic stimuli have previously been linked [26]. Early studies on the regulation of Myc in the cell focused on the transcriptional control of the MYC gene. MYC was the first gene identified to be controlled via the process of transcriptional elongation, which is often lost in cancer [27,28]. Similarly, with MYC mRNA turnover, there are both translation dependent and independent mechanisms that regulate mRNA expression. These mechanisms can also be disrupted in cancer as is evidenced by the ability of increased MYC mRNA to drive cancer formation [29].

Myc protein regulation has been well studied, particularly the phosphorylation of residues Thr58 and Ser62, which are important for Myc protein stability and Myc activity [30,31]. Ser62 phosphorylation by kinases such as mitogen-activated protein kinase (MAPK), c-JUN N-terminal kinase (JNK), and cyclin-dependent kinase 1 (CDK1) is a pre-requisite for Thr58 phosphorylation [32]. GSK-3β is the kinase responsible for phosphorylation of Thr58; Thr58 phosphorylation marks Myc for recognition by the E3 ubiquitin ligase FBXW7, which will result in SCF^{FBXW7} complex recruitment, and subsequent Myc ubiquitination and degradation [33,34]. The importance of the Thr58 residue for normal regulation of Myc protein levels is underscored by the documentation of frequent cancer-associated Thr58 mutations that were shown to increase the oncogenic transformation potential of Myc [35,36]. In addition to SCF^{FBXW7} complex degradation of Myc protein, the SCF^{SKP2} complex has also been shown to contribute to Myc protein regulation, however no phosphorylation signal on Myc has been shown to be required for this interaction, unlike Thr58 for FBXW7 [37]. Studies have also suggested that prior to proteasome-mediated degradation, the SCF^{SKP2} complex

interaction with Myc stimulates Myc transcriptional activity, although it is not yet known how this stimulation of Myc function might occur [38] .

Myc protein can also be acetylated at certain lysine residues, such as Lys323 or Lys417. It is not yet clear what the function of acetylation at these lysine residues is for Myc activity or regulation, or whether they could act as docking sites for other proteins. However, lysine residues that can be acetylated can also be ubiquitinated. An inverse relationship has been established between an increase in Myc acetylation and a decrease in ubiquitination, which results in an increase in Myc stability [39,40]. Thus, many signaling pathways and mechanisms contribute to the complex regulation of Myc levels in cells.

MYC Deregulation in Cancer

Since the discovery that MYC is a driver of cancer through chromosomal translocation, MYC deregulation has been found to occur by various other means, including gene amplification, point mutations, or activation of upstream signaling pathways that lead to elevated Myc expression. [41,42]. Following analysis of more than 12 different cancer types, the frequency of MYC amplification was estimated to be around 14% [1,43]. In lung squamous cell carcinoma, breast, and ovarian cancers, MYC amplification is the most common copy-number alteration [44]. MYC point mutations, while being relatively uncommon, have been identified, mostly in the highly conserved MYC Homology Box I (MBI). In Burkitt lymphoma, the MYC T58 residue of MYC is frequently mutated, amongst other hotspot mutations [45]. Mutations in the T58 residue increase Myc stability, suggesting that this increase in protein stability is a mechanism of oncogenic transformation [46]. Mouse model studies of the T58A mutation suggested that in fact the tumorigenic potential of this mutation is found in the inability to upregulate the pro-apoptotic protein BIM [47].

Aside from alterations to the MYC gene itself, there are many signaling pathways involved in the initiation and progression of cancer that consequently result in Myc activation. Mutations in the PI3K/AKT pathway can increase Myc stability through hyper-activation of AKT, which decreases GSK3 mediated proteasomal degradation of Myc [48,49]. The MAPK pathway also regulates Myc. Signaling through the RAS oncoprotein leads to activation of the effector protein ERK which is directly responsible for regulating Myc stability and activity by phosphorylation of Myc on S62, and may phosphorylate other Myc residues that contribute to the regulation of protein stability [50,51]. RAS family members such as KRAS and BRAF are frequently mutated in cancer, leading to unregulated MAPK signaling and increased Myc protein stability and expression. These are only a few examples of how dysregulated signaling pathways in cancer lead to Myc activation. Other implicated pathways include BCR-ABL1 signaling, ER signaling in breast cancer, the WNT pathway, and NOTCH signaling in T-cell acute lymphoblastic leukemia [52]. The multiple means by

which Myc is deregulated in cancer all result in growth-factor independent expression of Myc and uncontrolled Myc activity that is no longer regulated by cellular and extracellular signals.

Inhibition of MYC as a Cancer Therapeutic Strategy

Numerous studies have established that Myc plays an important role not only in tumor initiation, but also in tumor maintenance [53,54]. Early on, Myc was shown to drive tumorigenesis in multiple transgenic mouse models [29,55]. Then later on, MYC inactivation was found to lead to regression of established tumors [56,57]. For this reason, considerable efforts have been made to inhibit Myc function. However, transcription factors are notoriously challenging to target pharmacologically due to their lack of hydrophobic pockets and large interaction surface areas, which are at odds with the standard binding models of small drug molecules [58]. Therefore, additional efforts have been made to inhibit MYC expression and to target signaling pathways that activate Myc.

BET bromodomain family members have a high affinity for P-TEFb complexes containing CDK-9 [59]; it was thus hypothesized that these proteins might function in the recruitment of CDK-9 to sites of highly acetylated chromatin and contribute to Myc-mediated transcriptional elongation. BET inhibition down-regulates the Myc transcriptional program, but also down-regulates the MYC gene itself [60]. Following the discovery that the BET transcriptional regulator BRD4 can bind to the MYC promoter and regulate MYC expression, investigators have begun to explore the therapeutic use of BRD4 inhibitors to treat cancer; however, this strategy may not be suitable for all cancer types [61]. In addition to BET proteins, Myc also interacts with histone acetyltransferase enzymes such as TIP60, CBP/P300, and GCN5. These interactions promote Myc stability and activity, thus inhibiting this group of enzymes could serve as another path to inhibiting Myc in cancer.

A Myc dominant-negative peptide named Omomyc was developed as an alternative to disrupting MYC transcription [62–64]. The peptide, which binds Myc and prevents Myc:Max heterodimerization, and has anti-tumor activity in experimental models of non-small cell lung cancer [65]. Finally, numerous upstream signaling pathways deregulate Myc activity, such as Notch, WNT,

PI3K, and MAPK pathways, for which small molecule inhibitors exist and are currently undergoing pre-clinical and clinical trials [66].

Contribution of MYC to Apoptosis

Although efforts are being made to inhibit Myc activity due to its contribution to tumor initiation and maintenance, paradoxically it has long been appreciated that Myc can also promote cell death. For example, in a Myc-driven cancer such as Burkitt lymphoma, tumor cells are highly proliferative but at the same time also display high levels of cell death [67]. Early studies revealed that Myc can trigger apoptosis, a form of cell death [68,69]. Later studies found that Myc deregulation leads to apoptosis through activation of the tumor suppressor p53 via ARF upregulation. To avoid this consequence of Myc activity, many Myc-driven tumors inactivate this pro-apoptotic pathway, as was seen in MYC-driven murine transgenic lymphomas that inactivate Arf or p53 [70,71]. This disabling of the p53 pro-apoptotic pathway is a mechanism by which MYC-driven tumors can survive with such high levels of Myc without triggering cell death. The disabling of Myc-driven apoptosis can be crucial for tumor initiation and progression, as demonstrated by the robust acceleration in tumorigenesis upon loss of the ARF-MDM2-p53 pathway in mouse models of MYC-driven cancers [72,73]. Although p53 is the main effector of Myc-mediated apoptosis, p53-independent mechanisms have also been identified; however, the different means by which Myc triggers p53-independent cell death are not completely understood. In *Eμ-Myc* murine lymphomas, Myc suppresses the anti-apoptotic proteins BCL-2 and BCL-XL [74,75]. Myc also activates the pro-apoptotic proteins BAX and BIM in different models of Myc-driven cancers [76–78].

In addition to amplifying intrinsic or mitochondrial cell death, Myc also modulates extrinsic, or death-receptor mediated cell death. Myc can sensitize cells to signaling though the death receptor CD95/Fas [79]. Many extrinsic apoptosis genes are in fact direct transcriptional targets of Myc, as is the case with CFLAR/FLIP, which is directly repressed by Myc, or Fas ligand, which is directly upregulated by Myc [80,81]. Alternatively, extrinsic apoptosis genes can be indirectly affected

by Myc expression, as with the TRAIL receptor DR5, which is upregulated at the cell surface upon Myc activation [82].

A full understanding of Myc-driven apoptosis brings with it the potential to re-engage Myc-driven apoptosis for therapeutic benefit. It is imperative to understand what factors determine whether Myc will act in a pro-survival or a pro-apoptotic manner. *In vivo* studies with a finely controlled Myc allele suggest that there are thresholds for Myc activity- a modest increase in the level of Myc led to oncogenesis, but a much larger increase was required to trigger apoptosis [83]. This would suggest that in the context of cancer, there could be a certain threshold for Myc that when reached, could activate cell death.

Chemotherapy and Apoptosis

Almost all cancer therapies exert their anti-tumor effect by triggering apoptosis in tumor cells [84,85]. Apoptosis is a well characterized form of cell death that features morphological hallmarks such as nuclear DNA fragmentation, membrane blebbing, and decrease in cell size [86]. Although different cancer therapies enact their anti-tumor effect through various means, ultimately DNA damage is a critical common component. DNA damage followed by cellular stress response signaling through molecules such as c-Jun N-terminal kinase (JNK), mitogen-activated, protein kinase (MAPK)/extracellular signal-regulated protein kinase (ERK), nuclear factor kappa B (NF-kB) eventually lead to activation of caspases, the effector molecules of apoptosis [87–89]. Caspases are activated following cleavage at specific aspartate residues, and once a caspase is activated it can cleave and further activate other caspases, thereby propagating the apoptotic signal. Two main pathways upstream of caspases lead to caspase activation-- the intrinsic, or mitochondrial, apoptotic pathway, and the extrinsic, or death receptor, apoptotic pathway (Fig. 2) [90].

As suggested in the pathway name, extrinsic apoptosis is initiated from the cell surface by extracellular ligands binding to death receptors. Death receptors are part of the tumor necrosis factor (TNF) receptor gene superfamily. Four death receptors have been well studied so far: CD95/Fas, TNF receptor 1 (TNFRI), TNF-related apoptosis-inducing ligand-receptor 1 and 2 (TRAIL-R1/DR4 and TRAIL-R2/DR5); their corresponding ligands are as follows: CD95 ligand (CD95L/FasL), TNF-α, and TRAIL [91]. All death receptors are composed of an extracellular ligand-binding domain, a membrane-spanning region, and an intracellular domain. This cytosolic domain contains a characteristic ~80 amino acid sequence known as the death domain, which is required for induction of apoptosis [92]. Upon ligand binding in the extracellular domain, the receptor undergoes a conformational change that leads to the recruitment of adaptor proteins such as Fas-associated protein with death domain (FADD) [93]. Adaptor proteins like FADD contain a death domain that allows for association with the receptor, and also death effector domains that facilitate

the recruitment of initiator caspases like caspase-8. At this stage, caspase-8 is still in its procaspase, inactive form, but upon formation of this so called death-inducing signaling complex (DISC), procapase-8 undergoes auto-catalytic cleavage and now becomes activated [94]. Activation of caspase-8 at the DISC can be inhibited by the short or long form of the cellular FLICE/caspase 8-like inhibitory protein ($cFLIP_S$ or $cFLIP_L$). These inhibitory proteins contain death effector domains that allow for their recruitment into the DISC and blocking of caspase-8 processing and activation [95]. The main cleavage targets of caspase-8 are the effector caspases (3, 6, and 7), which when activated will cleave and degrade critical cellular proteins, marking the beginning of the biological and morphological changes of an apoptotic cell.

Cytotoxic stimuli converge on the mitochondria to initiate intrinsic, or mitochondrial, apoptosis by permeabilization of the outer mitochondrial membrane [96,97]. Bax and Bak are pro-apoptotic proteins that oligomerize and assist in forming pores in the mitochondrial outer membrane. Following disruption of the outer membrane, proteins found in between the outer and inner membranes are released. This includes cytochrome *c*, which when released will directly activate caspase-3 by formation of an apoptosome complex with Apaf-1 and caspase-9 [98]. Anti-apoptotic proteins of the Bcl-2 family, such as Bcl-2, Bcl-xL, Bcl-w, and Mcl-1, are responsible for antagonizing intrinsic apoptosis [99].

There can be convergence between these two apoptotic pathways. Following activation in the DISC, caspase-8 can cleave Bid, a pro-apoptotic Bcl-2 family protein, which then induces oligomerization of Bax and Bak and leads to the release of cytochrome *c* from the mitochondria [100]. Another intersection between these pathways is the ability of caspase-9, which gets activated downstream of the mitochondria, to activate death receptor mediated apoptosis by cleavage of caspase-8 [101].

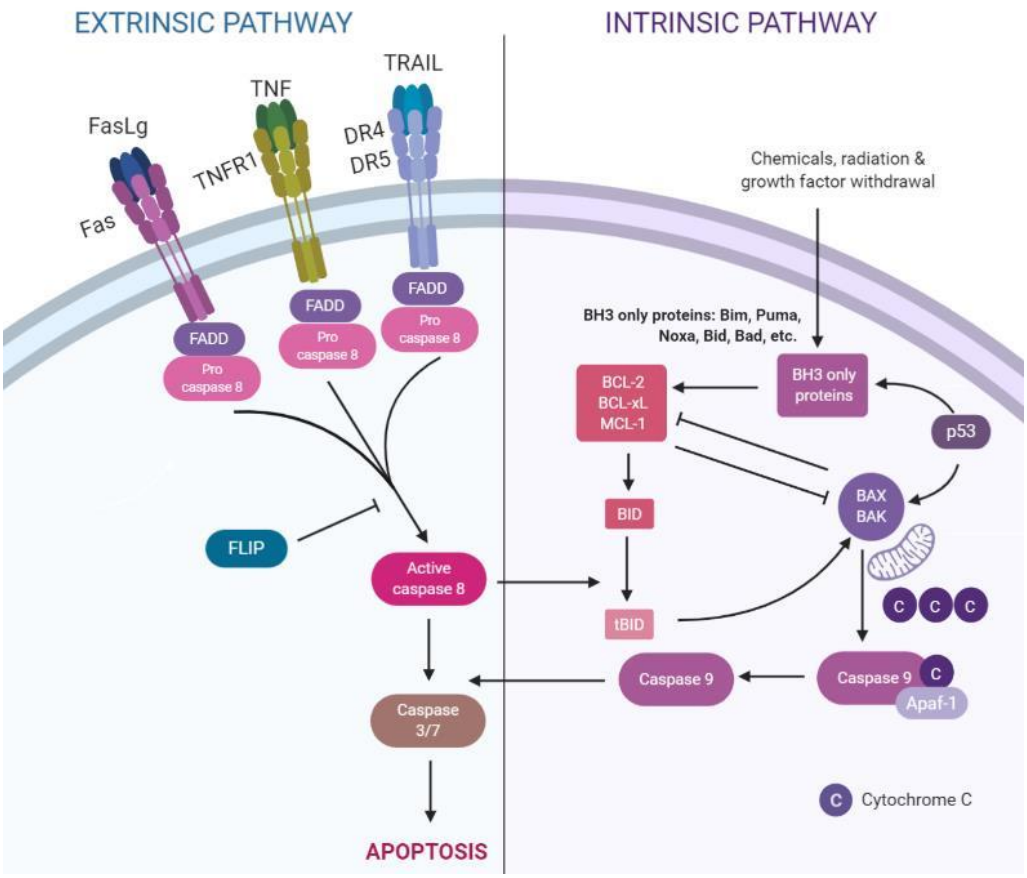

Figure 2. Extrinsic and intrinsic apoptotic pathways.

Mechanisms of Chemotherapy Resistance

Inherent frequency of resistance to a tumor-targeting drug falls between one in one million or one in one billion cells. Tumor cells frequently develop resistance to chemotherapy by disrupting both intrinsic and extrinsic apoptotic pathways. With regards to the death receptor pathway, there have been documentations of chemotherapy-resistant leukemia and neuroblastoma downregulating CD95/Fas expression [102,103]. In fact, mutations in Fas have been identified in multiple solid and hematologic cancers [104]. In colon cancer, inhibition of DR4 and DR5 transportation to the plasma membrane is a mechanism of resistance to the death ligand TRAIL [105]. Chromosome 8p, the region that contains DR4 and DR5, is a region of common loss of heterozygosity (LOH) in cancer, and many cancers that have this LOH event will delete or mutate the other copy of DR4 or DR5 resulting in a complete loss of these death receptors [106–108]. As mentioned previously, isoforms of cFLIP can block extrinsic apoptosis. Therefore, many tumors harbor high levels of FLIP, which has been correlated with a resistance to apoptosis following TRAIL, FasL, and chemotherapy [109,110].

In addition to these common, cancer-associated alterations in the extrinsic pathway, intrinsic apoptosis genes are also frequently mutated or altered in cancer and associated with chemotherapy resistance. The Bcl-2 oncogene is translocated and overexpressed in many cancers. High Bcl-2 expression is found in multiple hematologic malignancies, including follicular lymphoma where ~90% of patients have a chromosomal translocation involving Bcl-2 [111,112]. High Bcl-2 expression has also been found in solid tumors including those of the prostate, breast, and lung [113]. Inactivating mutations in the pro-apoptotic gene BAX have also been identified in colon cancer and some hematologic malignancies, and deletions in the region of the genome harboring BIM, another pro-apoptotic Bcl-2 family member, have been found in cases of mantle cell lymphoma [114–116]. Mutations in the tumor suppressor TP53, the most common genetic feature of human cancers, is a major source of chemotherapy resistance. Other mechanisms of

chemotherapy resistance exist in addition to the ones described here. Once example is the ability of ATP-binding cassette (ABC) transporters to pump anti-cancer drugs out of the cell, leading to multi-drug resistance [117]. These mechanisms and others oppose the potential efficacy of cancer chemotherapy.

Summary

In this study, we aim to leverage Myc-driven apoptosis to improve the response of chemoresistant tumors. For our model system, we have employed Myc-driven Burkitt lymphoma (BL). BL is an aggressive subtype of non-Hodgkin's lymphoma that arises from germinal center B-cells [118]. The cytogenetic hallmark of BL is the t(8;14) chromosomal translocation that results in a fusion between Myc coding sequence and the immunoglobulin heavy locus (IgH) enhancer. Less commonly MYC is translocated to the immunoglobulin light chain loci, IgK or IgL [119]. Given the prevalence of Myc as an oncogenic driver in BL and other cancers [120], numerous efforts have been made to develop Myc-targeting therapeutics [121]. However, in pre-clinical and clinical settings, such compounds are usually tested as monotherapies, often ignoring the question of their interactions with existing standards of care.

The interplay between Myc-targeting compounds and other anti-cancer modalities is made more complicated by the fact that Myc, while driving enhanced growth and proliferation, can also trigger cell death [122,123]. This occurs primarily through p53, a well-established tumor suppressor that activates intrinsic/mitochondrial apoptosis [70]. P53 inactivating mutations and Myc deregulation co-occur in >30% of BL tumor samples [124], essentially abrogating this signaling axis and conferring chemoresistance. Not surprisingly, doxorubicin (Dox)-based EPOCH-R (etoposide, prednisone, vincristine, cyclophosphamide, and doxorubicin with rituximab) and similar regimens, which are standards of care for Burkitt and other aggressive B-lymphomas, fail to cure a significant number of patients, especially those with relapsed or refractory disease [125]. Nevertheless, p53-independent, Myc-driven cell death has been reported by several laboratories [reviewed in [122]].

In principle, the pro-apoptotic activity of Myc could be leveraged for improved treatment outcomes even in chemoresistant tumors. However, apoptosis is triggered by much higher Myc levels than proliferation (Fig. 3) [83]. Thus, there could be proliferation without apoptosis but not

apoptosis without proliferation. A potential solution to this problem is to transiently increase Myc levels immediately prior to chemotherapy, reap therapeutic benefits, and then allow Myc to return to baseline.

We and others have reported that strengthening the CD19-PI3K-AKT axis is a reliable method to boost Myc protein stability in B-lymphoid cells [126–128]. This finding is consistent with the propensity of glycogen synthase kinase 3 beta (GSK-3β), which is inhibited by Akt, to phosphorylate Myc at Thr-58, which marks Myc for recognition by the E3 ubiquitin ligase Fbxw7 and subsequent degradation [reviewed in [129]]. Here we report that adding GSK-3 inhibitors to Dox significantly improves therapeutic apoptosis in B-cell lymphomas with inactive p53 and dissect the underlying molecular mechanisms.

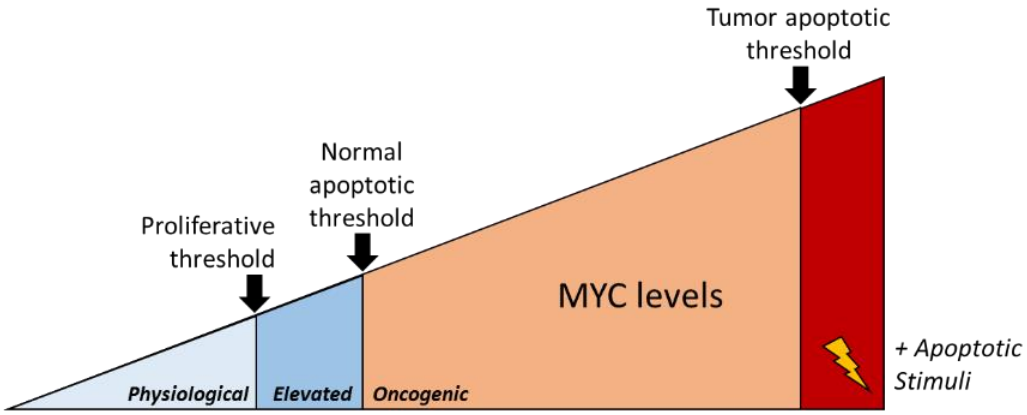

Figure 3. Model of MYC thresholds for proliferation versus apoptosis.

CHAPTER 2: Materials and Methods

Cell Culturing

Burkitt lymphoma and B-lymphoid cell lines were cultured and maintained in RPMI 1640 medium supplemented with 10% fetal bovine serum (FBS), 2mM L-glutamine, penicillin/streptomycin (p/s) at 37°C and 5% CO2. P493-6 cells and Burkitt lymphoma cell lines Ramos, Daudi, Raji, and Mutul were acquired from Drs. Chi Dang and Riccardo Dalla-Favera. P493-6 cells were authenticated in 2010 through targeted resequencing of the transgenic *MYC* allele. P53ER/MYC cells were established and cultured as described previously [130–133]. PDX MAP-GR-C95-BL-1 cells were cultured in RPMI 1640 medium supplemented with 2% FBS, 2mM L-glutamine, p/s, and 2% glucose at 37°C and 5% CO2. HT-29 colorectal adenocarcinoma cells were cultured in DMEM supplemented with 10% FBS, p/s, and 1% non-essential amino acids (NEAA).

siRNA Knockdowns and Viral Infections

SMARTpool siRNA for Fadd or RIPK1 (Dharmacon) were transfected at 300 nM or 200 nM, respectively, into Ramos cells by electroporation using the AMAXA system program 0-006 and Reagent V (Lonza). siRNA knock-down efficiency was measured 24h after transfection by RT-qPCR. For infection of Ramos cells with pMx-Ires-FLIP and MIGR1-Bcl2, retroviral particles were generated by transfection of 293GP cells with Lipofectamine-2000 (Invitrogen). Viral supernatants were harvested 24h, 36h and 48h after transfection and used to infect cells in the presence of polybrene (4 μg/ml). Selection of infected cells was done with 4 ug/ml Blasticidin over 1.5 weeks for pMx-Ires-FLIP or by cell sorting for GFP positive cells for MIGR1-Bcl2. For infection of P493-6 cells with two different p53shRNA constructs, lentiviral particles were generated by transfection of 293GP cells with Lipofectamine-2000 (Invitrogen). Viral supernatants were harvested 3 and 5 days

after transfection and were concentrated using Amicon centrifugal filters (UFC901024). Concentrated virus was used to infect cells in the presence of polybrene (2 μg/ml). Selection of infected cells was done with 2 ug/ml Puromycin over 1.5 weeks.

Drug Treatments

Tetracycline HCL (Sigma T7660), CHIR99021 (Biovision #1677-5), lithium chloride (Amresco K445), tamoxifen (Sigma H6278), Dox or vincristine (CHOP Pharmacy), mafosfamide (Santa Cruz sc-211761) and TRAIL (Calbiochem 616374) were added to cell culture medium as indicated. Mapatumumab was provided under the Material Transfer Agreement with Human Genome Sciences. For mRNA stability experiments, cells were treated with Actinomycin D (Sigma A9415) at a concentration of 3.5 μg/ml. For protein stability experiments, cells were treated with 20 μg cycloheximide (Sigma, C4859). For Myc transcription inhibition experiments, cells were treated with iBet-151 as described in the text. For a position control detection of necroptosis, Z-VAD-FMK (R&D FMK001), SM-164 (APExBio A8815), and TNF-α (R&D 210-TA-005) was added to cell culture media as indicated.

Cytotoxicity and Caspase Activity Assays

For cytotoxicity assays, 8 x 10^4 cells or 5 x 10^5 cells (for p493-6 p53shRNA and p493-6 p53KO) per well of a 96-well plate were treated in triplicate with DMSO, 3 μM CHIR, or 5 ng/mL tetracycline and indicated concentrations of chemotherapeutic drugs, TRAIL, or mapatumumab. After 48-72 hours, cell viability was measured using CellTiter-Glo (Promega, G7570) according to the manufacturer's protocol. Luminescent signal was read using a Synergy 2 plate reader (BioTek Instruments, Winooski, VT, USA). GraphPad Prism software (version 7) was used for log-transformed nonlinear regression curve fitting (4 parameter analysis). For caspase activity assays,

cells were treated with DMSO or 3 μM CHIR and indicated concentrations of Dox or vincristine. 5 x 10^4 cells were plated in triplicate in a 96-well plate and caspase activity was measured using Caspase-Glo 3/7 Assay (Promega, G8091). Signals were analyzed in a Synergy 2 plate reader.

Allograft and Xenograft Studies

Syngeneic tumors of P53ER/MYC cells were established in flanks of F1 hybrid B6129PF1/J 6-8 week old female mice (Jackson Laboratories stock no. 100492) as described previously [130–133]. Administration of drugs was started once tumors were palpable. 8 mg/kg Dox was delivered via intraperitoneal injection. CHIR99021 was dissolved in 10% DMSO, 45% polyethylene glycol 400 (Fisher Scientific, P167-1) and 45% of .9% NaCl (Sigma S8776) and delivered via intraperitoneal injection (100 mg/kg). All animal work was conducted under a protocol approved by the Children's Hospital of Philadelphia Animal Care and Use Committee (protocol IAC 15-000902) and by the Gustave Roussy Animal Care and Use Committee (protocol APAFIS#9399-2017032714402416v3). Xenograft tumors of PDX-MAP-GR-C95-BL-1 cells were established in flanks of ATHYM-Foxn1nu/nu 5-6 week old male mice. Once tumors became palpable, mice were treated with CHIR99021 and/or Dox as described above. The model was developed in female NSG mice of 6–8 weeks at engraftment within the project Development of Pediatric PDX Models, approved by the experimental ethic committee 26 (CEEA26—Gustave Roussy) under the number 2015032614359689v7, and in accordance with European legislation, as ancillary study of the clinical MAPPYACTS trial (ClinicalTrials.gov identifier NCT02613962).

CRISPR Constructs and Genome Editing

LentiCRISPRv2GFP was a gift from David Feldser (Addgene plasmid 82416) [134]. sgRNAs for TNFRSF10A (DR4), TNFRSF10B (DR5), and Fas were designed to target exons in the first half

of the gene using the Genetic Perturbation Platform (https://portals.broadinstitute.org/gpp/public/) to minimize off-target effects in the human genome. sgRNAs were cloned into the LentiCRISPRv2GFP vector via Golden Gate assembly using *Bsm*BI (New England BioLabs #R0580S). The sgRNA sequences are as follows:

Tnfrsf10A: 5'- CTTCAAGTTTGTCGTCGTCG-3', 5'-CCCATGTACAGCTTGTAAAT-3', 5'-AGGTCAAGGATTGTACGCCC-3'

Tnfrsf10B: 5'- GCAAATATGGACAGGACTAT-3', 5'-TGTGCCGGAAGTGCCGCACA-3', 5'-TGCAGCCGTAGTCTTGATTG-3'

Fas: 5'-GCATCATGATGGCCAATTCT-3', 5'-TAGGGACTGCACAGTCAATG-3', 5'-ATGTGAACATGGAATCATCA-3'

The scrambled sequence used is 5'-GCACTACCAGAGCTAACTCA-3'. For infection of Ramos cells with LentiCRISPRv2GFP plasmids, lentiviral particles were generated by transfection of 293GP cells with Lipofectamine-2000 (Invitrogen). Viral supernatants were harvested 24h, 36h and 48h after transfection and used to infect the Ramos cell lines in the presence of polybrene (4 μg/ml). After one week GFP positive cells were sorted and collected, and receptor knockout was confirmed by flow cytometry and western blot.

For CRISPR knockout of p53 in p493-6 cells, 1 x 10^6 cells were electroporated with 1 μg each of p53-Cas9 knockout plasmid (Santa Cruz sc-416469) and p53-homology directed repair (HDR) plasmid (Santa Cruz sc-416469-HDR) using the AMAXA system program M-013 and Reagent V (Lonza). Each knockout plasmid mixture contains a mix of three plasmids targeting TP53, and each HDR plasmid mixture contains a mix of three plasmids with homology arms specific for each of the knockout plasmids. Upon homology arm-directed recombination, puromycin is inserted at the site of CRISPR editing. Following electroporation with the plasmids, edited cells were selected for with puromycin (1 μg/ml) for two weeks.

Retroviral and Lentiviral Constructs

pLKO-p53-shRNA-427 and pLKO-p53-shRNA-941 were gifts from Todd Waldman (Addgene plasmid 25636, 25637) [135]. Human CFLAR cDNA was purchased from Dharmacon (MHS6278-202828910) and digested into a 1.1 kb piece using BamHI/XhoI restriction enzymes and a 865 bp piece using BamHI digestion. A retroviral construct expressing FLIP cDNA was generated by digestion of pMX-IRES-Blasticidin vector (RTV-016, Cell Biolabs) with BamHI/XhoI restriction enzymes followed by ligation of the 1.1 kb piece. This plasmid was then digested with BamHI restriction enzyme followed by ligation of the 865 bp piece to generate the pMx-Ires-FLIP plasmid. The BCL2-expressing retrovirus was generated using MIGR1 as a backbone.

Flow Cytometry

Live cells were stained with Annexin V and propidium iodide (BD Pharmingen 556547 and 556463), Yo-Pro (Invitrogen Y3607), TMRE (Enzo Life Sciences ENZ-52309) or antibodies against cleaved caspase-3 (Cell signaling 9603), APC anti-DR4 (BioLegend 307207), APC anti-DR5 (BioLegend 307407), and APC anti-FAS (Thermo Fischer Scientific MA1-10313) and analyzed in an AccuriC6 cytometer as previously described [136].

Western Blotting and Antibodies

Whole cell protein lysates were prepared in RIPA buffer (0.15 M NaCl:l% (w/v) sodium deoxycholate:0.1 % (w/v) sodium dodecyl sulfate: 1%(v/v) Triton X-100:1 mM phenylmethylsulfonyl fluoride in 0.05 M Tris-HCl, pH 7.4) containing protease and phosphatase inhibitors (Pierce Halt Inhibitor Cocktail, Thermo Scientific). Protein concentrations were estimated by Biorad colorimetric assay (BCA). Immunoblotting was performed as described previously [126]. Signals were detected by ECL (Pierce) or by Odyssey Infrared Imager (LI-COR Biosciences). The following primary

antibodies were used: P53, Santa Cruz sc-6243; Actin, Sigma A3853; Myc 9E10, Calbiochem OP10; Myc XP, Cell Signaling 5605; Myc T58, Abcam ab28842; β-catenin, BD Transduction Labs 610153; GAPDH, Abcam ab8245; PARP, Cell Signaling 9542; Caspase 3/Cleaved Caspase-3, Cell Signaling 9665; Bcl2, Cell Signaling 15071; Cleaved Caspase-8, Cell signaling 9496; CFLAR/c-FLIP, Enzo Life Sciences ALX-804-961-0100; RIPK1, BD Biosciences 610458; MLKL, Cell Signaling 14993; Phospho-MLKL (Ser358), Cell Signaling, 91689; DR4, Prosci 1139; DR5, Abcam ab181846; Fas, Santa Cruz sc-1023. The following secondary antibodies were used: goat anti-rabbit-HRP, GE Healthcare NA934V; goat anti-mouse HRP, GE Healthcare NA931V; goat anti-mouse-680, Licor 925-32220; donkey anti-rabbit-800, Licor 926-32213.

RNA Isolation and Reverse Transcriptase (RT)-qPCR

Total RNA was isolated using TRIzol ® (Invitrogen). cDNAs were prepared with random hexamers using High Capacity cDNA RT kit (Life Technologies). RT-qPCR was performed using PowerSYBR Green PCR Master Mix (Life Technologies) and gene-specific oligo pairs. Quantitative PCR reactions were performed on an Applied Biosystems Viia7 machine and analyzed with Viia7 RUO software (Life Technologies). The following Forward (F) and Reverse (R) primers were used:

Bax F- CGTGTCTGATCAATCCCCGAT | R- TGAGCAATTCCAGAGGCAGT

Bak F- GGCACCTCAACATTGCATGG | R- CAGTCTCTTGCCTCCCCAAG

Bim F- AGACAGAGCCACAAGCTTCC | R- ATACCCTCCTTGCATAGTAAGCG

Noxa F- ATTACCGCTGGCCTACTGTG | R- ATGTGCTGAGTTGGCACTGA

DR4 F- TTGCTTGCCTCCCATGTACAG | R- CAGGGACTTCTCTCTTCTTCA

DR5 F- TGTCGCCGCGGTCCT | R- TGGGTGATCAGAGCAGACTCAG

Fas F- GGGCATCTGGACCCTCCTAC | R- GATAATCTAGCAACAGACGTAAGAACCA

TNFR1 F- CCCGAGTCTCAACCCTCAAC | R- ATTCCCACCAACAGCTCCAG

TNF F- ATCCTGGGGGACCCAATGTA | R- AAAAGAAGGCACAGAGGCCA

TRAIL F- TATGATGGAGGTCCAGGGGG | R- CTGCAGGAGCACTGTGAAGA

FLIP F- TTTACCACCCAGAGACACGC | R- AGAACCTCTGCCTGCTGAAC

Fadd F- CACAGACCACCTGCTTCTGA | R- CTGGACACGGTTCCAACTTT

RIPK1 F- AGTCCTGGTTTGCTCCTTCCC | R- GCGTCTCCTTTCCTCCTCTCTG

MLKL F- CTCTTTCCCCACCATTTGAA | R- TCATTCTCCAGCATGCTCAC

RNA-Sequencing

Biological triplicates of Ramos cells treated with 0, 3, or 6 hours of 3 μM CHIR99021 were subjected to RNA-sequencing. Raw RNA-seq reads were aligned using GSNAP (version 2016-04-01) [137] and quantified with htseq-count [138] using the Ensembl genome and gene annotation (GRCh37 release 75) [139]. After filtering low expressed genes, differential expression was determined using the voom method in the bioconductor package limma (version 3.30.0) [140,141]. The volcano plot was generated using R (version 3.3.2 (2016-10-31)) package ggplot2 (version 2.2.0) and genes annotated in the apoptosis pathway as annotated in the KEGG PATHWAY database (hsa04210) [142,143]. Data was uploaded to GEO under accession number GSE126529.

Immunohistochemistry

Following excision, flank tumors were fixed in 10% buffered formalin and transferred to PBS the following day. Tissue was dehydrated, embedded in paraffin and sectioned by the CHOP Pathology Core. Immunohistochemical staining for cleaved caspase-3 was carried out on paraffin-embedded tumor sections using R&D Systems antibody AF835 following standard procedures. Positive staining for cleaved caspase-3 analysis was performed using Aperio Positive Pixel Count Algorithm (version 9.1; Leica, Buffalo Grove, IL). Normal tonsils and Burkitt lymphoma clinical

samples were immunohistochemically stained for DR4 (TNFRSF10A) with the LSBio antibody LS-B2073-50 following standard procedures.

Statistical Analysis

Statistical analysis was performed on GraphPad Prism software (version 7) by unpaired student's t-test for two group comparisons or one-way ANOVA correcting for multiple comparisons, with similar variance between groups being compared. Error bars represent s.e.m. ± SD, and $P<0.05$ was considered statistically significant. For these experiments, each group is made up of at least three samples to achieve 80% power. No randomization nor blinding of investigators was performed.

CHAPTER 3: Results

Myc Sensitizes B-lymphoid cells to Doxorubicin

To address the role of Myc in responses to chemotherapy, we utilized the B-lymphoid cell model p493-6, which expresses a tetracycline-repressible Myc allele and endogenous Myc [144]. However, these cells are TP53 wild-type and do not recapitulate the genetics of BL where p53 is mutated at a frequency of ~30% [124].To make these cells a more suitable model of r/r BL, we infected cells with lentiviruses encoding two different p53-directed shRNA hairpins and selected the best knockdown for further use (Fig. 4A, arrow). In response to Dox treatment, p53shRNA-infected cells exhibited impaired induction of p53 and also displayed a higher IC50 for Dox following 72 hours of treatment (Fig. 4B, C), making them representative of r/r BL. Of note, in the absence of a chemotherapeutic agent, we observed minimal cleavage of PARP in both 'high Myc' and 'low Myc' states, indicating the ability of this B-lymphoid cell model to tolerate fluctuations in Myc levels. Furthermore, in the 'high Myc' state, therapeutic apoptosis was quite robust, as evidenced by elevated levels of cleaved PARP (Fig. 5A, left two lanes). To our surprise, in the 'low Myc' state (Fig. 5A, right two lanes), there was minimal cleavage of PARP in response to Dox.

We wanted to measure the effect of manipulating Myc levels on apoptosis quantitatively, so we treated cells with vehicle or tetracycline and increasing concentrations of Dox for 72 hours and found that 'low Myc' cells (+ tetracycline) were much more resistant to Dox as measured by a 1-log increase in the IC50 (Fig. 5B). To determine whether sustained Myc expression is required for Dox sensitivity or whether acute Myc activation would suffice, we started with cells in a 'low Myc' state and, at the time of plating/Dox treatment, washed off tetracycline from half the cells, to allow for a quick accumulation of Myc. We found that cells with acute Myc activation ("high Myc") were much more sensitive to Dox as measured by a >1-log decrease in the IC50 (Fig. 5C).

We then asked what the contribution of Myc would be to therapeutic apoptosis in a model system completely lacking p53. To do this, we electroporated p493-6 cells with a pool of three p53-targeting CRISPR/Cas9 plasmids and a pool of three homology directed repair (HDR) template plasmids that insert puromycin at the site of editing. Once knockout (KO) cells were selected for with purmocyin treatment, p53 wild-type (WT) and knockout cell lines were treated for 24 hours with Dox. Western blotting confirmed that there was no induction of p53 expression in the KO line following Dox, and furthermore, that there was minimal induction of apoptosis compared to WT cells, as measured by greatly reduced cleaved PARP expression after 24 hours of treatment (Fig. 6A). To further demonstrate the Dox resistance in the KO cell line, WT and KO cells were treated with increasing concentrations of Dox for 72 hours. KO cells were vastly more resistant to Dox, as demonstrated by a roughly 1-log increase in IC50 compared to WT cells (Fig. 6B). To establish the role of Myc in this highly Dox-resistant, p53-null model, cells were treated as in Fig. 5C. Cells in a 'low Myc' state (+ tetracycline) either had tetracycline washed off, to allow for a quick accumulation of Myc at the time of Dox addition, or were kept in a low Myc state for the duration of the experiment. Just as in the p53shRNA model, acute accumulation of Myc (a "high Myc" state) led to a drastic increase in sensitivity to Dox, as seen by the > 1 log decrease in Dox IC50 (Fig. 6C). These counterintuitive data indicate that high Myc, while clearly oncogenic, is essential for Dox-mediated apoptosis. This finding prompted us to investigate how Myc could be pushed beyond the apoptotic threshold in r/r BL cells under normal growth conditions or upon exposure to chemotherapy.

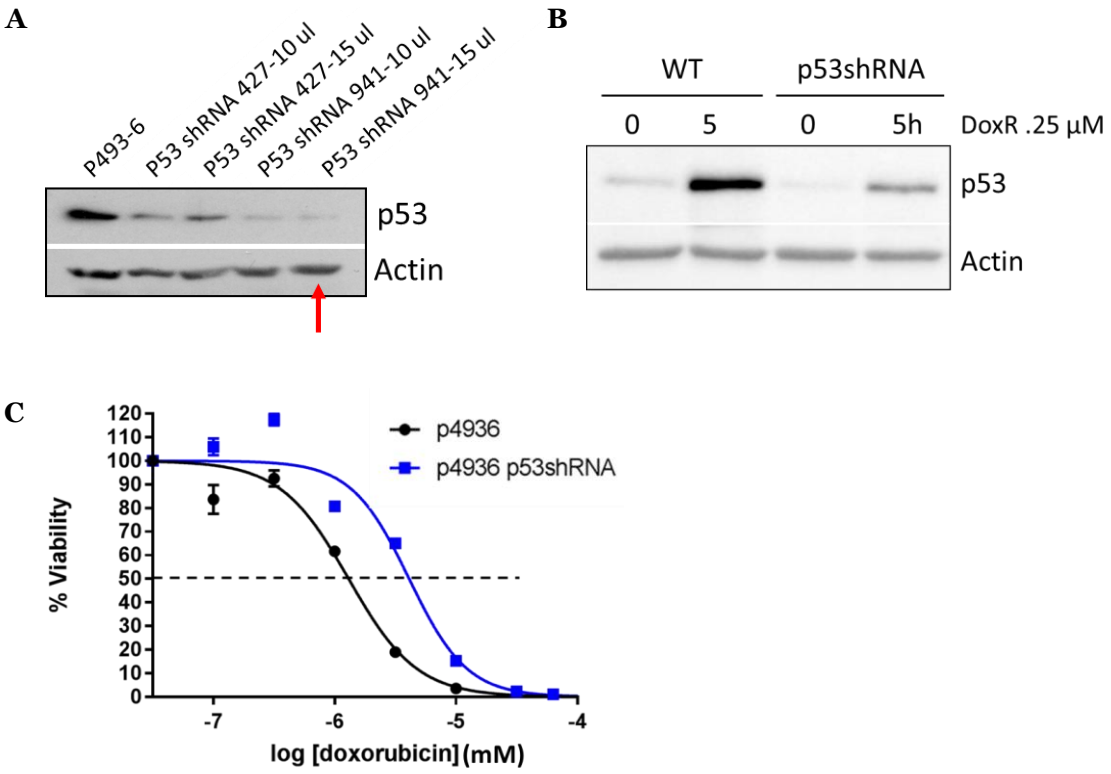

Figure 4. Generation and characterization of P493-6 p53shRNA cell line.
A) P493-6 cells were infected with two p53shRNA at two viral concentrations. P53 knockdown was assessed by western blotting. **B)** P493-6 WT and p53shRNA cells were treated for 5 hours with .25 µM doxorubicin. Induction of p53 was assessed by western blotting. **C)** 72 hour Dox dose response curve of p493-6 WT and p53shRNA cells; survival was assessed using CellTiter-Glo and plotted using GraphPad Prism.

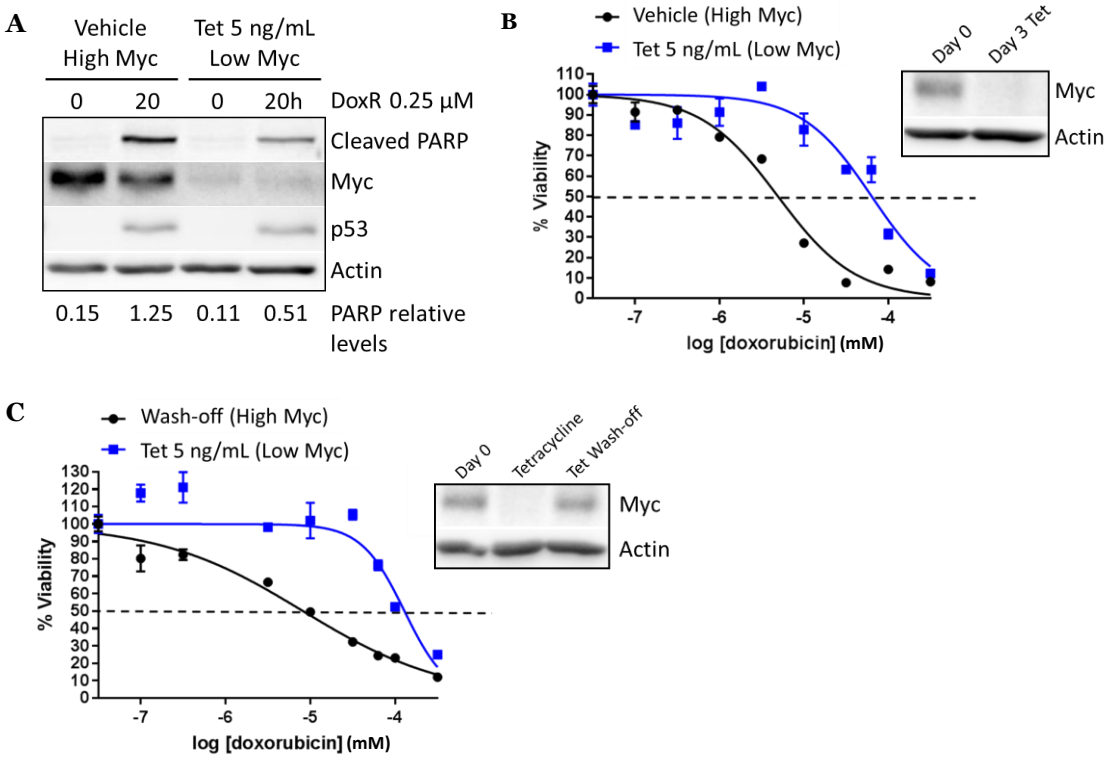

Figure 5. Myc is critical for doxorubicin sensitivity in Myc-repressible p53shRNA B-lymphoid model.
A) P493-6 p53shRNA cells were treated with vehicle (high Myc) or 5 ng/mL tetracycline (low Myc) for 5 hours and doxorubicin as indicated. Western blotting was performed for cleaved PARP, Myc, p53 and actin loading control. Levels of cleaved PARP (indicated below) were quantified using Image J software and plotted with GraphPad Prism. **B)** 72 hour Dox dose response curve of p493-6 p53shRNA cells treated with 5 ng/mL tetracycline or vehicle; survival was assessed using CellTiter-Glo and plotted on GraphPad Prism. Cells were harvested at day 0 and day 3 to assess Myc levels by western blotting. **C)** P493-6 p53shRNA cells were treated with 5 ng/mL tetracycline or vehicle overnight. The next day, tet was removed from half of the cells. Cells were harvested at day 0, after overnight tet, and 48 hours after tet wash-off to assess Myc levels by western blotting. All cells were then treated with increasing concentrations of doxorubicin for 48 hours and cell survival was measured as in B).

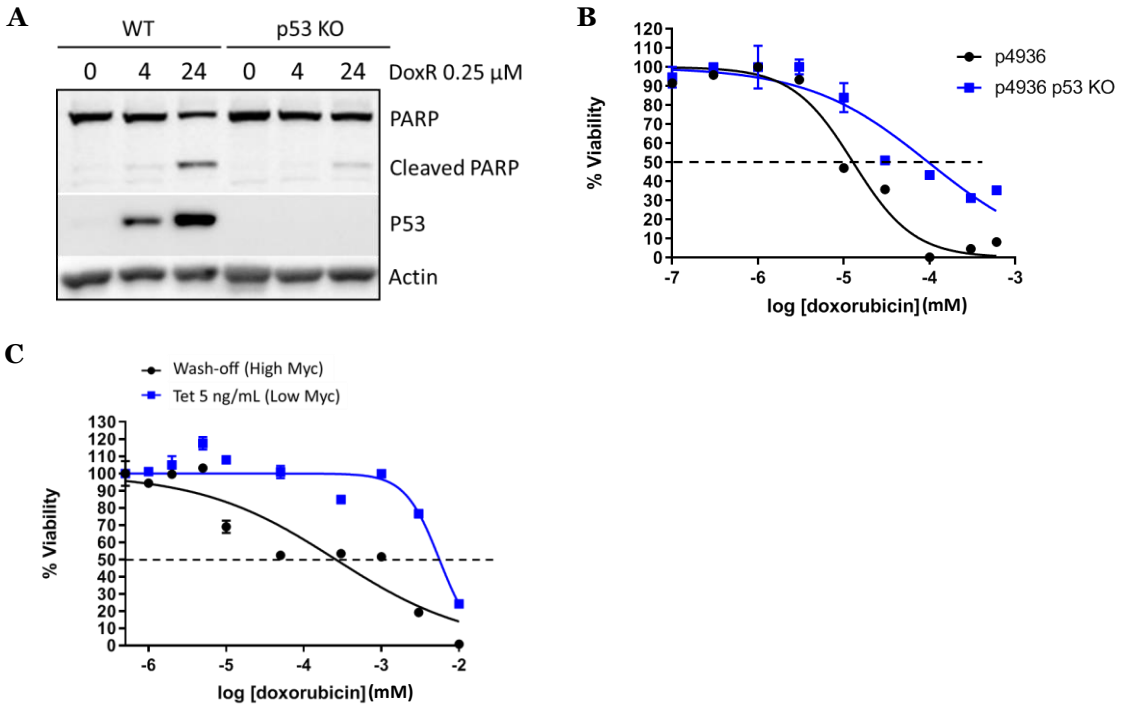

Figure 6. Myc is critical for doxorubicin sensitivity in Myc-repressible p53 knockout B-lymphoid model.
A) P493-6 p53 WT and KO cells were treated for 4 or 24 hours with .25 µM doxorubicin. Western blotting was performed for cleaved PARP, p53 and actin loading control. **B)** 72 hour Dox dose response curve of p493-6 WT and p53 KO cells; survival was assessed using CellTiter-Glo and plotted using GraphPad Prism. **C)** P493-6 p53KO cells were treated with 5 ng/mL tetracycline or vehicle overnight. The next day, tet was removed from half of the cells. All cells were then treated with increasing concentrations of doxorubicin for 48 hours and cell survival was measured as in B).

GSK-3 inhibition stabilizes Myc in Burkitt lymphoma cell lines

Since Myc is regulated post-translationally by GSK-3β phosphorylation on the Thr58 residue, we reasoned that treating B-lymphoid cells with GSK-3 inhibitors such as lithium chloride [145] or the more specific small molecule CHIR99021 [146] would elevate Myc to levels sufficient to trigger cell death (Fig. 7A). We first treated a panel of BL cell lines bearing wild-type or Thr58-mutant Myc with CHIR99021. β-catenin, a well-known GSK-3β target [147] was stabilized in all cell lines irrespective of Myc status and thus was used as a readout for GSK-3 inhibition in subsequent experiments (Fig. 7B). In contrast, only wild-type Myc was transiently stabilized by CHIR99021 treatment (Fig. 7B). This stabilization was accompanied by the loss of the inhibitory Myc-Thr58 phosphorylation. We also observed Myc stabilization in the Ramos cell line (p53 mutant, Myc wild-type) upon GSK-3 inhibition with lithium chloride (Fig. 7C). To determine the mechanism of Myc transient stabilization, we pre-treated Ramos cells with DMSO or CHIR99021, then blocked new mRNA synthesis with actinomycin D. We found no apparent difference in mRNA stability between treatment conditions (Fig. 8A). Ramos cells pre-treated with DMSO or CHIR99021 were then exposed to cycloheximide to inhibit new protein synthesis. In DMSO treated cells, Myc protein was rapidly degraded, with almost all pre-existing protein disappearing after 80 minutes (Fig. 8B, DMSO lanes). In contrast, Myc protein in CHIR99021-treated cells was stable over 80 minutes (Fig. 8B, CHIR lanes). Thus, increased protein stability underlies CHIR99021-mediated increases in Myc.

Both Myc and β-catenin are able to promote cell cycle progression and in some cases survival, thus we considered the possibility that treatment with CHIR99021 alone could promote neoplastic growth. To address this, CHIR99021-treated Ramos cells were assessed for cell cycle distribution, nuclear membrane integrity, and mitochondrial membrane depolarization using flow cytometry for propidium iodide (PI) uptake, Annexin V, and TMRE, respectively. We found no differences in cell cycle distribution or apoptosis (Fig. 8C), suggesting that while short-term

treatment with CHIR99021 is unlikely to accelerate cancer progression, it will not be effective as a monotherapy either and would have to be combined with cytotoxic drugs.

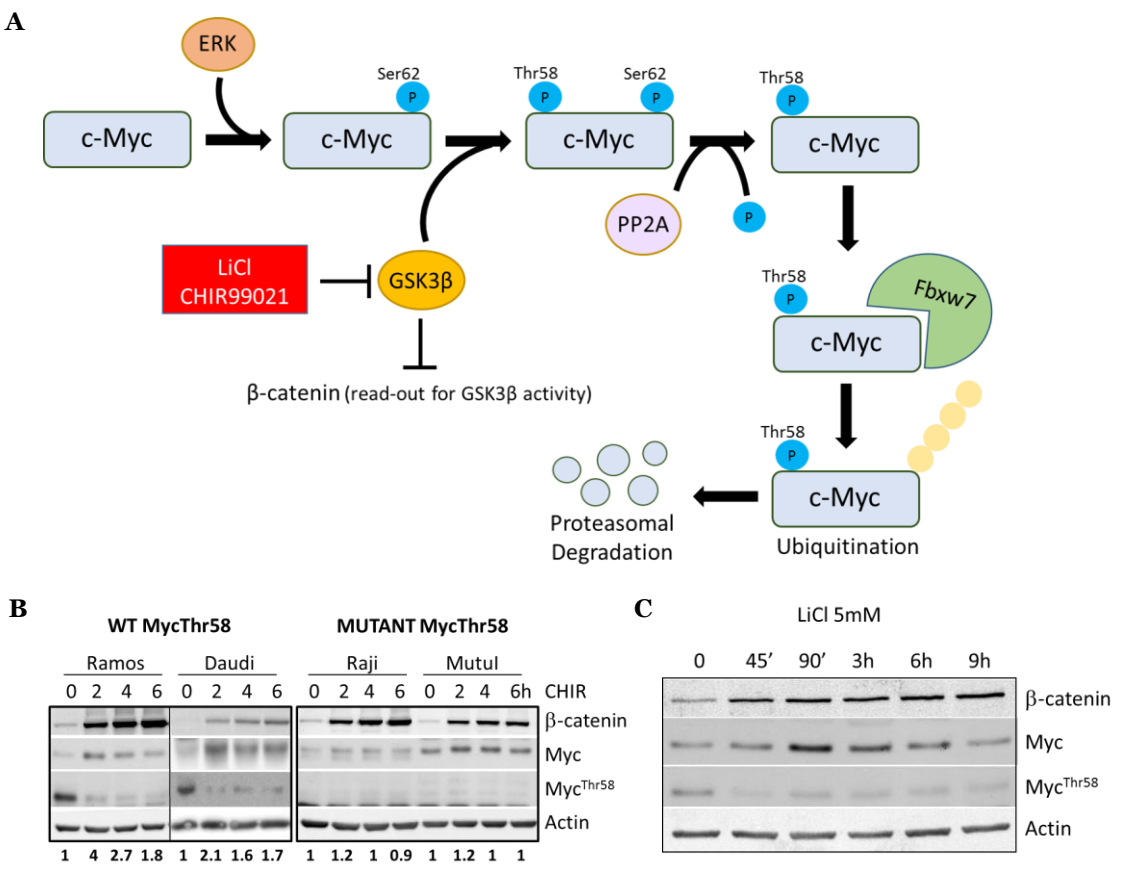

Figure 7. GSK-3 inhibition results in a transient increase in Myc Thr58 wild-type protein. **A)** Model of Myc protein regulation by GSK-3. **B)** Myc wild type (left) & Thr58 mutant (right) Burkitt lymphoma cell lines were treated with 3 μM CHIR99021 for a 6 hour time course. Western blotting was performed for β-catenin, Myc, Myc^{Thr58} phosphorylation and actin control, with Myc quantification using ImageJ below. **C)** Ramos cells were treated with LiCl as indicated. Western blotting was performed for β-catenin, Myc, and Myc^{Thr58} phosphorylation.

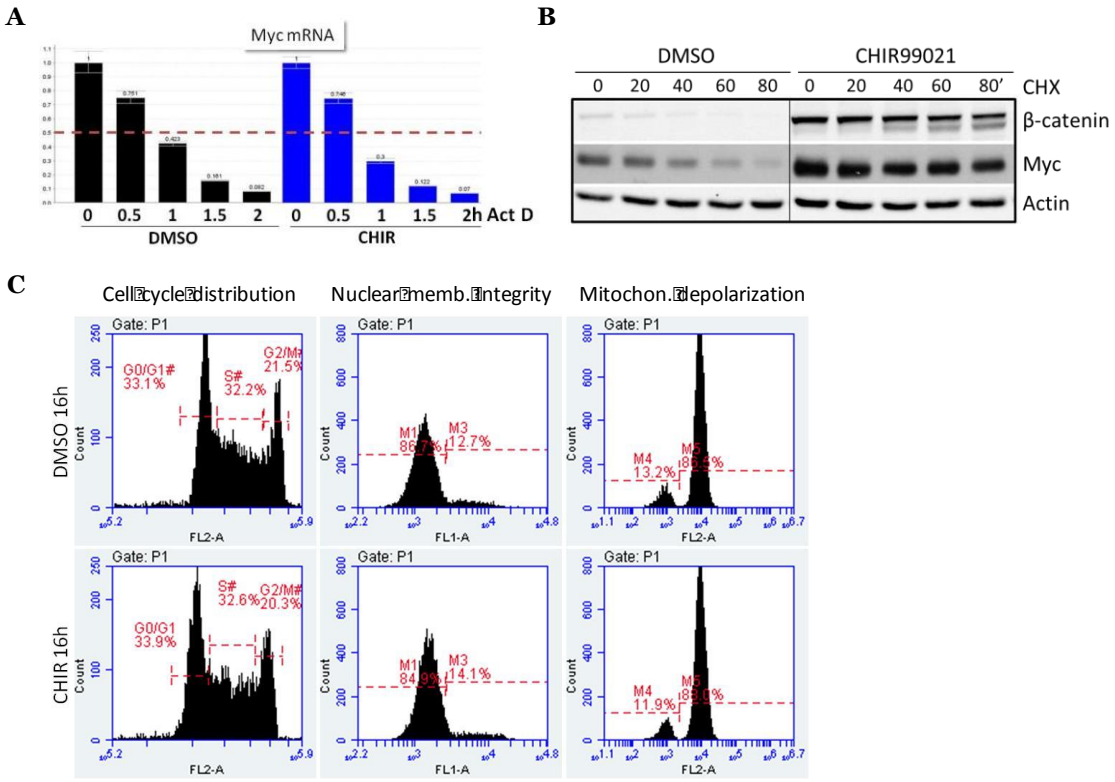

Figure 8. GSK-3 inhibition leads to an increase in Myc levels through transient stabilization of Myc at the protein level.
A) Ramos cells were treated with DMSO or 3 μM CHIR99021 for 16 hours followed by actinomycin D. Bar graphs show qRT-PCR for Myc mRNA. **B)** Ramos cells were treated as in B) but followed by cycloheximide treatment. Western blotting was performed for Myc, β-catenin, and GAPDH control. **C)** Ramos cells were treated with DMSO or 3 μM CHIR99021 for 16 hours, then stained with PI, Yo-Pro, or TMRE (left, middle, and right columns), and analyzed by flow cytometry. Percentage of cells in each phase of cell cycle are shown (left column). Positive and negative cells are shown for Yo-Pro and TMRE staining.

GSK-3 inhibition aids chemotherapy in BL by a Myc-dependent mechanism

To determine whether GSK-3 inhibition potentiates therapeutic apoptosis, we chose a two-hour CHIR99021 pre-treatment interval, which coincides with the spike in Myc levels (Fig. 7B). Ramos cells pretreated with DMSO or CHIR99021 were exposed to Dox. We found that CHIR99021 treatment increased activation of apoptosis as measured by enhanced PARP cleavage (Fig. 9A). We also measured apoptosis activation by the Caspase-Glo 3/7 assay, which detects the release of aminoluciferin from the cleaved caspase-3/7-specific substrate. We found that CHIR99021 boosted the activation of caspases 3/7 in response to Dox (Fig. 9B). As expected, by flow cytometric analysis we observed an increase in cleaved caspase-3 staining between Dox alone and its combination with CHIR99021 (Fig. 9C). As a result of detecting an increase in apoptosis activation, the IC50 for Dox was significantly reduced across multiple experiments (Fig. 9D). In the Burkitt lymphoma cell line Daudi (p53 mutant, Myc Thr58 wild type), CHIR99021 also reduced the IC50 for Dox, albeit to a lesser degree (Fig. 9E). Collectively these data demonstrate that GSK-3 inhibition enhances the response of Burkitt lymphoma cells to the chemotherapeutic drug doxorubicin.

Doxorubicin is not the only chemotherapeutic drug that is used to treat Burkitt lymphoma, so we wanted to test the cooperation between GSK-3 inhibition and other anti-cancer drugs. We combined CHIR99021 pre-treatment with 4 or 7 hours of vincristine in Ramos cells, and similarly to the result with Dox, we found that CHIR99021 increased vincristine-induced apoptosis as seen by an increase in cleaved PARP (Fig. 10A). Using the Caspase-Glo 3/7 assay, we detected an increase in activated caspases 3/7 following CHIR99021 + vincristine compared to DMSO + vincristine (Fig. 10B). These measured increases in apoptosis translated to about a half a log reduction in the IC50 for vincristine when Ramos cells were also cultured with CHIR99021 for 72 hours (Fig. 10C). CHIR99021 treatment also lead to a >0.5 log reduction in the IC50 for a different

chemotherapeutic drug mafosfamide, a cyclophosphamide analog that does not require hepatic activation to induce apoptosis (Fig. 10D).

Given that GSK-3 has targets other than Myc, we asked to what extent this pro-apoptotic effect was due to Myc stabilization. We began by anti-GSK-3 adjuvant therapy on the BL cell lines Raji and MutuI that are p53/MycThr58 mutant and did not exhibit a CHIR99021-mediated increase in Myc (Fig. 7B). Despite all of the other GSK-3 targets that could be modulated during CHIR99021 treatment, in both of these cell lines where Myc was not transiently stabilized addition of CHIR99021 did not alter the IC50 for Dox (Fig. 11A, B).

To test the involvement of Myc in a more direct genetic manner, p493-6 p53shRNA cells were treated with vehicle or low dose tetracycline to reduce Myc levels, followed by DMSO or CHIR99021 and Dox. In vehicle-treated cells, CHIR99021 lead to increased activation of apoptosis following Dox (Fig. 12A, 'Vehicle' columns). Tetracycline-treated cells expressed around ~50% less Myc, and apoptosis following Dox alone was reduced ~50%. Despite this, CHIR99021 no longer enhanced the apoptotic response to Dox (Fig. 12A, 'Tet' columns).

In parallel, we pharmacologically inhibited Myc expression in BL cells. Because Myc is regulated at the transcriptional level by BRD4 [60,61], we employed the BRD4 inhibitor iBet-151 (a.k.a. GSK1210151A) [148] to blunt Myc transcription in the context of CHIR99021 treatment. First, we treated Ramos cells with increasing concentrations of iBet-151 and determined that 500 nM was the lowest dose at which Myc protein levels were adequately suppressed without evidence of cell death (Fig. 12B). We then cultured Ramos cells in 500 nM iBet-151 or control media for 24 hours followed by anti-GSK-3 adjuvant therapy. We found that when Myc expression was reduced, the cooperation between CHIR99021 and Dox was almost fully abrogated, as evidenced by the abolishment of apoptosis markers (Fig. 12C). To measure apoptosis quantitatively, we subjected cells treated with Dox, iBet-151 + Dox, CHIR + Dox, or all three drugs to flow cytometric analysis for apoptosis marker Annexin V. We found that Dox alone did not induce apoptosis very efficiently

(<15% Annexin V-positive cells) and adding iBet-151 to Dox made apoptosis even less efficient (-7% net change). Combining CHIR99021 and Dox more than doubled the percentage of Annexin V positive cells as compared to Dox alone (~30%). However, treatment with all three compounds completely blocked apoptosis (Fig. 12D). Collectively, these data suggest that Myc is a key GSK-3 target involved in CHIR99021-facilitated sensitization to chemotherapy.

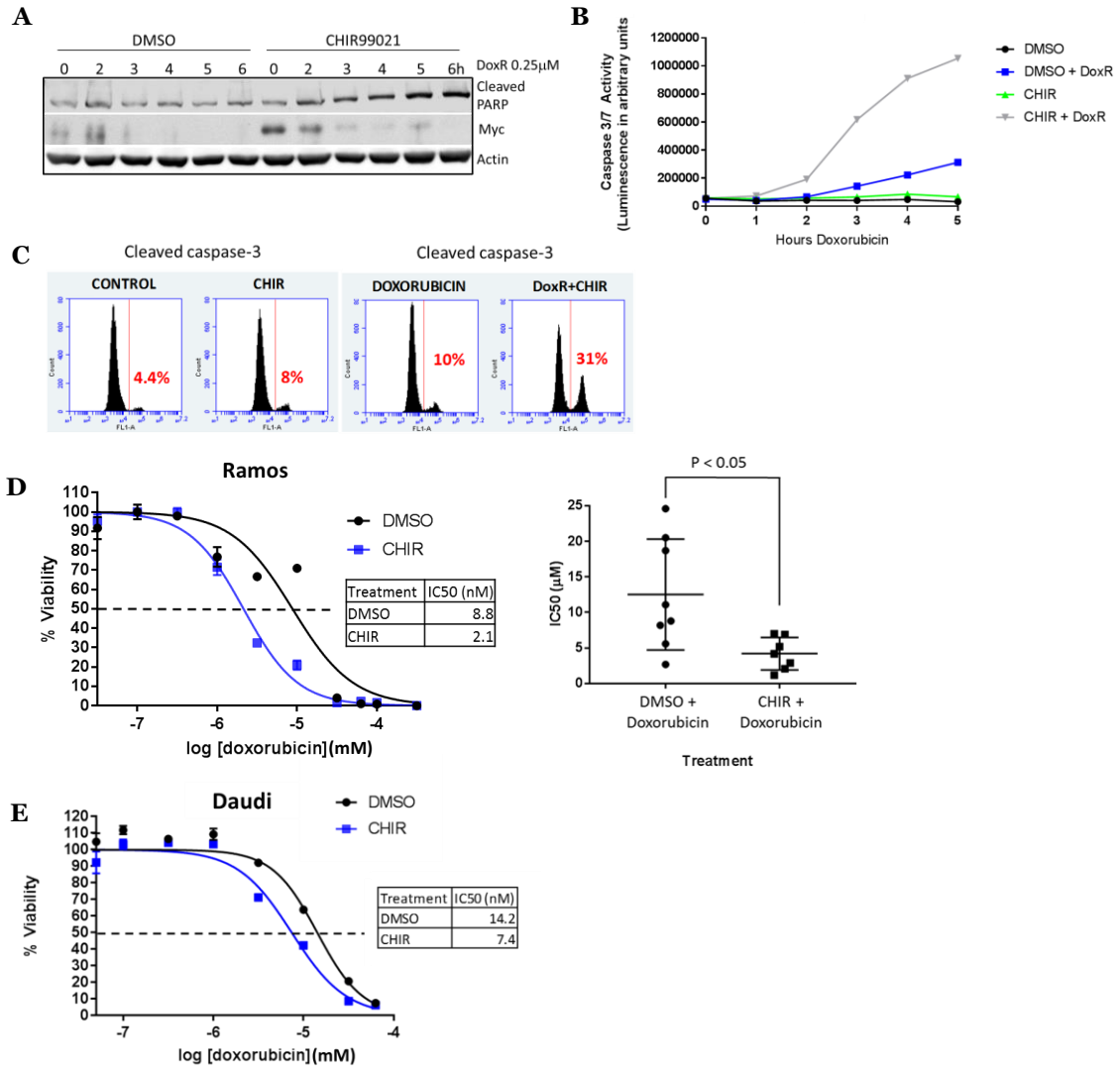

Figure 9. GSK-3 inhibition with CHIR99021 increases sensitivity to doxorubicin in Myc wild-type Burkitt lymphoma cell lines.
A) Ramos cells were treated with DMSO or 3 µM CHIR99021 for 2 hours followed by doxorubicin as indicated. Western blotting was performed for cleaved PARP, Myc, and actin control. **B)** Ramos cells were treated as described in A). Cleaved caspase-3 expression was analyzed by flow cytometry after 6.5 hours of doxorubicin; percentages of positive cells are indicated. **C)** Ramos cells were treated as described in A). Caspase 3/7 Glo assay was performed and luminescence data points for each treatment group are plotted. **D)** Left: Ramos cells were treated with DMSO or 3 µM CHIR99021 and increasing concentrations of doxorubicin for 72 hours. Cell survival was assessed using CellTiter-Glo and plotted using GraphPad Prism. Right: Graph of means ± SEM analyzed by unpaired t-test for experimental repeats. **E)** Daudi cells were treated and analyzed as described in D).

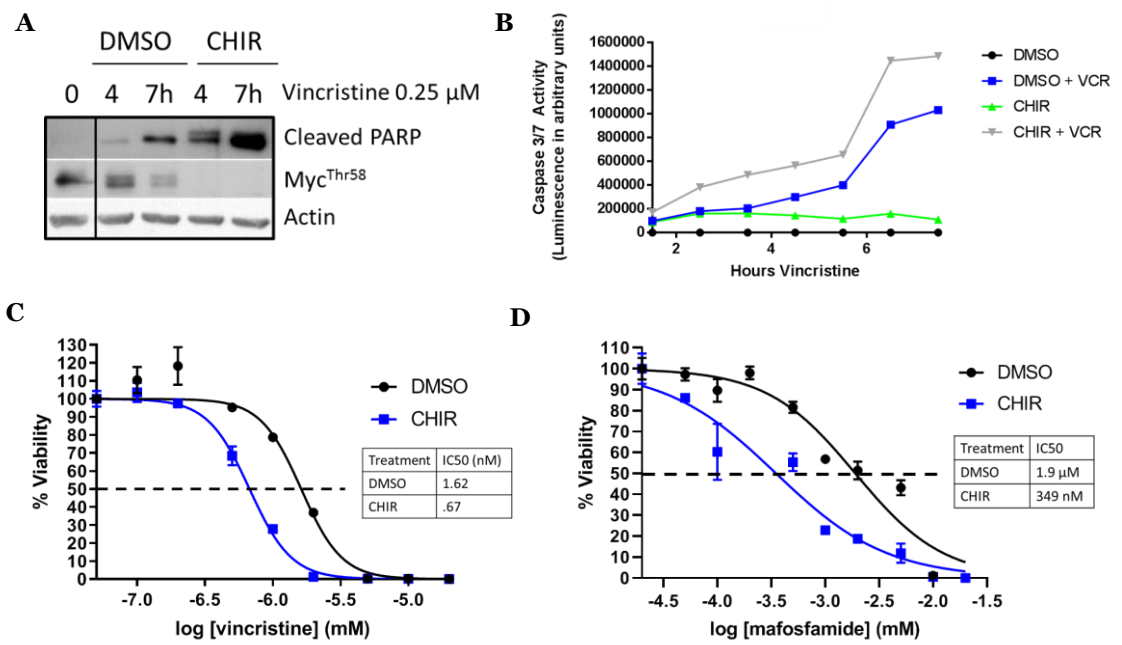

Figure 10. GSK-3 inhibition increases sensitivity to additional chemotherapeutic drugs. **A)** Ramos cells were treated with DMSO or 3 µM CHIR99021 for 2 hours followed by vincristine. Western blotting was performed for cleaved PARP, Myc^{Thr58} phosphorylation, and actin control. **B)** Ramos cells were treated with DMSO or 3 µM CHIR99021 for 2 hours followed by a 7.5 hour time course of .1 µM vincristine. Caspase 3/7 Glo assay was performed and luminescence data points plotted. **C)** Ramos cells were treated with DMSO or 3 µM CHIR99021 and increasing concentrations of vincristine for 72 hours. Cell survival was assessed using CellTiter-Glo and plotted using GraphPad Prism. **D)** Ramos cells were treated with DMSO or 3 µM CHIR99021 and increasing concentrations of mafosfamide for 72 hours. Cell survival was assessed as described in C).

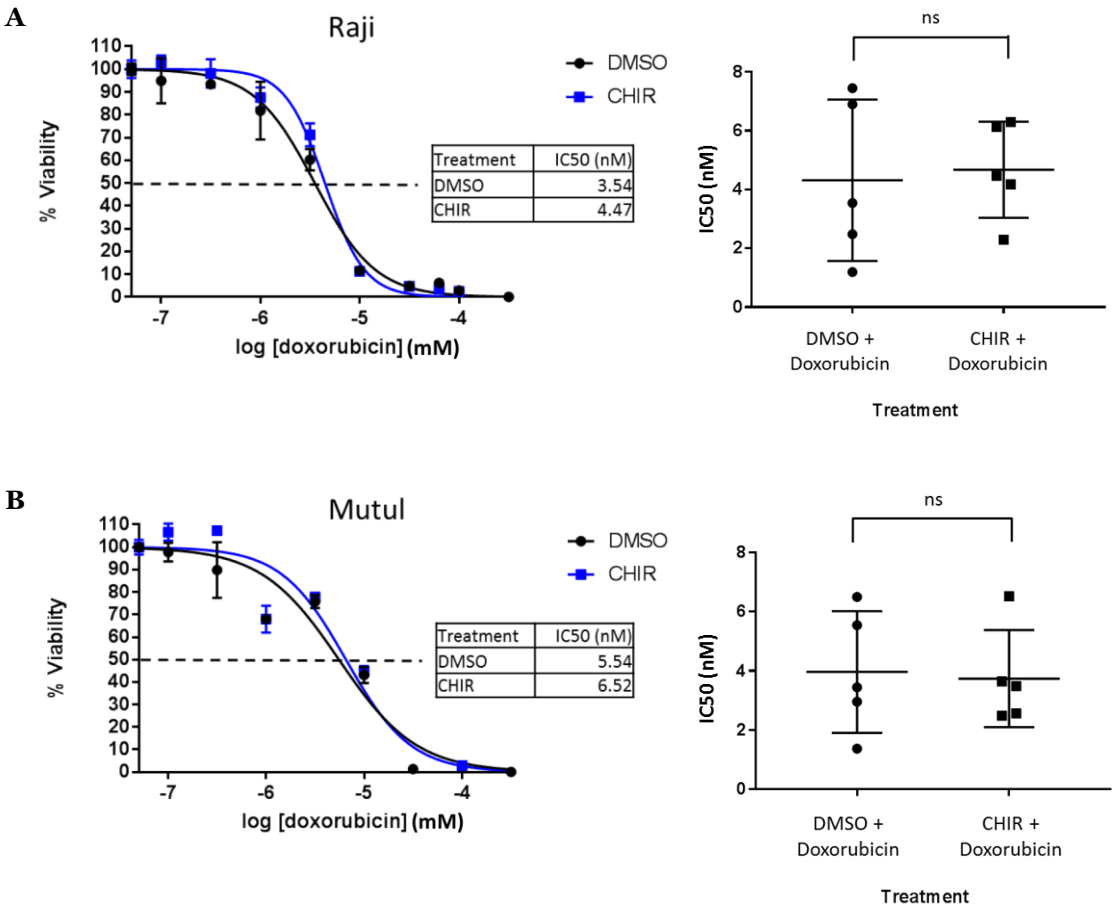

Figure 11. GSK-3 inhibition has no effect on doxorubicin sensitivity in Myc^{Thr58} mutant Burkitt lymphoma cell lines.
A) and **B)** Left: Raji (A) or Mutu1 (B) cells were treated with DMSO or 3 µM CHIR99021 and increasing concentrations of doxorubicin for 72 hours. Cell survival was assessed using CellTiter-Glo and plotted using GraphPad Prism. Right: Graph of means ± SEM analyzed by unpaired t-test for experimental repeats.

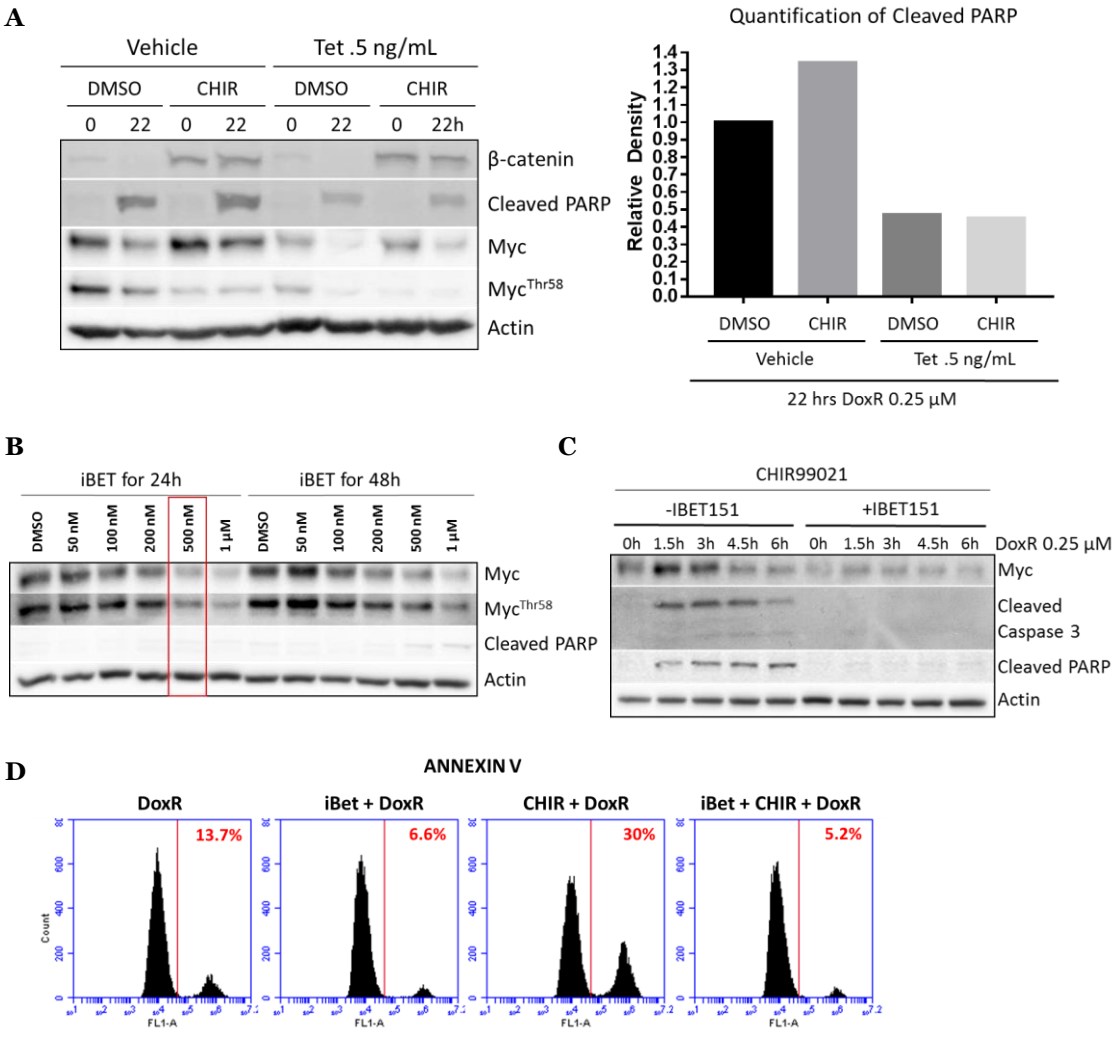

Figure 12. Myc is a key target of GSK-3 responsible for CHIR99021-mediated sensitization to doxorubicin.
A) Left: P493-6 p53shRNA cells were treated with vehicle or tetracycline for 5 hours, followed by 2 hours or DMSO or CHIR and doxorubicin. Western blotting was done for β-catenin, cleaved PARP, Myc, Myc^{Thr58} phosphorylation and actin control. Right: Levels of cleaved PARP were quantified with Image J software and plotted with GraphPad Prism. **B)** Ramos cells were treated with increasing concentrations of iBet-151 or DMSO for 24-48 hours. Myc repression and cell death was assayed by western blotting. **C)** Ramos cells were treated with 500 nM iBet-151 or DMSO for 24 hours followed by 2 hours of 3 µM CHIR99021 and doxorubicin as indicated. Western blotting was performed for Myc and markers of cell death. **D)** Same experiment setup as in C). Annexin V expression was analyzed by flow cytometry after 6 hours of doxorubicin. Gates were drawn based on untreated cells.

GSK-3 inhibition increases sensitivity to chemotherapy *in vivo*

To test anti-GSK-3 adjuvant therapy *in vivo*, we first utilized a previously generated non transgenic p53 conditionally-deficient B-lymphoma model (dubbed 'p53ER/MYC') [130,133] wherein bone marrow cells were isolated from p53ER^{TAM} knock-in mice [149] and transduced with retrovirus expressing constitutively active Myc [150]. We confirmed that CHIR99021 treatment transiently stabilized Myc in p53ER/MYC cells (Fig. 13A). In the context of inactive p53 (cells grown without the estrogen receptor (ER) agonist 4-OHT), there was a notable increase in cleaved PARP and cleaved caspase-3 protein following CHIR + Dox, indicating that Myc stabilization potentiates p53-independent apoptosis in this cell model *in vitro* (Fig. 13B). This pro-apoptotic effect of CHIR99021 was not seen when cells were treated in the context of functional p53 (cells grown in 4-OHT; Fig. 13C). Subsequently, p53ER/MYC allografts grown in mice without 4-OHT treatment were intraperitoneally injected with increasing doses of CHIR99021. Tumors were harvested at 1.5 and 3 hours to probe for Myc levels. An increase in total Myc protein and a loss of Myc-Thr58 phosphorylation was observed at a dose of 100 mg/kg, but not lower doses (Fig. 14A, data not shown). For this reason, 100 mg/kg was the selected dose of CHIR99021 to use in further experiments. P53ER/MYC allografts were then subjected to anti-GSK-3 adjuvant therapy; mice received one intraperitoneal injection of vehicle, CHIR99021, vehicle + Dox, or CHIR99021 + Dox. Tumors were harvested 24 hours later and subjected to IHC staining for cleaved caspase-3. We noted a significant increase in positive cells after CHIR99021 + Dox treatment compared to Dox alone (Fig. 14B, C).

We also developed a patient-derived xenograft (PDX MAP-GR-C95-BL-1) model representing a p53 mutant BL. The model is derived from the pancreatic metastasis of a refractory BL with a TP53 p.Cys135Phe mutation and LOH as well as a MYC p.Pro78Ser mutation and the subclonal presence of a t(8;14) translocation involving Myc. We confirmed the PDX p53 defect by observing minimal induction of p53 protein following Dox (Fig. 15A). We then inhibited GSK-3 in

cultured MAP-GR-C95-BL-1 cells with CHIR99021 or LiCl; both resulted in transient Myc stabilization similar to other Myc WT BL cell lines tested (Fig. 15B, C). As in Ramos cells, CHIR99021 lowered the IC50 for Dox by roughly half a log, and this decrease in IC50 was significant across multiple experiments (Fig. 16A). To test this adjuvant therapy *in vivo*, mice bearing MAP-GR-C95-BL-1 flank xenografts were treated with one intraperitoneal injection of vehicle, Dox, or CHIR99021 + Dox; tumors were harvested 24 hours later and processed for IHC measurement of cleaved caspase-3 positive cells. Upon analysis, CHIR99021 + Dox treated tumors were significantly more positive than Dox alone- or vehicle treated tumors (Fig. 16B). These findings demonstrate that GSK-3 inhibition with CHIR99021 can enhance *in vivo* p53-independent apoptosis in both allograft and PDX models.

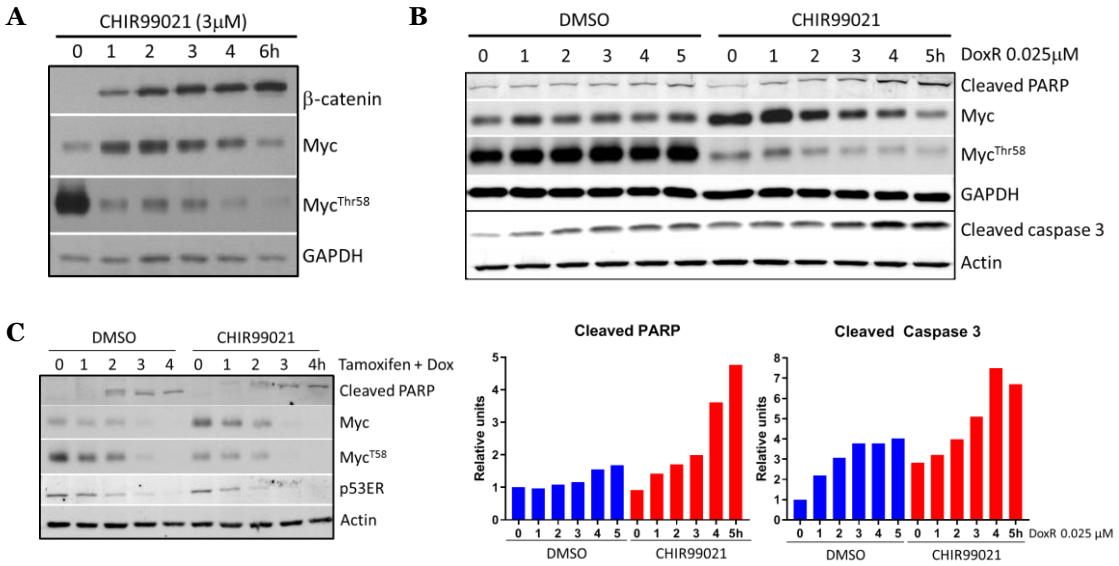

Figure 13. GSK-3 inhibition enhances p53-independent apoptosis *in vitro* in murine model of B-cell lymphoma.
A) p53ER/MYC cells were treated with CHIR99021 as indicated. Western blotting was performed for markers of GSK-3β inhibition. **B)** Top: p53ER/MYC cells were grown without 4-OHT (p53-inactive). Cells were treated with DMSO or 3 μM CHIR99021 for 2 hours followed by doxorubicin as indicated. Western blotting was performed for markers of GSK-3 inhibition, apoptosis, and loading controls. Bottom: Quantification of cleaved PARP and cleaved caspase-3 western blots. **C)** p53ER/MYC cells were treated with DMSO or 3 μM CHIR99021 for 2 hours followed by 250 nM 4OHT and .025 μM doxorubicin as indicated. Western blotting was performed for markers of GSK-3 inhibition, apoptosis, p53ER, and loading control actin.

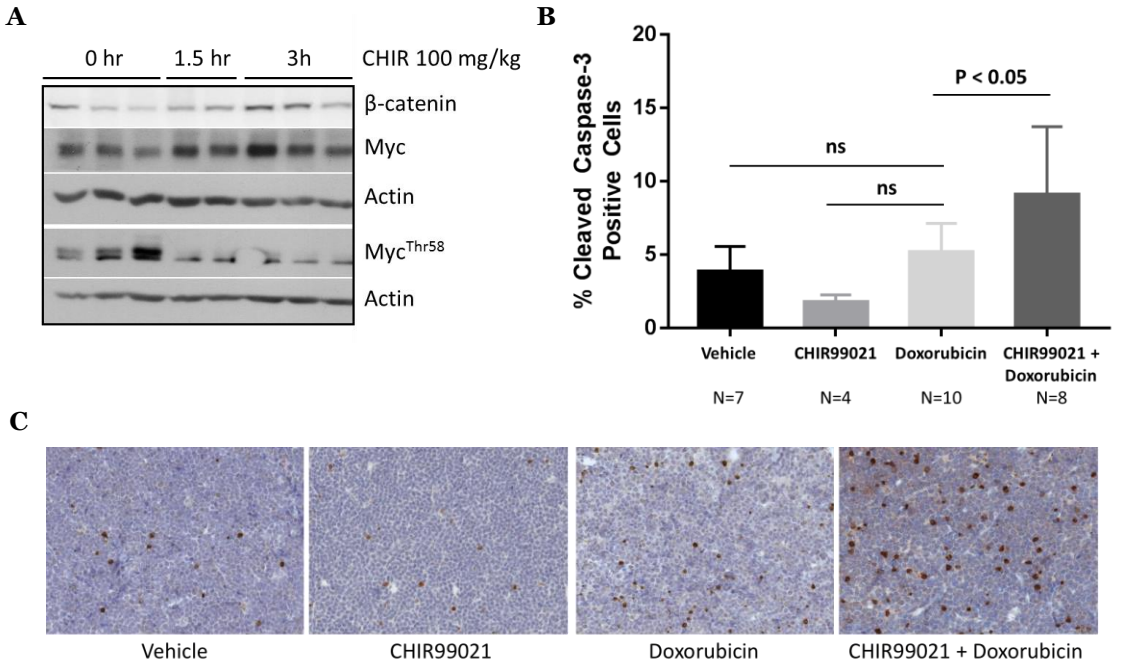

Figure 14. GSK-3β inhibition enhances p53-independent apoptosis *in vivo* in syngeneic murine B-cell neoplasms.
A) F1 hybrid B6129PF1/J mice bearing p53ER/MYC subcutaneous grafts were intraperitoneally injected with vehicle or 100 mg/kg CHIR99021 and tumors were harvested at indicated time points. Western blotting was performed for markers of GSK-3β inhibition and actin loading control. **B)** F1 hybrid B6129PF1/J mice bearing p53ER/MYC subcutaneous grafts were intraperitoneally injected with vehicle, vehicle + 8 mg/kg doxorubicin, 100 mg/kg CHIR99021, or 100 mg/kg CHIR99021 + 8 mg/kg doxorubicin. Tumors were harvested after 18 hours for immunohistochemistry (IHC) staining for apoptosis marker cleaved caspase-3. Graph depicts aperio positive pixel count quantification of cleaved caspase-3 IHC staining for each treatment group (number per group indicated below). Error bars represent mean + SEM analyzed by one-way ANOVA with correction for multiple comparisons. **C)** Representative images of cleaved caspase-3 stains (brown) are shown for each treatment group from B).

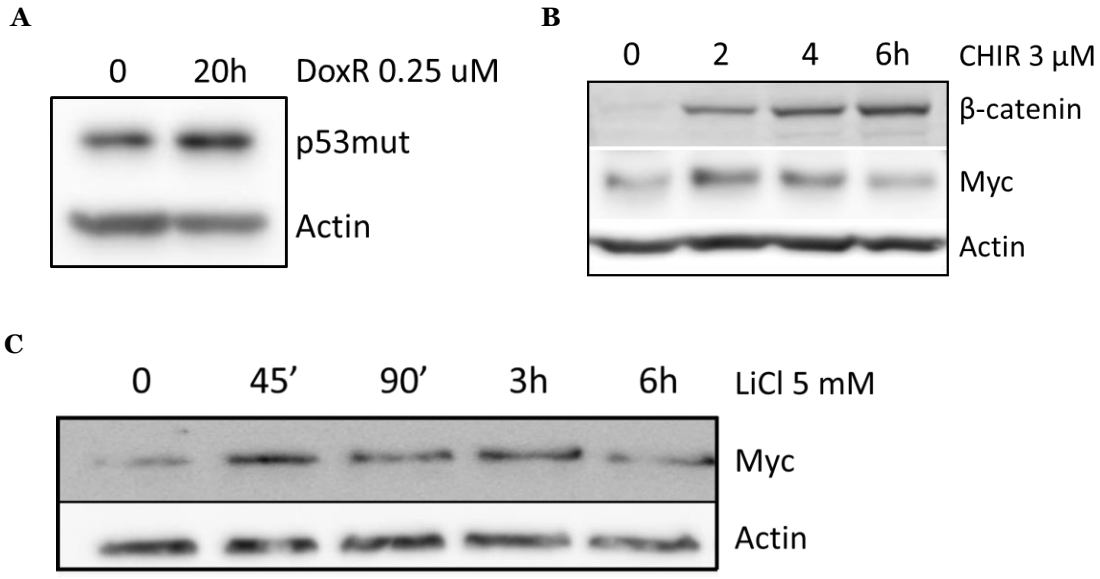

Figure 15. GSK-3β inhibition stabilizes Myc protein in p53 mutant Burkitt lymphoma PDX. **A)** PDX MAP-GR-C95-BL-1 cells were treated with doxorubicin as indicated. P53 induction was measured by western blotting. **B)** PDX MAP-GR-C95-BL-1 cells were treated with CHIR99021 as indicated. Western blotting was performed for β-catenin and Myc. **C)** PDX MAP-GR-C95-BL-1 cells were treated with LiCl as indicated, and Myc levels were assessed by western blotting.

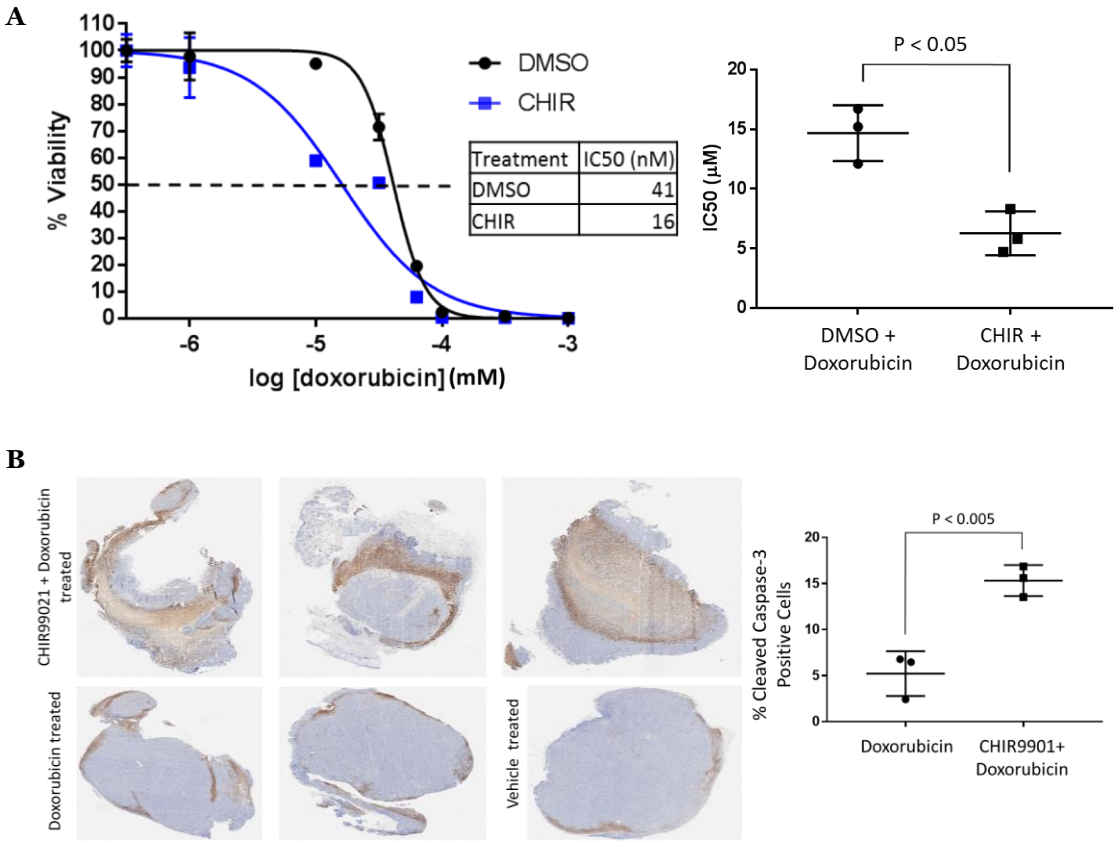

Figure 16. GSK-3β inhibition increases sensitivity to doxorubicin in Burkitt lymphoma PDX. **A)** Left: PDX MAP-GR-C95-BL-1 cells were treated with DMSO or 3 µM CHIR99021 and increasing concentrations of doxorubicin for 72 hours. Cell survival was assessed using CellTiter-Glo and plotted using GraphPad Prism. Right: IC50s of multiple experiments were statistically analyzed by unpaired t-test. **B)** Left: ATHYM-Foxn1nu/nu mice bearing MAP-GR-C95-BL-1 xenografts were intraperitoneally injected with 8 mg/kg doxorubicin or 100 mg/kg CHIR99021 + 8 mg/kg doxorubicin. Tumors were harvested after 24 hours for immunohistochemistry (IHC). Representative images of whole tumors stained for cleaved caspase-3. Right: Aperio positive pixel count quantification of cleaved caspase-3 IHC staining of MAP-GR-C95-BL-1 xenografts was statistically analyzed by unpaired t-test.

Anti-GSK-3 adjuvant therapy modulates members of the extrinsic apoptotic pathway

To determine the underlying mechanism downstream of Myc, we profiled CHIR99021-mediated transcriptional changes by performing RNA-Seq analysis on Ramos cells treated for 0, 3, or 6 hours with CHIR99021. We confirmed that there was a relatively equivalent read count between biological replicates (Fig. 17A) and that the three treatment groups clustered together based on gene expression (Fig. 17B). We then looked for overlap between CHIR99021-induced transcriptome changes and previously reported Myc signatures in two datasets pertaining to p493-6 cells- from microarray profiling ("Psathas Affy" [126]) and array-based nuclear run-on (ANRO) assay ("Dang NRO" [151]). We compared activated genes between the three datasets and found that there were highly statistically significant overlaps between the CHIR99021 and Myc datasets, attesting to the fact that Myc is a key downstream effector of GSK-3 (Fig. 17C).

We then further analyzed our RNA-seq dataset at the single gene level to examine how apoptosis-related genes were being affected. We confirmed that canonical Myc targets, such as ODC1 [20]**,** were being modulated as expected (Fig. 17C). We then visualized up or down-regulated KEGG apoptosis pathway genes (Fig. 17D). Of the significantly altered genes, many were related to extrinsic/death receptor-driven apoptosis, such as up-regulation of RIPK1/TNFR-STK, TRAIL-R4, Death Receptor 4, and down-regulation of CFLAR/FLIP, the negative regulator of extrinsic apoptosis. Extrinsic apoptosis is triggered by binding of death ligands FasLG, TNF, and TRAIL to their cognate receptors Fas, TNFR1, and DR4/DR5, which triggers formation of the death-inducing signaling complex (DISC) with Fadd and caspase-8, leading to activation of caspase-8 and downstream caspases (Fig. 18A). In contrast, intrinsic/mitochondrial apoptotic genes such as BAX, BAK, and NOXA, which are pro-apoptotic proteins involved in facilitating cytochrome C release from the mitochondria to activate downstream caspases, were not significantly altered.

We validated the RNA-sequencing findings in cells treated with both CHIR99021 and Dox via qRT-PCR. Once again, we did not observe differential expression in the examined intrinsic apoptosis genes (Fig. 18B). We then re-examined expression of death receptors (Fas, TNFR1, DR4, and DR5), their cognate ligands (FasLg, TNF, and TRAIL), and CFLAR/FLIP. Largely consistent with our RNA-Seq data, we observed up-regulation of DR4 and DR5, and down-regulation of CFLAR/FLIP (Fig. 18C, yellow arrows); expression of other genes was either absent (FASL; data not shown) or unaffected by CHIR99021. Interestingly, with Dox alone we saw robust upregulation of Fas and TNF, suggesting that chemotherapy alone might engage extrinsic apoptosis to some degree (Fig. 18C).

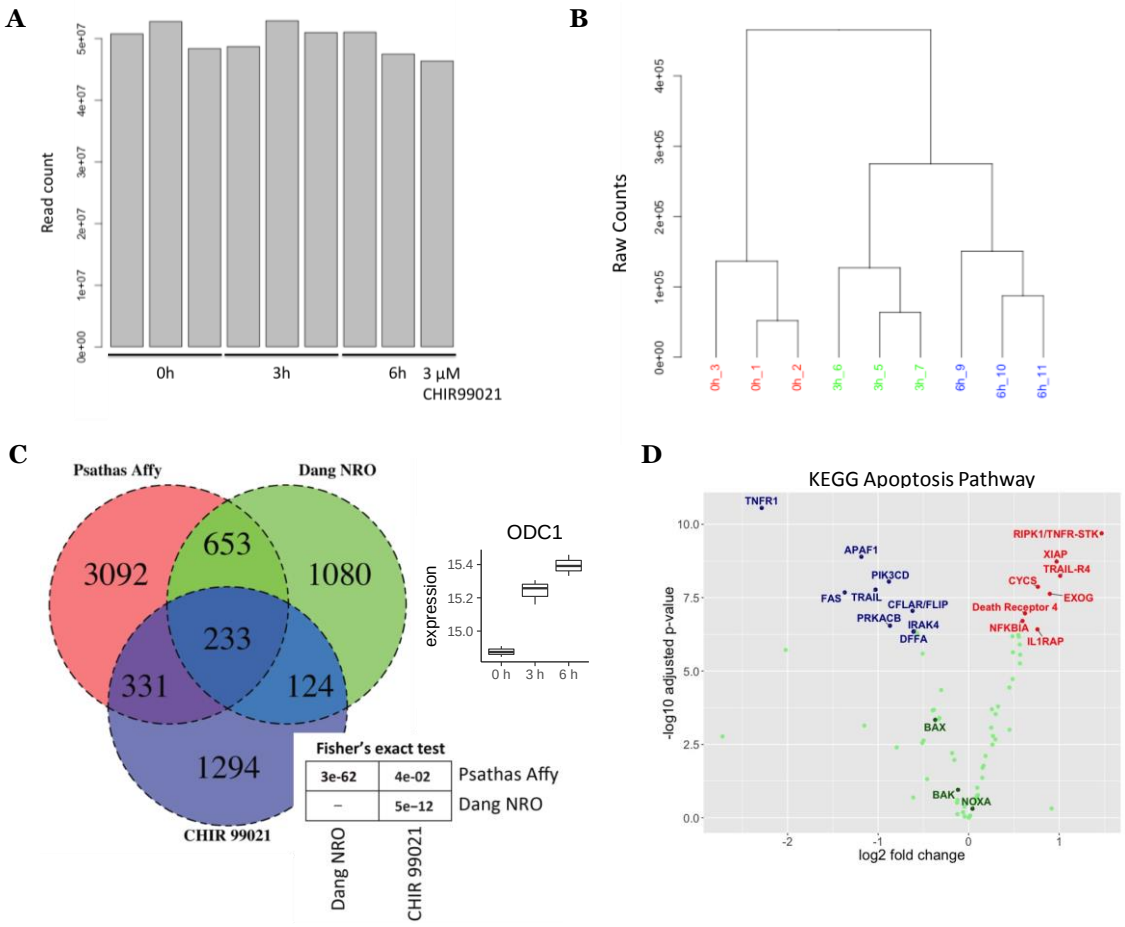

Figure 17. GSK-3β inhibition alters expression of extrinsic apoptosis genes.
A) RNA-sequencing read counts for 0, 3, and 6 hour biological triplicates. **B)** Clustering analysis of RNA-sequencing samples. **C)** Left: Venn diagrams showing overlap of activated genes between three datasets (CHIR99021, Psathas Affy, and Dang NRO). Right: Change in expression level of ODC1 from RNA-sequencing. **D)** Volcano plot of KEGG apoptosis genes derived from RNA-Seq data on Ramos cells treated for 3 hours with 3 μM CHIR99021 in biological triplicates. Key apoptotic genes are labeled, with genes in blue being down-regulated, genes in red being up-regulated, and genes in green having no significant changes.

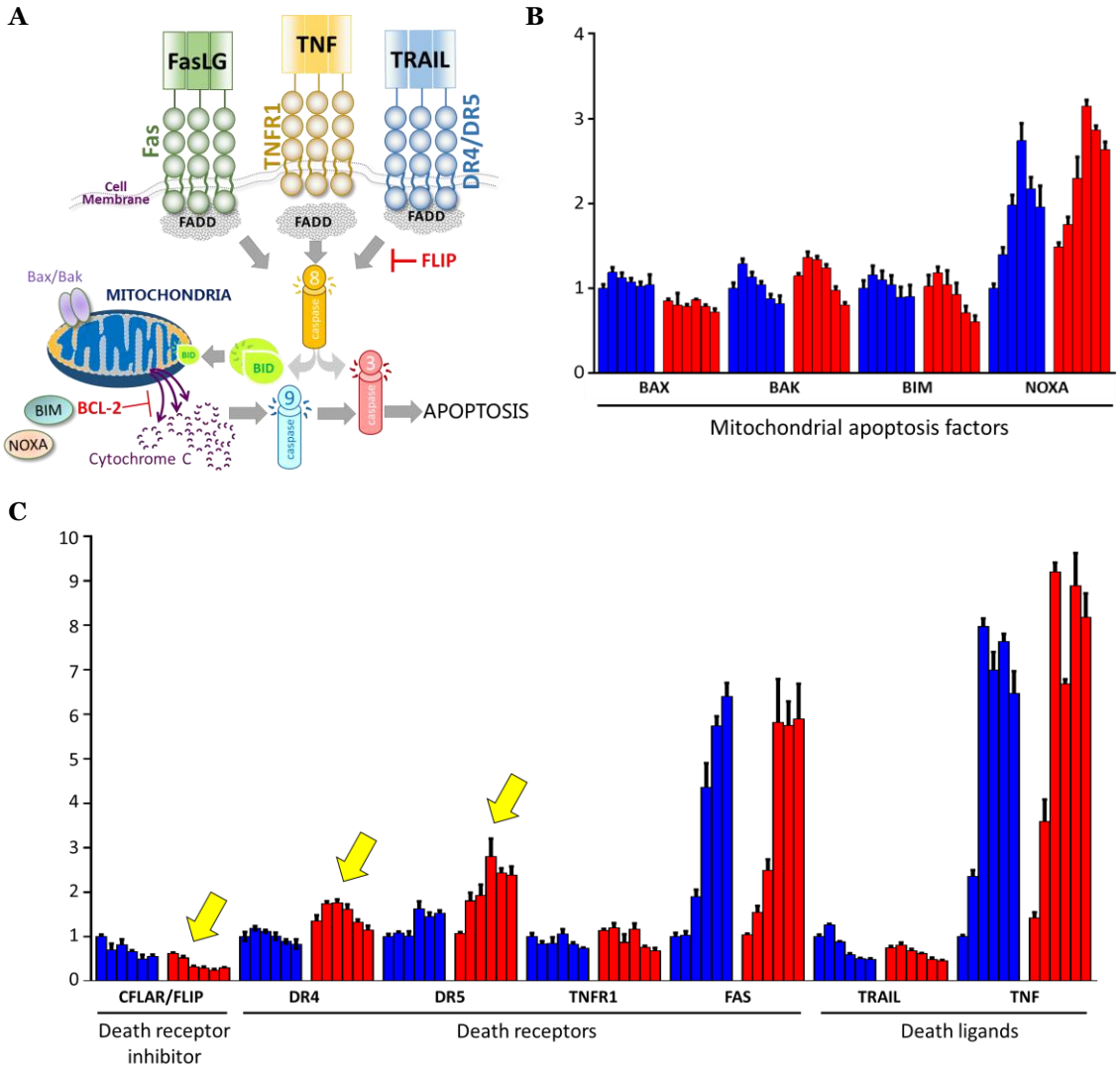

Figure 18. Anti-GSK-3β adjuvant therapy alters expression of extrinsic, not intrinsic, apoptosis genes.
A) Schematic of the extrinsic apoptotic pathway and its interplay with the intrinsic (mitochondrial) pathway. **B)** qRT-PCR expression analysis for known Myc-dependent intrinsic/mitochondrial apoptotic factors was performed on Ramos cells treated for 2 hours with DMSO (blue bars) or 3 μM CHIR99021 (red bars) followed by a 6 hour time course of .25 μM doxorubicin. **C)** qRT-PCR expression analysis for extrinsic apoptosis factors was performed on Ramos cells treated as in B). Notable changes are indicated with yellow arrows.

Anti-GSK-3 adjuvant therapy does not depend on intrinsic apoptosis or necroptosis

To define the role of both apoptotic pathways experimentally, we first over-expressed the pathway inhibitor Bcl-2 in Ramos cells (Fig. 19A). When we compared CHIR99021-aided apoptosis in empty vector and Bcl-2 expressing cells, we observed enhanced PARP cleavage with CHIR99021 pre-treatment in both cell lines (Fig. 19B). Furthermore, we saw significant activation of caspases-3/7 in both empty vector and Bcl-2 cells treated with CHIR99021 + Dox (Fig. 19C), although both basal and GSK3i-aided apoptosis were somewhat reduced by Bcl-2 overexpression, attesting to the involvement of the intrinsic pathway.

We also considered the possibility that necroptosis might be involved in anti-GSK-3 adjuvant therapy, given that RIPK1 was one of the most robustly and significantly altered genes in our RNA-sequencing data from CHIR99021 treated Ramos cells (Fig. 17D). Necroptosis is an alternative mode of programmed cell death that bears resemblance to certain features of both apoptosis and necrosis. RIPK1 is a kinase that contains a death domain which allows it to associate with death receptors in the extrinsic apoptotic pathway, as well as extrinsic apoptosis adaptor proteins [152,153]. However, it is the association of RIPK1 with RIPK3 and downstream phosphorylation of MLKL that triggers necroptosis.

To evaluate whether necroptosis was playing a role in our experimental system, we first looked at the change in RIPK1 RNA following CHIR99021 treatment. From RNA-sequencing, we observed a sharp increase in expression at 3 hours of CHIR99021, which began to taper off by 6 hours (Fig. 20A). This was confirmed by qRT-PCR and western blotting for RIPK1 in Ramos cells treated with 3 μM CHIR99021 for a more detailed time course (Fig. 20B top, C). We also observed an upregulation of MLKL expression in CHIR99021 treated Ramos cells (Fig. 20B, bottom). We then used siRNA to knock down RIPK1 expression in Ramos cells treated with anti-GSK-3 adjuvant therapy. Despite an efficient knockdown, loss of RIPK1 expression had no effect on apoptosis, as

seen by similar levels of cleaved PARP in the siRNA control vs. RIPK1 samples (Fig. 20D). Given that we detected an increase in MLKL expression and that this protein is downstream of RIPK1 in the necroptosis pathway, we wanted to look for activated MLKL in CHIR99021 + doxorubicin treated cells. As a positive control for necroptosis, we used a well-documented system whereby HT-29 colon carcinoma cells are treated with 20 μM of the pan-caspase inhibitor Z-VAD, 20 ng/ml of TNF-α, and 100 nM of the Smac mimetic SM-164, which leads to the induction of necroptosis as identified by detection of MLKL phosphorylation at Thr357/Ser358 [154]. When we ran this positive control alongside Ramos cells treated with CHIR99021 followed by doxorubicin, we were able to detect phosphorylated MLKL in the positive control but not in the other samples, suggesting that necroptosis does not play a contributing role in mediating cell death following anti-GSK-3 adjuvant therapy (Fig. 20E).

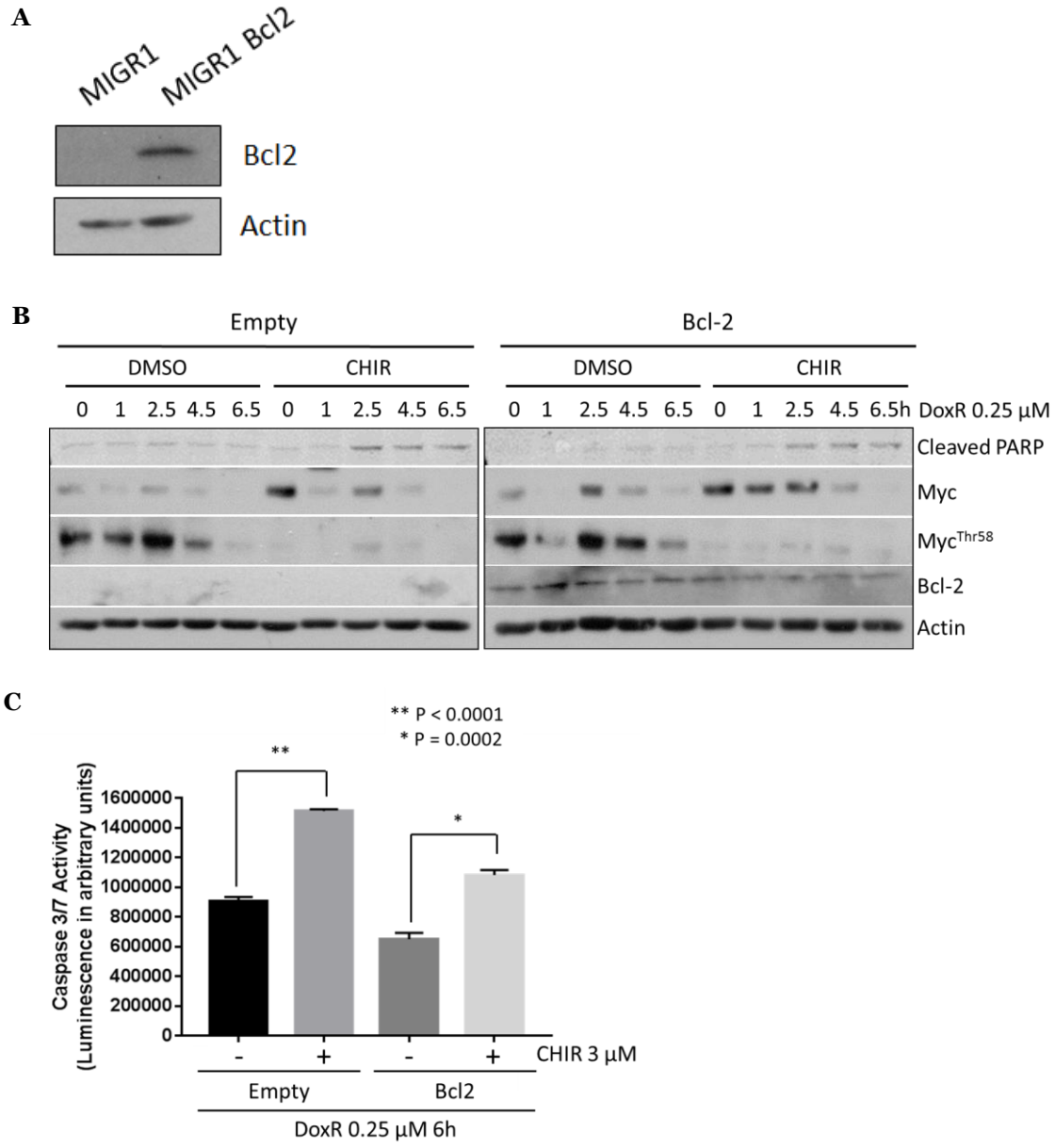

Figure 19. Anti-GSK-3β adjuvant therapy efficacy is unaffected by blocking intrinsic apoptosis. **A)** Western blotting confirming retroviral over-expression of Bcl-2 in Ramos cells. **B)** Ramos cells expressing an empty vector construct or the Bcl-2 construct were treated for 2 hours with DMSO or 3 µM CHIR99021 followed by a 6.5 hour time course of .25 µM doxorubicin. Western blotting was performed for Myc, Myc^{Thr58} phosphorylation, cleaved PARP, and Bcl-2. **C)** Caspase 3/7 Glo luminescence assay was performed on Ramos empty vector or Bcl-2 expressing cells treated as in B). Luminescence was plotted and statistically analyzed by unpaired t-test.

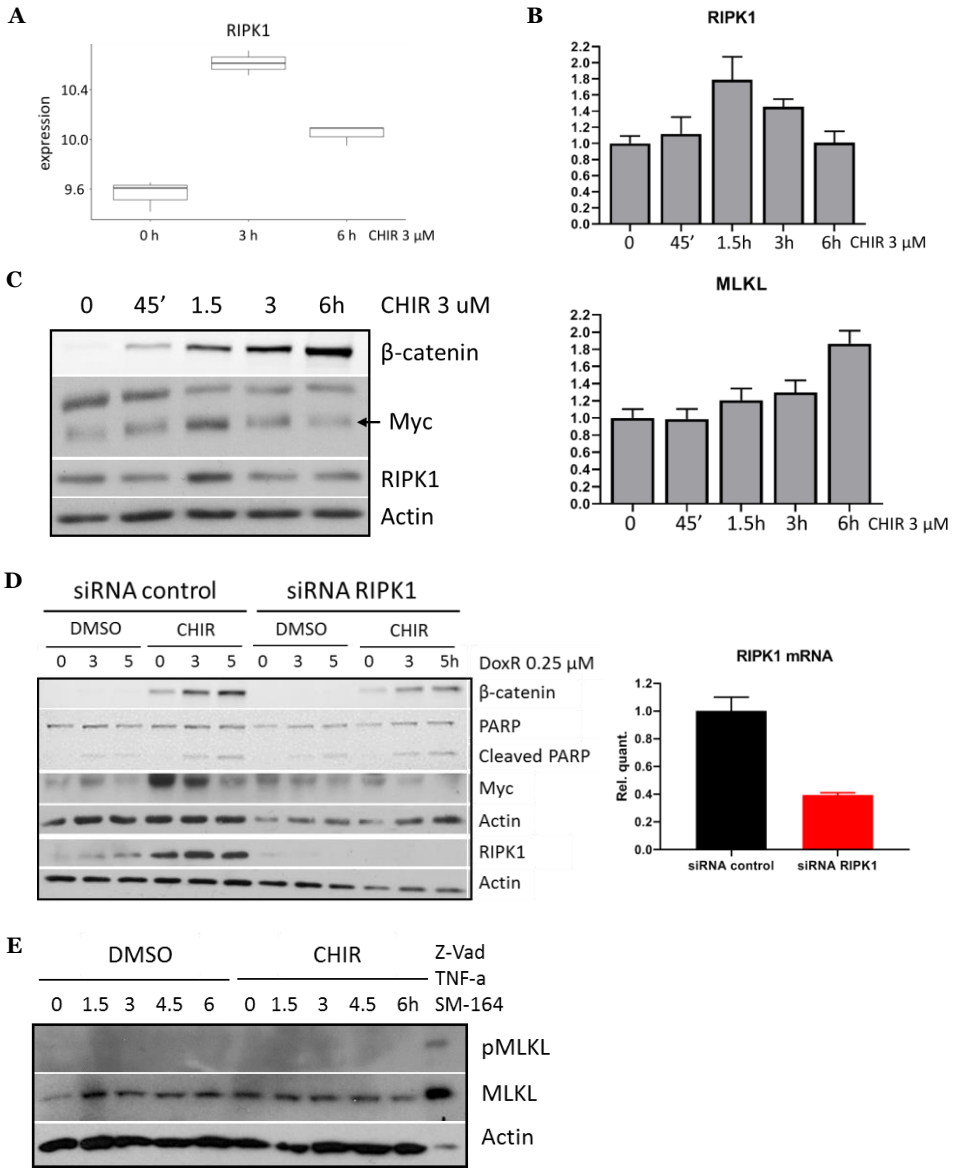

Figure 20. Anti-GSK-3β adjuvant therapy does not engage or rely on necroptosis.
A) Change in expression level of RIPK1 from RNA-sequencing. **B)** qRT-PCR expression analysis for necroptosis pathway members RIPK1 and MLKL in Ramos cells treated with a time course of 3 μM CHIR99021. **C)** Western blotting for RIPK1 protein in Ramos cells treated with a time course of 3 μM CHIR99021. Also probed for markers of GSK-3β inhibition and actin loading control. **D)** Left: Ramos cells were treated with control or RIPK1 siRNA for 24 hours followed by DMSO or CHIR and doxorubicin as indicated. Western blotting was performed for markers of GSK-3β inhibition, apoptosis, RIPK1, and actin loading control. Right: qRT-PCR demonstrating knockdown of RIPK1 mRNA with RIPK1-directed siRNA. **E)** Ramos cells were treated with DMSO or 3 μM CHIR99021 for 2 hours followed by doxorubicin as indicated. A positive control for necroptosis was included (HT-29 cells treated with 20 μM Z-VAD for 30 minutes followed by 7 hours of 20 ng/ml TNF-α and 100 nM SM-164). Western blotting was performed for MLKL, p-MLKL Ser358, and actin loading control.

Anti-GSK-3 adjuvant therapy engages and relies on extrinsic apoptosis

Given that changes in intrinsic apoptosis had limited effects on therapy efficacy and necroptosis was not found to be involved, we tested the contribution of the extrinsic apoptotic pathway. First, cleaved caspase-8, which is specific to extrinsic apoptosis, was higher in CHIR99021 + Dox treated Ramos cells (Fig. 21A). We also found that CHIR99021 treatment downregulated FLIP protein (Fig. 21B). To test the importance of extrinsic apoptosis, we genetically manipulated members of this pathway. First, we knocked down the extrinsic adaptor protein Fadd mRNA using siRNA and subjected the cells to anti-GSK-3 adjuvant therapy. Despite a modest knockdown (~30%, Fig. 21C, left), therapeutic apoptosis was markedly diminished, as evidenced by reduced cleaved caspase-8 (Fig. 21C, right). To corroborate this observation, we overexpressed caspase-8 competitor CFLAR (a.k.a c-FLIP) in Ramos cells (Fig. 22A). FLIP overexpressing cells were functionally tested to have compromised extrinsic apoptosis activity. Compared to empty-vector cells, FLIP expressing cells displayed blunted expression of cleaved caspases 3 and 8 in response to the extrinsic ligand TRAIL (Fig. 22B). In empty-vector cells, apoptosis could be readily induced by anti-GSK-3 adjuvant therapy; however, there was an almost complete abrogation of apoptosis in CFLAR/FLIP-overexpressing cells, as evidenced by a strong reduction in cleaved PARP and cleaved caspase-8 (Fig. 22C). Similarly, we saw no significant increase in activated caspases in CFLAR/FLIP expressing cells compared to empty vector (Fig. 22D).

To analyze individual contributions of death receptors, we used the CRISPR/Cas9 system to knock-out Fas, DR4 and DR5. Short guide RNAs (sgRNAs) for Fas, DR4, DR5, and a scrambled control sequence were cloned into the LentiCRISPRv2GFP lentiviral vector and stably expressed in Ramos cells. GFP-positive cells were isolated and stained for surface expression of the targeted extrinsic receptor; the knockout (KO) lines displayed almost a complete loss of surface expression of each particular receptor compared to the scrambled control (Fig. 23A). Knockout was confirmed by western blot for Fas, DR4, and DR5 protein (Fig. 23B). DR4 and DR5 KO lines were further

characterized to be functional knockouts by comparing the IC50s for 72 hours of TRAIL treatment and observing that both knockouts, but especially the DR4 KO, were resistant to their cognate extrinsic ligand TRAIL compared to the scrambled cell line (Fig. 23C). We began by testing the involvement of the Fas receptor, as it was highly upregulated upon both doxorubicin and CHIR99021 + doxorubicin (Fig. 18C). However, we found that Fas KO did not abrogate the ability of CHIR99021 to sensitize cells to doxorubicin (Fig. 24A). Therefore, we tested the other extrinsic death receptor KO lines. The scrambled cell line 'Scrambled sgRNA', DR4 and DR5 KO lines were treated with DMSO or CHIR and dilutions of Dox for 72 hours. We found that knockout of either DR4 or DR5 did not affect the IC50 of DMSO + Dox compared to the scrambled control; however, in DR4 or DR5 KO lines, CHIR no longer sensitized cells to Dox, as observed across multiple experiments (Fig. 24B).

Consistent with engagement of extrinsic apoptosis, we found that CHIR99021 lowered the IC50 for the DR4/DR5 ligand TRAIL by 1 log (Fig. 25A). Apoptosis in response to TRAIL or CHIR + TRAIL could be blunted by overexpression of FLIP as seen by a reduction in cleaved caspase-3 and -8 expression in FLIP expressing cells compared to empty-vector cells (Fig. 25B). Additionally, we utilized the human DR4 agonist antibody mapatumumab (a.k.a. HGS-ETR1) [155]. Similar to the results with TRAIL, CHIR99021 sensitized Ramos cells to mapatumumab as seen by a half-log reduction in IC50 (Fig. 25C). We wanted to know if DR4 involvement is clinically relevant, so we analyzed 10 Burkitt lymphoma clinical samples for IHC expression of DR4 and compared them to 5 normal tonsils. The tonsillar germinal center showed weak cytoplasmic staining, while the lymphoma samples displayed robust membrane and cytoplasmic staining (Fig. 25D). Collectively these data demonstrate that GSK-3 inhibition potentiates the apoptotic activity of death receptors such as DR4 and reveals the critical dependence of anti-GSK-3 adjuvant therapy on extrinsic apoptosis.

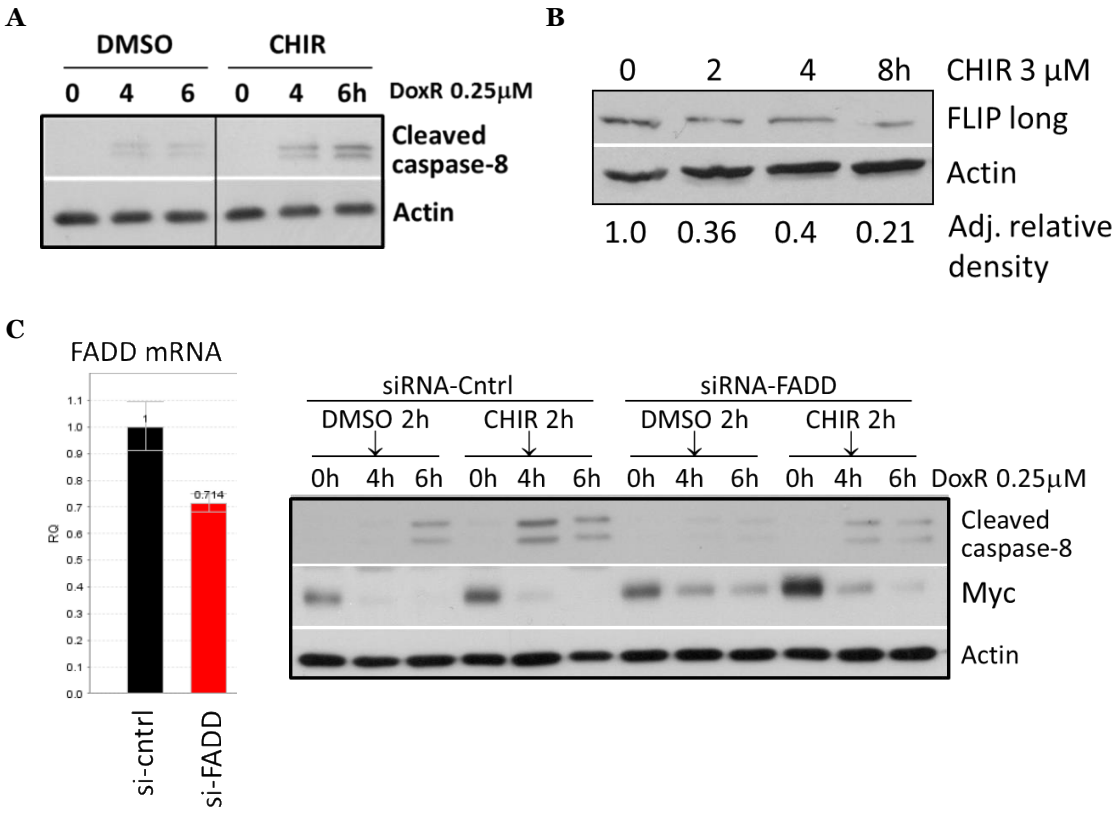

Figure 21. Extrinsic apoptosis is active during anti-GSK-3β adjuvant therapy which is disrupted by knockdown of Fadd.
A) Ramos cells were treated for 2 hours with DMSO or 3 µM CHIR99021 followed by doxorubicin. Cleaved caspase-8 levels were assessed by western blotting. **B)** Ramos cells were treated with a time course of 3 µM CHIR99021 and western blotting was performed for FLIP long and actin loading control. **C)** Left: qRT-PCR demonstrating modest knockdown of FADD mRNA with FADD-directed siRNA. Right: Ramos cells were treated with control or FADD siRNA for 24 hours followed by DMSO or CHIR and doxorubicin as indicated. Western blotting was used to assess activation of caspase-8 and Myc levels.

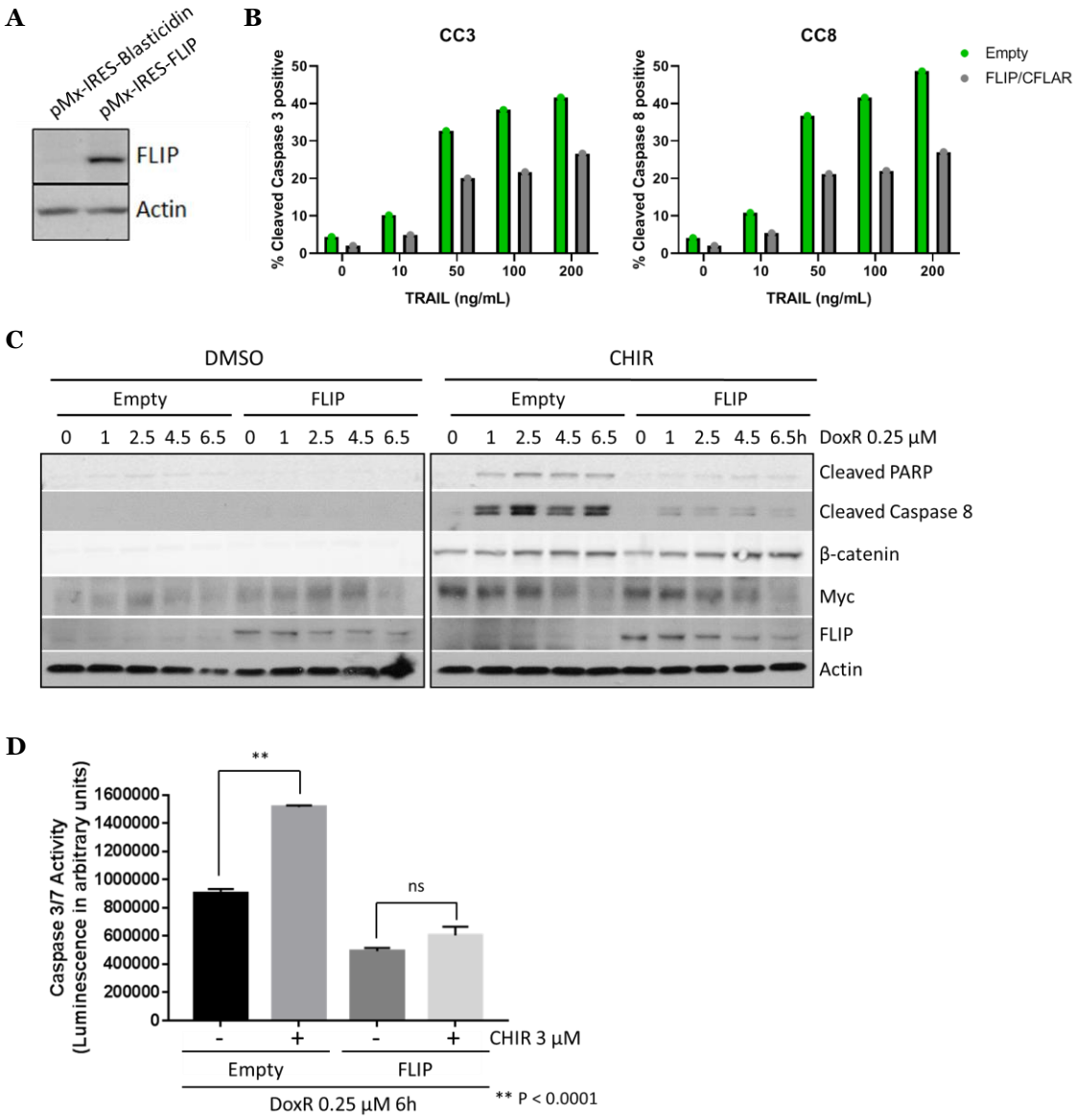

Figure 22. Blocking the extrinsic apoptotic pathway abrogates the pro-apoptotic effects of anti-GSK-3β adjuvant therapy.
A) Western blotting confirming retroviral over-expression of FLIP in Ramos cells. **B)** Ramos empty vector and FLIP expressing cells were treated with increasing concentrations of the extrinsic ligand TRAIL. Cleaved caspase-3 and 8 (CC3 and CC8) expression was analyzed by flow cytometry after 6 hours of treatment; percentages of positive cells are plotted. **C)** Ramos cells expressing an empty vector construct or FLIP construct were treated for 2 hours with DMSO or 3 µM CHIR99021 followed by a 6.5 hour time course of .25 µM doxorubicin. Western blotting was performed for markers of GSK3-β inhibition, cell death, and FLIP expression. **D)** Caspase 3/7 Glo luminescence assay was performed on Ramos empty vector or FLIP expressing cells treated as in C). Luminescence was plotted and statistically analyzed by unpaired t-test.

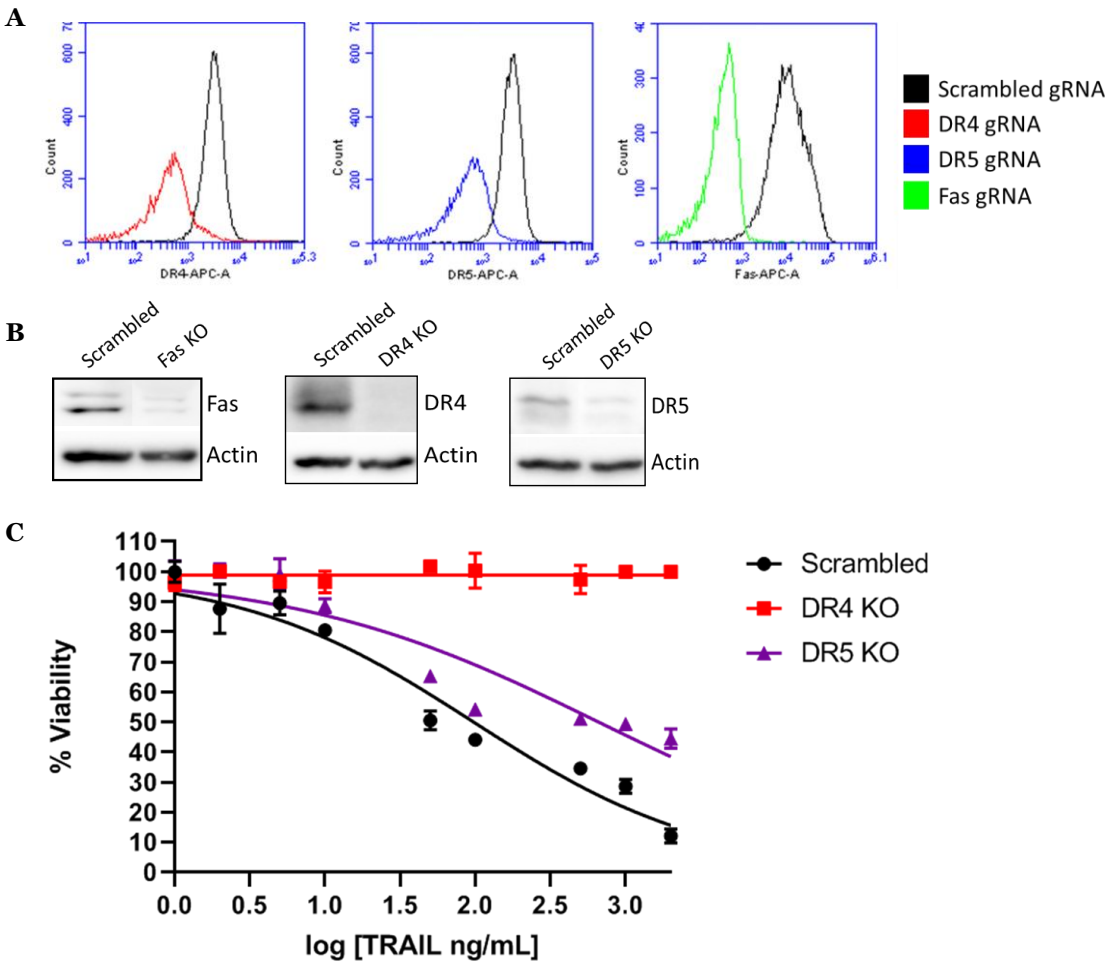

Figure 23. Generation of death receptor CRISPR knockout cell lines.
A) Confirmation of CRISPR knockout of death receptors. Ramos derivatives with scrambled, DR4, DR5, or Fas gRNA were stained for surface expression of DR4 (left), DR5 (middle), or Fas (right) and analyzed with flow cytometry. Gates were set based on scrambled cells stained with IgG-APC control. **B)** Western blotting confirming protein knockout of DR4, DR5, and Fas. **C)** Ramos scrambled gRNA and DR4 or DR5 KO cells were treated with increasing concentrations of TRAIL for 72 hours. Cell survival was assessed using CellTiter-Glo and plotted using GraphPad Prism.

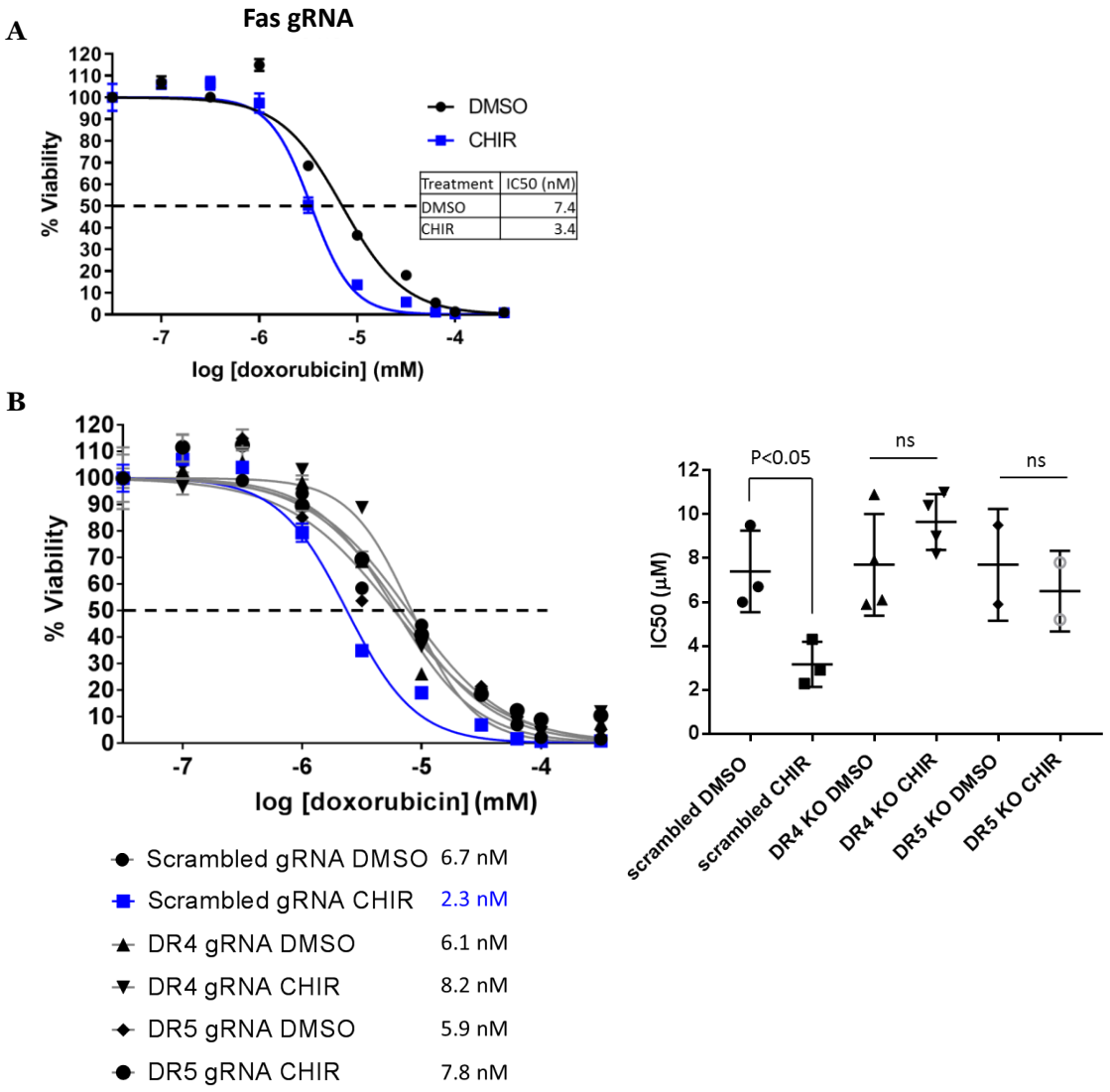

Figure 24. Anti-GSK-3β adjuvant engages and relies on the extrinsic apoptotic pathway.
A) Ramos Fas KO cells were treated with DMSO or 3 µM CHIR99021 and increasing concentrations of doxorubicin for 72 hours. Cell survival was assessed using CellTiter-Glo and plotted using GraphPad Prism. **B)** Left: Ramos derivative cell lines with scrambled gRNA, DR4 gRNA, and DR5 gRNA were treated and cell survival assessed as in A). IC50s of the curves are indicated below. Right: IC50s of multiple experiments as done on the left were statistically analyzed by unpaired t-test.

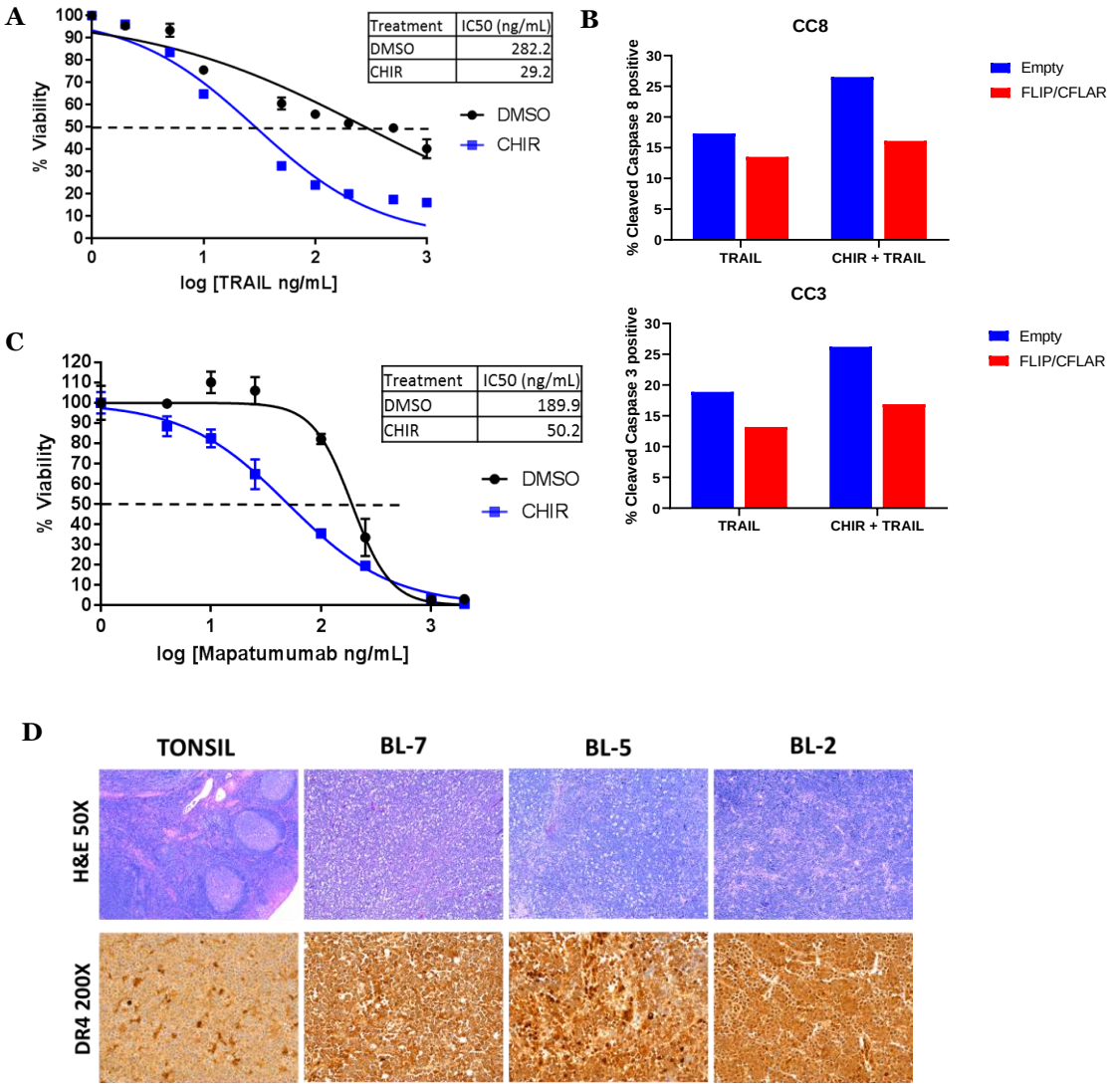

Figure 25. GSK-3β inhibition sensitizes to direct engagers of extrinsic apoptosis.
A) Ramos cells were treated with DMSO or 3 μM CHIR99021 and increasing concentrations of TRAIL for 72 hours. Cell survival was assessed using CellTiter-Glo and plotted using GraphPad Prism. **B)** Ramos empty vector and FLIP expressing cells were treated with DMSO or 3 μM CHIR99021 and 50 ng/mL TRAIL for 6 hours. Cleaved caspase-8 and 3 (CC8 and CC3) expression was analyzed by flow cytometry; percentages of positive cells are plotted. **C)** Ramos cells were treated with DMSO or 3 μM CHIR99021 and increasing concentrations of the DR4 agonist antibody mapatumumab for 72 hours. Cell survival was assessed and plotted as in A). **D)** Immunohistochemical staining was performed on human Burkitt lymphomas or normal tonsils. Representative images of hematoxylin and eosin (H&E) and DR4 stains at indicated magnification.

Discussion

Our studies using murine allografts, human Burkitt lymphoma cell lines and PDXs demonstrate the benefits of adding GSK3 inhibitors to chemotherapeutic drugs in the R-CHOP/EPOCH-R regimens. They also firmly implicate Myc as the key downstream target of GSK-3 and a master regulator of chemosensitivity in refractory B-cell lymphomas. Finally, we have learned that Myc-dependent chemosensitivity relies on the extrinsic apoptotic pathway, with direct involvement of death receptors such as DR4, whose ligands and agonists function better when GSK-3 is inhibited and Myc is stabilized (Fig. 26). All three key conclusions would be impossible to predict in theory because both GSK-3 and Myc have multitudes of targets with non-overlapping and often conflicting functions.

The literature on the role of GSK-3 in modulating apoptosis is complex, with some evidence that GSK-3 inhibits the extrinsic apoptotic pathway [reviewed in [156]]. For example, GSK-3β was found to localize to extrinsic apoptotic receptors DR5/TRAIL-R2, DR4/TRAIL-R1, and Fas; GSK-3 was shown to be part of an anti-apoptotic complex that also contained the anti-apoptotic proteins DDX3 and cIAP-1, and inhibition of GSK-3 lead to increased apoptosis following extrinsic receptor stimulation [157]. Conversely, GSK-3 potentiates the intrinsic pathway through mechanisms such as facilitating pro-apoptotic disruption of the mitochondria and increasing intrinsic pro-apoptotic family members like p53 and Bcl-2 [reviewed in [156]]. Thus, its overall contribution to cell survival in the face of genotoxic therapy remains controversial and likely cell type-specific. A 2008 study demonstrated that GSK-3 inhibition in glioblastoma multiforme results in decreased NF-κB activity [158]**.** Simultaneously, another group reported the beneficial effects of targeting GSK-3 in a preclinical murine model of MLL leukemia, with the underlying mechanism being stabilization of the cyclin-dependent kinase inhibitor p27 [159]. Another firmly established GSK-3 target is the tumor suppressor PTEN, which is phosphorylated by GSK-3 on Thr-366 and Ser-362 [160]. While Thr366

phosphorylation is thought to lead to PTEN destabilization [161], the contribution of Ser-362 phosphorylation to PTEN function is not known. Given that this tumor suppressor is known to contribute to both intrinsic survival pathways [48] and the extrinsic cell death pathways [162,163], the overall effect of GSK-3 inhibition on therapeutic apoptosis in B-lymphoid malignancies would have been difficult to predict with certainty. The fact that one of its key targets Myc has manifold effects on tumor cell survival only adds to the complexity of this system.

The role of Myc in cell death has been incompletely understood, despite the large amount of published studies. While Myc is best known to induce p53-dependent, intrinsic apoptosis, Myc has also been linked to the extrinsic pathway. Notably, it has been shown to participate in apoptosis induced by CD95/CD95L (Fas/FasL) [79] as well as TNFα [164]. Earlier work from our group in hypoxic solid tumors reported the relationship between inhibition of GSK-3β and subsequent increase in Myc and enhanced apoptosis in response to TRAIL [165], at least in part through the propensity of Myc to directly inhibit the extrinsic apoptosis negative regulator CFLAR/c-FLIP [80,166]. In parallel, in some solid cancers Myc elevates expression of the death receptors DR4 and DR5 and the extrinsic ligand FasL [81,82,167]**.** While these data, in particular regarding CFLAR/c-FLIP, are consistent with the pro-apoptotic function of Myc, there are reports challenging the notion that there is a linear correlation between FLIP levels and TRAIL resistance [see for example [168]]. In addition, our RNA-Seq experiment demonstrated that in Myc-stabilized cells other transcripts went in the opposite, pro-survival direction, with strong downregulation of pro-apoptotic genes TNFR1, Fas, and TRAIL, and significant upregulation of anti-apoptotic genes XIAP and the decoy death receptor TRAIL-R4. Thus, one could have predicted that stabilization of Myc would limit cell death and by inference confer chemoresistance – or that the effects of Myc on the extrinsic pathway would be irrelevant in the context of genotoxic chemotherapy.

Traditionally, chemoresistance is seen as a failure of the intrinsic pathway. This view is based on the fact that many pro- and anti-apoptotic members of the intrinsic pathway are altered in cancer. For example, IAPs (inhibitors of apoptosis proteins) frequently confer survival to

neoplastic cells, especially when overexpressed in tumor cells [169]. In pediatric B-cell malignancies, IAP has been identified as a valid therapeutic target and inhibitors against this target are being investigated in combination with other anti-tumor agents [170]. Furthermore, the expression and mutation status of Bcl-2 family members is predictive of responses to chemotherapy prognosis: both mutations in the pro-apoptotic gene BAX and over-expression of BCL-2 are common in many cancer types [171]. Therefore, the small molecular inhibitor of Bcl-2 venetoclax has shown considerable promise in preclinical and clinical trials, including those involving B-lymphoid malignancies [172].

Despite an established role for intrinsic apoptosis in resistance to chemotherapy, there is also a body of evidence that points to the importance of extrinsic apoptosis for responses to chemotherapy. Published data show that signaling through the death receptor CD95/Fas is critical for chemosensitivity [173]. Conversely, resistance to chemotherapy in leukemia and other cancers can be attributed to downregulation of this death receptor [102]. In addition, mutations in CD95 have been identified in many solid and hematopoietic tumors [reviewed in [104]]. Finally, upregulation of CFLAR/c-FLIP and its increased recruitment to CD95 has been observed in response to various chemotherapeutics in B-ALL and in fact is a resistance mechanism to chemotherapy treatment [174]. Utilizing Ramos Burkitt lymphoma cells, we observed robust upregulation of Fas mRNA in response to treatment with Dox, while there were minimal changes in intrinsic apoptosis genes. Over-expression of Bcl-2 conferred a very modest decrease in Dox induced apoptosis (~30% inhibition of caspase 3/7 activity). In contrast, we observed a sharp increase in chemoresistance via overexpression of CFLAR/c-FLIP or by CRISPR/Cas9 knockout of extrinsic death receptors DR4 or DR5. These data support the notion that extrinsic apoptosis is engaged by chemotherapy treatment and disruption of this pathway can lead to chemoresistance.

Data presented throughout the paper suggest that even in the absence of p53, stabilized Myc belongs firmly on the “cell death” side. Notably, when we inhibited Myc transcription with the Brd4 inhibitor iBet-151 at a sub-lethal concentration, there was actually a reduction in GSK3i-aided

apoptosis. Resistance to apoptotic stimuli was also observed when we shut off Myc transcription in a cell model bearing tetracycline-repressible Myc. Thus, in the context of chemotherapy regimens, inactivation of Myc would be counterproductive, as Myc potentiates doxorubicin-induced cell death by engaging extrinsic apoptosis. This observation adds a new wrinkle to the prevailing view that Myc contributes to B-lymphoma cell survival in the face of chemotherapy [see for example [175]].

As established through previous studies, there are thresholds for MYC that govern whether it will act in a pro-survival or pro-apoptotic manner. Because MYC stabilization will only enhance apoptosis in cells with MYC overexpression, the transient increase in MYC in non-tumor cells should not have negative effects. EPOCH-R and other chemotherapy regimens used to treat BL can result in both damage to tumor cells but also to dividing normal tissue as well. Doxorubicin in particular can induce cardiomyopathy through numerous proposed mechanisms [176]. We have shown here that GSK-3 inhibition increases sensitivity to doxorubicin, suggesting that lower doses of doxorubicin could be used to achieve the same clinical efficacy, thus having less off-tumor harmful effects.

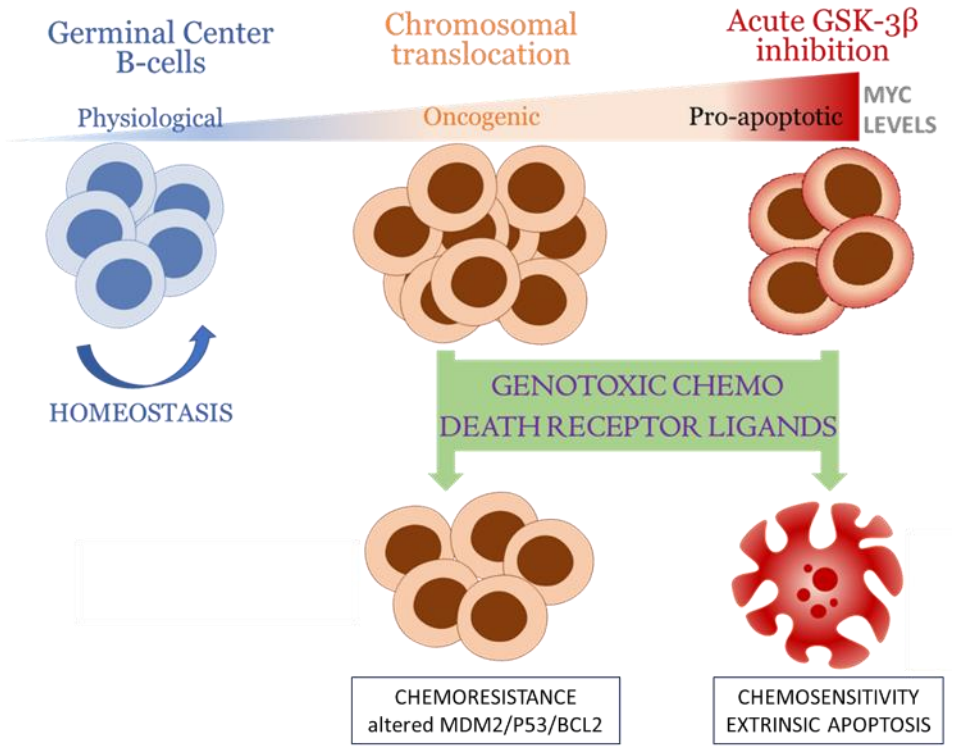

Figure 26. Model of sensitization of B-cell lymphomas to therapeutic agents by GSK-3 inhibition and stabilization of Myc.

CHAPTER 4: Conclusion and Future Directions

Improving Therapeutic Responses in B-Cell Lymphomas

Burkitt lymphoma (BL) is an aggressive subtype of Non-Hodgkin lymphoma that arises from germinal center B-cells [177]. It was first designated as a neoplasm and subtype of lymphoma in 1961 [178]. BL is characterized by translocations involving MYC on chromosome 8 with immunoglobulin (Ig) enhancers, typically the Ig heavy chain enhancer on chromosome 14, but less commonly to Ig light chain loci, IgK or IgL [119,179]. There are three epidemiological variants of BL: sporadic, endemic, and HIV associated. HIV-associated BL is infrequently associated with Epstein-Barr virus (EBV), and sporadic BL even less so (1-2%), however almost all of endemic BLs are EBV positive [180]. EBV contributes to the pathogenesis and survival of BL cells. It is hypothesized that EBV does this through increasing the likelihood of a chromosome translocation involving MYC and other genetic changes that drive tumorigenesis. It is also thought that EBV can support transformation by promoting the survival of cells bearing mutations that would otherwise lead to cell death and also by supporting cell survival in the absence of B-cell receptor survival signals. Aside from the MYC translocation, there are other common genetic signatures to Burkitt lymphoma. Sequencing of BL tumors identified mutations in P53, a well-established tumor suppressor with a role in the development of BL, as well as mutations in other genes that are less well studied or unstudied in BL. These include frequent mutations of ID3, chromatin remodelers SMARCA4 and ARID1A, and CCND3 [45,181]. Current studies are underway to evaluate the role of these frequently mutated genes in the pathogenesis of BL.

Clinically, BL is treated with intense, high-dose chemotherapy regimens, which can often lead to further toxicities. First line therapy for BL consists of cycles of chemotherapy drugs such as cyclophosphamide, vincristine, dexamethasone, and doxorubicin [182]. For patients with more

advanced disease, treatment regimens will include the addition of methotrexate, cytarabine, and occasionally the immunotherapy drug rituximab, a CD20 monoclonal antibody [183]. With these therapy regimens, a 3-year overall survival rate of over 80% can be achieved [184]. Despite the success of this first line therapy for most patients, those patients who relapse and become refractory to these treatments have a very poor prognosis and dismal survival rates [185,186]. Therefore, there is an unmet clinical need to identify therapies to improve the survival of this chemoresistant patient population.

The results of this study suggest several new ways to improve upon standard-of-care therapies for Myc-driven B-cell lymphomas. First, our data suggest that the addition of a GSK-3 inhibitor (LiCl, CHIR99021, or tideglusib currently in Phase II clinical trials for Alzheimer's disease) could enhance the response to chemotherapy even in cells where the intrinsic apoptotic pathway is suppressed [187]. Two such subtypes of B-cell lymphoma associated with poor response to therapy are double- and triple hit lymphomas (Myc and Bcl-2/Bcl-6 translocated) [188] as well as non-translocated lymphomas double-positive for Myc and Bcl-2 [189]. Double hit lymphomas can present with a variety of morphologies including acute lymphoblastic leukemia or lymphoma (ALL), diffuse large B-cell lymphoma (DLBCL), and rarely follicular lymphoma (FL) [190,191]. For triple-hit lymphomas, which are not as prevalent as double-hit, the immunophenotype tends to be that of germinal center B-cells, with most cases presenting as DLBCL or an unclassifiable B-cell lymphoma that is similar to BL [192]. The overall 5 year survival rate for these double and triple hit lymphomas fall around 50% [193]. Thus, there is much room for clinical improvement in the therapeutic targeting of these highly aggressive lymphomas.

Preliminary data in DLBCL cell lines show that GSK-3 inhibition modestly sensitizes MYC rearranged, P53 mutant, and Bcl-2 rearranged OCI-LY8 cells to doxorubicin (Fig. 27A). Additionally, in the MYC rearranged, P53 mutant DLBCL cell line Karpas 422, GSK-3β inhibition results in Myc stabilization (Fig. 27B) and deregulation of extrinsic apoptosis genes similar to what we saw in BL cell lines (Fig. 27C). These preliminary experiments will be expanded upon in further

studies, but initially indicate that GSK-3 inhibition could be a viable method to increase chemosensitivity in DLBCL.

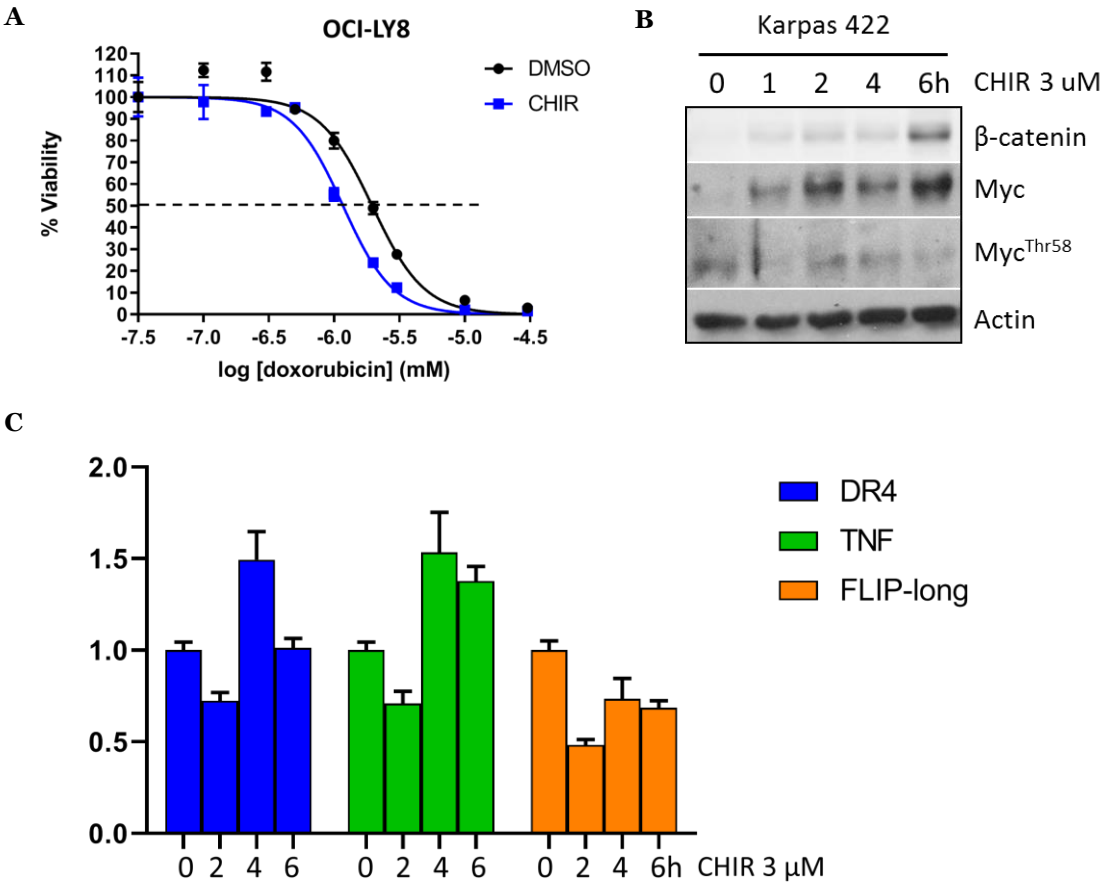

Figure 27. GSK-3 inhibition in MYC/Bcl-2 double hit lymphomas. **A)** DLBCL OCI-LY8 cells were treated with DMSO or 3 µM CHIR99021 and increasing concentrations of doxorubicin for 72 hours. Cell survival was assessed using CellTiter-Glo and plotted using GraphPad Prism. **B)** DLBCL Karpas 422 cells were treated with 3 µM CHIR99021 for a 6-hour time course. Western blotting was performed for β-catenin, Myc, Myc^{Thr58} phosphorylation and actin control. **C)** qRT-PCR expression analysis for extrinsic apoptosis factors performed on Karpas 422 cells treated with 3 µM CHIR99021 for a 6-hour time course.

Our findings that anti-GSK-3 adjuvant therapy engages extrinsic apoptosis provides a rationale for revisiting clinical trials of soluble TRAIL or agonistic antibodies targeting DR4 and DR5. Compared to the other extrinsic ligands, tumor cells were found to have a specific sensitivity to TRAIL-induced apoptosis over normal tissues [194,195]. Trials with recombinant TRAIL demonstrated safety and tolerability but there was no observed anti-cancer activity in combination with standard-of-care for the cancer types treated. Similarly, with trials using agonistic TRAIL receptor antibodies in combination with standards-of-care, there was a trend towards anti-cancer activity but no statistically significant results [196]. However, GSK-3 inhibition and ensuing Myc stabilization could make tumor cells more susceptible to the pro-apoptotic actions of TRAIL or death receptor targeting antibodies such as mapatumumab [197]. The potential to re-purpose the FDA approved GSK-3 inhibitor lithium chloride makes this adjuvant therapy strategy particularly viable as the process to transition this psychiatric drug to cancer therapy would be relatively unchallenging. Long-term usage of lithium chloride is not correlated with an increase in cancer incidence so it appears to be a safe adjuvant [198].

Limitations to Oncogene Targeting as a Therapeutic Strategy

Therapeutic targeting of initiating oncogenes is the mainstay of precision medicine. It is thought to be most effective in cancers with a single dominant genetic event, of which Burkitt lymphoma is a prime example. The rationale for targeting cancer oncogenes is based on the phenomenon known as "oncogene addiction" [199]. Oncogene addiction can be described as a tumor's dependency upon one protein or signaling pathway. These oncogenic proteins and pathways are poised as valuable therapeutic targets because normal cells should not exhibit this cancer-specific dependency; thus, cancer cells can be specifically killed while leaving normal tissue mostly unharmed. As one of the first identified oncogenes, tumor cell addiction to Myc has also been described such that brief inactivation of Myc leads to a reversal in tumorigenesis [57]. Oncogene addiction has also been described for other oncogenes like RAS, HER2, and certain kinases that are frequently altered in cancer [200]. Many tyrosine kinase inhibitors have been clinically approved, yet the clinical responses for these targeted therapies are often short-lived and followed by disease relapse. Thus, acquired drug resistance to targeted therapies is a frequent short-coming of this treatment strategy. Drug resistance tends to arise by two main mechanisms, with the first being the acquisition of mutations in the target that preclude binding of the drug [201]. An alternate mechanism of resistance arises when tumor cells activate a redundant survival pathway to compensate for the presence of the oncogene-targeting drug and inhibition of the main pathway being targeted [202].

In addition to the issue of drug resistance that arises upon targeting of oncogenic pathways, one must address the paradoxical nature of oncogenes and their dual promotion of pro-survival and pro-apoptotic pathways. Other oncogenes in addition to MYC can promote apoptosis. Following premature entry into the S phase of the cell cycle, the transcription factor E2F1 can activate apoptosis in conjunction with p53 [203]. Extensive work has uncovered how RAS induces apoptosis with a number of interacting partners [204]. In clinical trials for oncogene-targeted therapies, compounds are frequently tested as monotherapies. It may be more relevant or realistic to conduct

a trial where new therapies are combined with the standard of care to determine how the two will function together. In the case of Myc, therapies that aim to inhibit Myc function might have some level of efficacy on their own, as exemplified by BRD4 inhibitors currently in clinical trials [205]. But given what we know about Myc and its ability to engage apoptosis, compounds that inhibit MYC could end up having no effect or worsening the effects of standard chemotherapies, which inherently rely on engaged apoptotic signaling. Thus, the opposing pro-survival and pro-apoptotic nature of many oncogenes complicates the incorporation of targeted therapies into current therapeutic regimens and warrants further studies.

MYC Stabilization and the Cooperation with Additional Anti-Cancer Agents

In this study we have evaluated the cooperation between Myc stabilization and chemotherapy drugs that are part of the clinical regimens for BL, as well as ligands for extrinsic apoptosis receptors. However, there are many varieties of chemotherapy and other anti-cancer drugs that warrant the evaluation of their interaction with stabilized Myc. Chemotherapy drugs target the cell cycle at different points and have different mechanisms of action and could cooperate differently with a Myc-driven apoptotic program. Many chemotherapeutics cause cell death by inducing DNA damage. Alkylating agents or platinum-based drugs, such as cyclophosphamide and cisplatin, add alkyl groups to guanine bases to prevent formation of normal DNA secondary structures which leads to DNA damage. Anthracyclines like daunorubicin or doxorubicin intercalate into DNA and interfere with DNA replication to induce DNA damage. Topoisomerase inhibitors such as irinotecan and etoposide also interfere with DNA replication, but they do so by forming stable complexes with topoisomerases. Not all chemotherapy drugs induce DNA damage as their mechanism of action. Some examples include mitotic inhibitors, such as vincristine and docetaxel, which interfere with mitosis, the enzyme L-asparaginase, which degrades the cancer-essential compound asparagine, and the proteasome inhibitor bortezomib. It would be prudent to determine the similarities or differences of how Myc stabilization cooperates with these categories of chemotherapies. If Myc stabilization via GSK-3 sensitized to certain classes of chemotherapy better than others, this could inform clinical decisions about how best to integrate GSK-3 inhibitors into current chemotherapy regimens.

From our studies it is apparent that Myc stabilization can sensitize BL cells to DNA damaging compounds, amongst other anti-cancer agents. There are other compounds aside from the classes of chemotherapy mentioned above that cause DNA damage and could be worthwhile to test in combination with GSK-3 inhibition. One such group of compounds are inhibitors of the DNA damage response. The DNA damage response (DDR) is activated when cellular sensors

detect unresolved DNA single or double stranded breaks. Upon sensing DNA damage, cell cycle checkpoints become activated; Chk1 and Chk2 enzymes become activated and pause the cell cycle to allow for repair of the DNA damage. Cancer cells often harbor a compromised DDR compared to normal cells; in fact, deficiencies in the DDR can be a driver of oncogenesis. In the face of deficiencies in certain DNA repair pathways, of which there are numerous, tumors then become more reliant on the remaining intact DNA repair pathways. MYC overexpression has been found to drive genomic instability in cancer. Specifically, cells with an overexpression of MYC were found to have increased DNA replication stress, which lead to an increase in DNA damage and potentially explains why Myc-driven tumors often have chromosomal aberrations such as gene amplifications [206,207]. Taking these two cancer phenomena together, Myc-driven cancers that lack proper DNA damage checkpoints have increased sensitivity to Chk1 inhibitors [208,209]. Since it is the high level of Myc in Myc-driven tumors like BL or neuroblastoma that sensitize to Chk1 inhibition, it is plausible that increasing Myc levels even more via GSK-3 inhibition would render these tumors even more sensitive to Chk1 inhibition. Furthermore, GSK-3 inhibitors could potentially be used in tumors where Myc is at an intermediate level and not profoundly overexpressed via chromosomal translocation like in BL. If Myc levels similar to those found in BL could be achieved in other types of tumors, then perhaps these tumors would similarly become as sensitive to Chk1 inhibition due to Myc-induced replication stress and DNA damage.

The fact that Myc-driven tumors are more sensitive to Chk1 inhibition is an example of synthetic lethality. Synthetic lethality occurs when two genetic events are compatible with cell survival on their own, but when together, leads to cell death. In this example, the two genetic events in question are MYC over-expression and Chk1 loss of function. There are other genes aside from Chk1 that have been found to be synthetically lethal with MYC over-expression. CDK1 was identified from RNAi screens to be synthetically lethal with MYC overexpression and inhibiting CDK1 in Myc-driven lymphoma and neuroblastoma models lead to apoptosis and decreased tumor growth [210]. MYC overexpression has also been found to increase the dependence of tumor cells

on exogenous glutamine for survival, such that inhibition of glutamine metabolism selectively induced cell death in Myc-driven cancers [211,212]. These Myc dependencies could be exploited further in non-MYC-driven cancers by Myc stabilization via GSK-3 inhibition.

GSK-3 Inhibition in the Era of Immunotherapy

In this new era of immunotherapy, one should also consider how GSK-3 inhibition might cooperate with the immune system and with immunotherapies used to treat BL. Immune surveillance for malignant, cancerous cells culminates with immune mediated killing by cytotoxic T cells (CTLs) and natural killer (NK) cells. Both of these immune cell types secrete or increase membrane abundance of death ligands to induce extrinsic apoptosis in tumor cells and eliminate them from the body [213,214]. Immunotherapies to boost the activity of CTLs have been developed and are in clinical trials; this strategy is deemed immune checkpoint blockade and is mediated through antibody blockade of CTLA-4 or the PD-1/PD-L1 pathway, two pathways that serve to inhibit anti-tumor activity of CTLs [215]. NK cells also have immune checkpoints for which blocking antibodies have been developed and are being tested in clinical trials, including anti-PD-1/PD-L1 antibodies for a subset of NK cells that express PD-1 [216]. Increasing extrinsic apoptotic activity via GSK-3β inhibition in tumors combined with boosting anti-tumor activity of the immune system via checkpoint blockade could result in better immune-mediated elimination of malignant cells.

One issue with death-receptor agonists as cancer therapy is that there is no specificity for binding to the tumor over normal tissue. To combat this, researchers have found a way to target TRAIL to the surface of CTLs to increase tumor-specific TRAIL targeting of cancer cells [217]. Another strategy has been to use bispecific antibodies that recognize both a unique tumor surface protein and an extrinsic apoptosis receptor. One aspect of current immunotherapy strategies aims to identify so called “tumor neo-antigens”, thus there is more readily available data on membrane surface proteins that are either found in normal tissue yet exclusively expressed on the surface of tumor cells, or those that arise from tumor-specific mutations and thus are solely found on tumors. One such example is the generation of a bispecific antibody for the melanoma-specific MCSP protein and DR5 [218]. Thus, with this one bispecific antibody, DR5 can be stimulated specifically on melanoma cells expression MCSP. Therein lies the potential for GSK-3 inhibitors to cooperate with

immunotherapy strategies that engage extrinsic apoptosis, as GSK-3 inhibition increases the levels of death receptors that are targeted by these tumor-specific immunotherapies, and thus would augment the killing of tumor cells. The limitation to this strategy is that it requires the existence of tumor-specific surface proteins, which are more abundant in a tumor with a high-mutational burden such as melanoma, but less abundant, yet still present, in a tumor with a low-mutational burden as is the case with certain types of B-cell lymphoma [219]. Finally, CD19-targeted chimeric antigen receptor T-cell (CAR-T cell) therapy has revolutionized the treatment of CD19 positive B-cell malignancies [220]. It is not yet clear what role death receptor signaling may have in CAR-T cell mediated cell killing, although a recent study has implicated the disruption of extrinsic apoptosis in the tumor as a mechanism of inherent resistance to CAR-T cell killing activity [221]. Further studies into what influence death receptor signaling has on CAR-T cell function would be worthwhile to fully understand what role this apoptotic pathway plays in the tumor and in the CAR-T cell during CAR-T cell mediated tumor killing.

Future Directions

Further In-Vivo Testing of anti-GSK-3β adjuvant therapy

An immediate next step of this study is to further evaluate anti-GSK-3 adjuvant therapy *in vivo* by utilizing the numerous tumor models at our disposal. Our group has previously characterized the response of p53ER/MYC tumors to cyclophosphamide. One dose of cyclophosphamide will lead to tumor regression, followed by tumor reoccurrence after a few days [130]. We have also shown that the addition of the autophagy inhibitor chloroquine can extend this time to tumor reoccurrence, which we use as a surrogate for measurements of progression-free survival. With this model, we could similarly determine whether the addition of GSK-3 inhibitors can extend the time to tumor reoccurrence following treatment with chemotherapy. Preliminary experiments have shown that doxorubicin similarly leads to a brief tumor regression followed by reoccurrence. Further studies will optimize the treatment regimens such that the additive effect of GSK-3 inhibition can be properly evaluated. Other models that can be tested *in vivo* include Ramos cells labeled with GFP and our BL PDX that we developed. With Ramos-GFP cells, anti-GSK-3 adjuvant therapy can be tested on a systemic model of Burkitt lymphoma as supposed to the subcutaneous models used in our study. The PDX provides the opportunity to test this therapeutic combination on a more clinically relevant model of BL. Preliminary studies demonstrate that the PDX subcutaneous tumors grown with reproducible kinetics and will serve as a useful model for testing anti-GSK-3 adjuvant therapy. If PDX cells can be manipulated to express GFP, they too can be used as a systemic BL model upon which we can test our therapeutic regimen.

Drop-out CRISPR screen for sensitizers to doxorubicin

Another future step for this study is to interrogate what can sensitize tumors to chemotherapy in an unbiased manner. In our study detailed here we chose GSK-3 inhibition as a

method to chemosensitize tumors based on what we know about Myc biology and its promotion of apoptosis. However, there are likely not yet identified pathways or proteins that when inhibited will increase apoptosis following chemotherapy. With the development of CRISPR-screening methodologies, it is now feasible to perform genome-wide interrogations for chemosensitizers. For example, a negative-selection genome wide CRISPR screen was recently used to identify mediators of sensitization to temozolomide in glioblastoma stem cells [222]. This type of screen is referred to as a CRISPR-drop out screen or a negative-selection screen [223]. After subjecting cells to the CRISPR library, edited cells are cultured with a sub-lethal dose of drug, and following treatment, deep genomic sequencing is done on the remaining cells and the represented guide RNAs (gRNAs) are compared to the gRNAs of untreated cells. Those gRNAs that are not present, or have dropped out, in the chemotherapy treated cells indicate a gene that when present, impedes the response to chemotherapy, but when absent, promotes chemosensitivity. By subjecting the negatively selected genes to pathway analysis, one can determine if there are certain biological pathways that can be inhibited to increase chemosensitivity. It would also be beneficial to cross-reference the drop-out gene hits to a dataset of FDA-approved inhibitors and/or inhibitors in clinical trials to determine if there are clinically targetable present in the drop-out hits. With these steps, novel methods to chemosensitize BL would be identified.

Drop-out CRISPR screen for synthetic lethality with MYC transient stabilization

CRISPR screening could also be used to identify genes that cooperate or interfere with MYC stabilization via GSK-3 inhibition. The experimental workflow would be similar to that of the CRISPR drop-out screen- cells subjected to the CRISPR library would be treated with a GSK-3 inhibitor and the changes in the gRNA pool compared to untreated cells would be assessed. As with the drop-out screen in the presence of chemotherapy, genes that have dropped out in this screen are genes that when absent reduce cell viability in the presence of GSK-3 inhibition, and

when present mediate resistance to GSK-3 inhibition. Enriched gRNAs represent genes that are required for apoptosis following GSK-3 inhibition or when inhibited, result in a resistance phenotype. This information could be beneficial to know because if knockout of gene X lead to GSK-3 inhibitor resistance, then one would want to avoid treating tumors with loss-of-function mutations or deletions in this gene lest GSK-3 inhibition actually promote tumor growth.

Summary and Final Conclusions

The work presented here demonstrates the therapeutic potential of targeting GSK-3 and transiently stabilizing Myc to improve chemotherapeutic responses of P53-mutant, chemoresistant B-cell lymphoma. Myc has been shown to be a critical mediator of doxorubicin-induced apoptosis. GSK-3 inhibition with compounds such as lithium chloride or CHIR99021 transiently stabilized wild type Myc protein in Burkitt lymphoma cell lines and PDX, yet had no effect on the stability of Myc in cell lines with a mutation of Thr58. As such, GSK-3 inhibition with CHIR99021 increased sensitivity to chemotherapeutic drugs such as doxorubicin, vincrinstine, and the cyclophosphamide analog mafosfmamide *in vitro* and *in vivo*. This effect is dependent upon Myc as no sensitization was seen in Myc Thr58 mutant cell lines nor when MYC transcription was inhibited in a tetracycline-repressible MYC model or pharmacologically inhibited in Burkitt lymphoma cells. The mechanism of anti-GSK-3 adjuvant therapy was reliant on the extrinsic apoptotic pathway, as extrinsic apoptotic pathway family members were altered upon GSK-3 inhibition, unlike intrinsic family members which were unchanged. Blocking the intrinsic pathway had no effect on anti-GSK-3 adjuvant therapy, yet blocking extrinsic apoptosis completed abrogated the pro-apoptotic effect of anti-GSK-3 adjuvant therapy. Furthermore, knockdown or knockout of various extrinsic pathway family members also diminished or abrogated apoptosis following treatment with anti-GSK-3 adjuvant therapy. We also found that GSK-3 inhibition sensitized Burkitt lymphoma cells to extrinsic apoptosis ligands and agonists. This work suggests that GSK-3 inhibition would not only improve the response to chemotherapy, but also the response to engagers of extrinsic apoptosis. Finally, this work implicates Myc as promoting apoptosis in the absence of functional p53 by engagement of the extrinsic apoptotic pathway.

BIBLIOGRAPHY

1. Beroukhim R, Mermel CH, Porter D, et al. The landscape of somatic copy-number alteration across human cancers. *Nature*. 2010. doi:10.1038/nature08822

2. Hu SSF, Lai MMC, Vogt PK. Genome of avian myelocytomatosis virus MC29: Analysis by heteroduplex mapping. *Proc Natl Acad Sci U S A*. 1979. doi:10.1073/pnas.76.3.1265

3. Sheiness D, Bishop JM. DNA and RNA from uninfected vertebrate cells contain nucleotide sequences related to the putative transforming gene of avian myelocytomatosis virus. *J Virol*. 1979.

4. Vennstrom B, Sheiness D, Zabielski J, Bishop JM. Isolation and characterization of c-myc, a cellular homolog of the oncogene (v-myc) of avian myelocytomatosis virus strain 29. *J Virol*. 1982.

5. Dalla-Favera R, Bregni M, Erikson J, Patterson D, Gallo RC, Croce CM. Human c-myc onc gene is located on the region of chromosome 8 that is translocated in Burkitt lymphoma cells. *Proc Natl Acad Sci U S A*. 1982. doi:10.1073/pnas.79.24.7824

6. Taub R, Kirsch I, Morton C, et al. Translocation of the c-myc gene into the immunoglobulin heavy chain locus in human Burkitt lymphoma and murine plasmacytoma cells. *Proc Natl Acad Sci U S A*. 1982. doi:10.1073/pnas.79.24.7837

7. Amati B, Brooks MW, Levy N, Littlewood TD, Evan GI, Land H. Oncogenic activity of the c-Myc protein requires dimerization with Max. *Cell*. 1993. doi:10.1016/0092-8674(93)90663-B

8. McMahon SB, Van Buskirk HA, Dugan KA, Copeland TD, Cole MD. The novel ATM-related protein TRRAP is an essential cofactor for the c- Myc and E2F oncoproteins. *Cell*.

1998. doi:10.1016/S0092-8674(00)81479-8

9. McMahon SB, Wood MA, Cole MD. The Essential Cofactor TRRAP Recruits the Histone Acetyltransferase hGCN5 to c-Myc. *Mol Cell Biol*. 2000. doi:10.1128/mcb.20.2.556-562.2000

10. Cheng SWG, Davies KP, Yung E, Beltran RJ, Yu J, Kalpana G V. c-MYC interacts with INI1/hSNF5 and requires the SWI/SNF complex for transactivation function. *Nat Genet*. 1999. doi:10.1038/8811

11. Eberhardy SR, Farnham PJ. c-Myc Mediates Activation of the cad Promoter via a Post-RNA Polymerase II Recruitment Mechanism. *J Biol Chem*. 2001. doi:10.1074/jbc.M109014200

12. Cowling VH, Cole MD. The Myc Transactivation Domain Promotes Global Phosphorylation of the RNA Polymerase II Carboxy-Terminal Domain Independently of Direct DNA Binding. *Mol Cell Biol*. 2007. doi:10.1128/mcb.01828-06

13. Penn LJ, Brooks MW, Laufer EM, Land H. Negative autoregulation of c-myc transcription. *EMBO J*. 1990. doi:10.1002/j.1460-2075.1990.tb08217.x

14. Penn LJ, Brooks MW, Laufer EM, et al. Domains of human c-myc protein required for autosuppression and cooperation with ras oncogenes are overlapping. *Mol Cell Biol*. 1990. doi:10.1128/mcb.10.9.4961

15. Li LH, Nerlov C, Prendergast G, MacGregor D, Ziff EB. c-Myc represses transcription in vivo by a novel mechanism dependent on the initiator element and Myc box II. *EMBO J*. 1994. doi:10.1002/j.1460-2075.1994.tb06724.x

16. Adhikary S, Marinoni F, Hock A, et al. The ubiquitin ligase HectH9 regulates transcriptional activation by Myc and is essential for tumor cell proliferation. *Cell*. 2005.

doi:10.1016/j.cell.2005.08.016

17. Mao DYL, Barsyte-Lovejoy D, Ho CSW, Watson JD, Stojanova A, Penn LZ. Promoter-binding and repression on PDGFRB by c-Myc are separable activities. *Nucleic Acids Res*. 2004. doi:10.1093/nar/gkh669

18. Eilers M, Picard D, Yamamoto KR, Bishop JM. Chimaeras of Myc oncoprotein and steroid receptors cause hormone-dependent transformation of cells. *Nature*. 1989. doi:10.1038/340066a0

19. Eilers M, Schirm S, Bishop JM. The MYC protein activates transcription of the alpha-prothymosin gene. *EMBO J*. 1991. doi:10.1002/j.1460-2075.1991.tb07929.x

20. Bello-Fernandez C, Packham G, Cleveland JL. The ornithine decarboxylase gene is a transcriptional target of c-Myc. *Proc Natl Acad Sci U S A*. 1993. doi:10.1073/pnas.90.16.7804

21. Marhin WW, Chen S, Facchini LM, Fornace AJ, Penn LZ. Myc represses the growth arrest gene gadd45. *Oncogene*. 1997. doi:10.1038/sj.onc.1201138

22. Dang C V., O'Donnell KA, Zeller KI, Nguyen T, Osthus RC, Li F. The c-Myc target gene network. *Semin Cancer Biol*. 2006. doi:10.1016/j.semcancer.2006.07.014

23. Patel JH, Loboda AP, Showe MK, Showe LC, McMahon SB. Analysis of genomic targets reveals complex functions of MYC. *Nat Rev Cancer*. 2004. doi:10.1038/nrc1393

24. Dani C, Blanchard JM, Piechaczyk M, El Sabouty S, Marty L, Jeanteur P. Extreme instability of myc mRNA in normal and transformed human cells. *Proc Natl Acad Sci U S A*. 1984. doi:10.1073/pnas.81.22.7046

25. Hann SR, Eisenman RN. Proteins encoded by the human c-myc oncogene: differential expression in neoplastic cells. *Mol Cell Biol*. 1984. doi:10.1128/mcb.4.11.2486

26. Kelly K, Cochran BH, Stiles CD, Leder P. Cell-specific regulation of the c-myc gene by lymphocyte mitogens and platelet-derived growth factor. *Cell*. 1983. doi:10.1016/0092-8674(83)90092-2

27. Bentley DL, Groudine M. A block to elongation is largely responsible for decreased transcription of c-myc in differentiated HL60 cells. *Nature*. 1986. doi:10.1038/321702a0

28. Eick D, Bornkamm GW. Transcriptional arrest within the first exon is a fast control mechanism in c-myc gene expression. *Nucleic Acids Res*. 1986. doi:10.1093/nar/14.21.8331

29. Leder A, Pattengale PK, Kuo A, Stewart TA, Leder P. Consequences of widespread deregulation of the c-myc gene in transgenic mice: Multiple neoplasms and normal development. *Cell*. 1986. doi:10.1016/0092-8674(86)90280-1

30. Hann SR. Role of post-translational modifications in regulating c-Myc proteolysis, transcriptional activity and biological function. *Semin Cancer Biol*. 2006. doi:10.1016/j.semcancer.2006.08.004

31. Vervoorts J, Lüscher-Firzlaff J, Lüscher B. The ins and outs of MYC regulation by posttranslational mechanisms. *J Biol Chem*. 2006. doi:10.1074/jbc.R600017200

32. Sears R, Leone G, DeGregori J, Nevins JR. Ras enhances Myc protein stability. *Mol Cell*. 1999. doi:10.1016/S1097-2765(00)80308-1

33. Gregory MA, Qi Y, Hann SR. Phosphorylation by Glycogen Synthase Kinase-3 Controls c-Myc Proteolysis and Subnuclear Localization. *J Biol Chem*. 2003. doi:10.1074/jbc.M310722200

34. Welcker M, Orian A, Jin J, et al. The Fbw7 tumor suppressor regulates glycogen synthase kinase 3 phosphorylation-dependent c-Myc protein degradation. *Proc Natl Acad Sci U S*

A. 2004. doi:10.1073/pnas.0402770101

35. Wang X, Cunningham M, Zhang X, et al. Phosphorylation regulates c-Myc's oncogenic activity in the mammary gland. *Cancer Res*. 2011. doi:10.1158/0008-5472.CAN-10-1032

36. Salghetti SE, Kim SY, Tansey WP. Destruction of Myc by ubiquitin-mediated proteolysis: Cancer-associated and transforming mutations stabilize Myc. *EMBO J*. 1999. doi:10.1093/emboj/18.3.717

37. Kim SY, Herbst A, Tworkowski KA, Salghetti SE, Tansey WP. Skp2 regulates Myc protein stability and activity. *Mol Cell*. 2003. doi:10.1016/S1097-2765(03)00173-4

38. Von Der Lehr N, Johansson S, Wu S, et al. The F-box protein Skp2 participates in c-Myc proteosomal degradation and acts as a cofactor for c-Myc-regulated transcription. *Mol Cell*. 2003. doi:10.1016/S1097-2765(03)00193-X

39. Vervoorts J, Lüscher-Firzlaff JM, Rottmann S, et al. Stimulation of c-MYC transcriptional activity and acetylation by recruitment of the cofactor CBP. *EMBO Rep*. 2003. doi:10.1038/sj.embor.embor821

40. Patel JH, Du Y, Ard PG, et al. The c-MYC Oncoprotein Is a Substrate of the Acetyltransferases hGCN5/PCAF and TIP60. *Mol Cell Biol*. 2004. doi:10.1128/mcb.24.24.10826-10834.2004

41. Sauter G, Carroll P, Moch H, et al. c-myc Copy number gains in bladder cancer detected by fluorescence in situ hybridization. *Am J Pathol*. 1995.

42. Boxer LM, Dang C V. Translocations involving c-myc and c-myc function. *Oncogene*. 2001. doi:10.1038/sj.onc.1204595

43. Zack TI, Schumacher SE, Carter SL, et al. Pan-cancer patterns of somatic copy number alteration. *Nat Genet*. 2013. doi:10.1038/ng.2760

44. Ciriello G, Miller ML, Aksoy BA, Senbabaoglu Y, Schultz N, Sander C. Emerging landscape of oncogenic signatures across human cancers. *Nat Genet*. 2013. doi:10.1038/ng.2762

45. Love C, Sun Z, Jima D, et al. The genetic landscape of mutations in Burkitt lymphoma. *Nat Genet*. 2012. doi:10.1038/ng.2468

46. Bahram F, Von Der Lehr N, Cetinkaya C, Larsson LG. c-Myc hot spot mutations in lymphomas result in inefficient ubiquitination and decreased proteasome-mediated turnover. *Blood*. 2000.

47. Hemann MT, Bric A, Teruya-Feldstein J, et al. Evasion of the p53 tumour surveillance network by tumour-derived MYC mutants. *Nature*. 2005. doi:10.1038/nature03845

48. Stambolic V, Suzuki A, De la Pompa JL, et al. Negative regulation of PKB/Akt-dependent cell survival by the tumor suppressor PTEN. *Cell*. 1998. doi:10.1016/S0092-8674(00)81780-8

49. Zhao L, Vogt PK. Helical domain and kinase domain mutations in p110α of phosphatidylinositol 3-kinase induce gain of function by different mechanisms. *Proc Natl Acad Sci U S A*. 2008. doi:10.1073/pnas.0712169105

50. Sears R, Nuckolls F, Haura E, Taya Y, Tamai K, Nevins JR. Multiple Ras-dependent phosphorylation pathways regulate Myc protein stability. *Genes Dev*. 2000. doi:10.1101/gad.836800

51. Hayes TK, Neel NF, Hu C, et al. Long-Term ERK Inhibition in KRAS-Mutant Pancreatic Cancer Is Associated with MYC Degradation and Senescence-like Growth Suppression. *Cancer Cell*. 2016. doi:10.1016/j.ccell.2015.11.011

52. Kalkat M, De Melo J, Hickman KA, et al. MYC deregulation in primary human cancers.

Genes (Basel). 2017. doi:10.3390/genes8060151

53. Gabay M, Li Y, Felsher DW. MYC activation is a hallmark of cancer initiation and maintenance. *Cold Spring Harb Perspect Med*. 2014. doi:10.1101/cshperspect.a014241

54. Flores I, Murphy DJ, Swigart LB, Knies U, Evan GI. Defining the temporal requirements for Myc in the progression and maintenance of skin neoplasia. *Oncogene*. 2004. doi:10.1038/sj.onc.1207796

55. Adams JM, Harris AW, Pinkert CA, et al. The c-myc oncogene driven by immunoglobulin enhancers induces lymphoid malignancy in transgenic mice. *Nature*. 1985. doi:10.1038/318533a0

56. Felsher DW, Bishop JM. Reversible tumorigenesis by MYC in hematopoietic lineages. *Mol Cell*. 1999. doi:10.1016/S1097-2765(00)80367-6

57. Jain M, Arvanitis C, Chu K, et al. Sustained loss of a neoplastic phenotype by brief inactivation of MYC. *Science (80-)*. 2002. doi:10.1126/science.1071489

58. Darnell J. E. J. Transcription factors as targets for cancer therapy. *Nat Rev Cancer*. 2002.

59. Yang Z, Yik JHN, Chen R, et al. Recruitment of P-TEFb for stimulation of transcriptional elongation by the bromodomain protein Brd4. *Mol Cell*. 2005. doi:10.1016/j.molcel.2005.06.029

60. Zuber J, Shi J, Wang E, et al. RNAi screen identifies Brd4 as a therapeutic target in acute myeloid leukaemia. *Nature*. 2011. doi:10.1038/nature10334

61. Delmore JE, Issa GC, Lemieux ME, et al. BET bromodomain inhibition as a therapeutic strategy to target c-Myc. *Cell*. 2011. doi:10.1016/j.cell.2011.08.017

62. Savino M, Annibali D, Carucci N, et al. The action mechanism of the Myc inhibitor termed

Omomyc may give clues on how to target Myc for cancer therapy. *PLoS One*. 2011. doi:10.1371/journal.pone.0022284

63. Soucek L, Jucker R, Panacchia L, Ricordy R, Tatò F, Nasi S. Omomyc, a potential Myc dominant negative, enhances Myc-induced apoptosis. *Cancer Res*. 2002.

64. Soucek L, Whitfield J, Martins CP, et al. Modelling Myc inhibition as a cancer therapy. *Nature*. 2008. doi:10.1038/nature07260

65. Beaulieu ME, Jauset T, Massó-Vallés D, et al. Intrinsic cell-penetrating activity propels omomyc from proof of concept to viable anti-myc therapy. *Sci Transl Med*. 2019. doi:10.1126/scitranslmed.aar5012

66. Eilers M, Eisenman RN. Myc's broad reach. *Genes Dev*. 2008. doi:10.1101/gad.1712408

67. O'Malley DP, Auerbach A, Weiss LM. Practical applications in immunohistochemistry: Evaluation of diffuse large B-cell lymphoma and related large B-cell lymphomas. *Arch Pathol Lab Med*. 2015. doi:10.5858/arpa.2014-0451-CP

68. Askew DS, Ashmun RA, Simmons BC, Cleveland JL. Constitutive c-myc expression in an IL-3-dependent myeloid cell line suppresses cell cycle arrest and accelerates apoptosis. *Oncogene*. 1991.

69. Evan GI, Wyllie AH, Gilbert CS, et al. Induction of apoptosis in fibroblasts by c-myc protein. *Cell*. 1992. doi:10.1016/0092-8674(92)90123-T

70. Zindy F, Eischen CM, Randle DH, et al. Myc signaling via the ARF tumor suppressor regulates p53-dependent apoptosis and immortalization. *Genes Dev*. 1998. doi:10.1101/gad.12.15.2424

71. Eischen CM, Weber JD, Roussel MF, Sherr CJ, Cleveland JL. Disruption of the ARF-Mdm2-p53 tumor suppressor pathway in Myc-induced lymphomagenesis. *Genes Dev*.

1999. doi:10.1101/gad.13.20.2658

72. Schmitt CA, Lowe SW. Apoptosis and therapy. *J Pathol*. 1999. doi:10.1002/(SICI)1096-9896(199901)187:1<127::AID-PATH251>3.0.CO;2-T

73. Jacobs JJL, Scheijen B, Voncken JW, Kieboom K, Berns A, Van Lohuizen M. Bmi-1 collaborates with c-Myc in tumorigenesis by inhibiting c-Myc- induced apoptosis via INK4a/ARF. *Genes Dev*. 1999. doi:10.1101/gad.13.20.2678

74. Eischen CM, Packham G, Nip J, et al. Bcl-2 is an apoptotic target suppressed by both c-Myc and E2F-1. *Oncogene*. 2001. doi:10.1038/sj.onc.1204892

75. Eischen CM, Woo D, Roussel MF, Cleveland JL. Apoptosis Triggered by Myc-Induced Suppression of Bcl-XL or Bcl-2 Is Bypassed during Lymphomagenesis. *Mol Cell Biol*. 2001. doi:10.1128/mcb.21.15.5063-5070.2001

76. Dansen TB, Whitfield J, Rostker F, Brown-Swigart L, Evan GI. Specific requirement for Bax, not Bak, in Myc-induced apoptosis and tumor suppression in vivo. *J Biol Chem*. 2006. doi:10.1074/jbc.M513655200

77. Eischen CM, Roussel MF, Korsmeyer SJ, Cleveland JL. Bax Loss Impairs Myc-Induced Apoptosis and Circumvents the Selection of p53 Mutations during Myc-Mediated Lymphomagenesis. *Mol Cell Biol*. 2001. doi:10.1128/mcb.21.22.7653-7662.2001

78. Egle A, Harris AW, Bouillet P, Cory S. Bim is a suppressor of Myc-induced mouse B cell leukemia. *Proc Natl Acad Sci U S A*. 2004. doi:10.1073/pnas.0401471101

79. Hueber AO, Zörnig M, Lyon D, Suda T, Nagata S, Evan GI. Requirement for the CD95 receptor-ligand pathway in c-myc-induced apoptosis. *Science (80-)*. 1997. doi:10.1126/science.278.5341.1305

80. Ricci MS, Jin Z, Dews M, et al. Direct Repression of FLIP Expression by c-myc Is a Major

Determinant of TRAIL Sensitivity. *Mol Cell Biol*. 2004. doi:10.1128/mcb.24.19.8541-8555.2004

81. Kasibhatla S, Beere HM, Brunner T, Echeverri F, Green DR. A “non-canonical” DNA-binding element mediates the response of the Fas-ligand promoter to c-Myc. *Curr Biol*. 2000. doi:10.1016/S0960-9822(00)00727-2

82. Wang Y, Engels IH, Knee DA, Nasoff M, Deveraux QL, Quon KC. Synthetic lethal targeting of MYC by activation of the DR5 death receptor pathway. *Cancer Cell*. 2004. doi:10.1016/S1535-6108(04)00113-8

83. Murphy DJ, Junttila MR, Pouyet L, et al. Distinct Thresholds Govern Myc’s Biological Output In Vivo. *Cancer Cell*. 2008. doi:10.1016/j.ccr.2008.10.018

84. Makin G, Hickman JA. Apoptosis and cancer chemotherapy. *Cell Tissue Res*. 2000. doi:10.1007/s004419900160

85. Fulda S. Targeting apoptosis signaling pathways for anticancer therapy. *Front Oncol*. 2011. doi:10.3389/fonc.2011.00023

86. Hengartner MO. The biochemistry of apoptosis. *Nature*. 2000. doi:10.1038/35037710

87. Davis RJ. Signal transduction by the JNK group of MAP kinases. *Cell*. 2000. doi:10.1016/S0092-8674(00)00116-1

88. Karin M, Cao Y, Greten FR, Li ZW. NF-κB in cancer: From innocent bystander to major culprit. *Nat Rev Cancer*. 2002.

89. Degterev A, Boyce M, Yuan J. A decade of caspases. *Oncogene*. 2003. doi:10.1038/sj.onc.1207107

90. Fulda S, Debatin KM. Extrinsic versus intrinsic apoptosis pathways in anticancer

chemotherapy. *Oncogene*. 2006. doi:10.1038/sj.onc.1209608

91. Walczak H, Krammer PH. The CD95 (APO-1/Fas) and the TRAIL (APO-2L) apoptosis systems. *Exp Cell Res*. 2000. doi:10.1006/excr.2000.4840

92. Ashkenazi A, Dixit VM. Death receptors: Signaling and modulation. *Science (80-)*. 1998. doi:10.1126/science.281.5381.1305

93. Wajant H. The Fas signaling pathway: More than a paradigm. *Science (80-)*. 2002. doi:10.1126/science.1071553

94. Kischkel FC, Hellbardt S, Behrmann I, et al. Cytotoxicity-dependent APO-1 (Fas/CD95)-associated proteins form a death-inducing signaling complex (DISC) with the receptor. *EMBO J*. 1995. doi:10.1002/j.1460-2075.1995.tb00245.x

95. Irmler M, Thome M, Hahne M, et al. Inhibition of death receptor signals by cellular FLIP. *Nature*. 1997. doi:10.1038/40657

96. Marzo I, Brenner C, Zamzami N, et al. Bax and adenine nucleotide translocator cooperate in the mitochondrial control of apoptosis. *Science (80-)*. 1998. doi:10.1126/science.281.5385.2027

97. Green DR, Kroemer G. The pathophysiology of mitochondrial cell death. *Science (80-)*. 2004. doi:10.1126/science.1099320

98. Cain K, Bratton SB, Langlais C, et al. Apaf-1 oligomerizes into biologically active ~700-kDa and inactive ~1.4-MDa apoptosome complexes. *J Biol Chem*. 2000. doi:10.1074/jbc.275.9.6067

99. Shamas-Din A, Kale J, Leber B, Andrews DW. Mechanisms of action of Bcl-2 family proteins. *Cold Spring Harb Perspect Biol*. 2013. doi:10.1101/cshperspect.a008714

100. Cory S, Adams JM. The BCL2 family: Regulators of the cellular life-or-death switch. *Nat Rev Cancer*. 2002. doi:10.1038/nrc883

101. Cowling V, Downward J. Caspase-6 is the direct activator of caspase-8 in the cytochrome c-induced apoptosis pathway: Absolute requirement for removal of caspase-6 prodomain. *Cell Death Differ*. 2002. doi:10.1038/sj.cdd.4401065

102. Friesen C, Fulda S, Debatin KM. Deficient activation of the CD95 (APO-1/Fas) system in drug-resistant cells. *Leukemia*. 1997. doi:10.1038/sj.leu.2400827

103. Fulda S, Scaffidi G, Susin SA, et al. Activation of mitochondria and release of mitochondrial apoptogenic factors by betulinic acid. *J Biol Chem*. 1998. doi:10.1074/jbc.273.51.33942

104. Debatin KM, Stahnke K, Fulda S. Apoptosis in hematological disorders. *Semin Cancer Biol*. 2003. doi:10.1016/S1044-579X(02)00132-3

105. Jin Z, McDonald ER, Dicker DT, El-Deiry WS. Deficient tumor necrosis factor-related apoptosis-inducing ligand (TRAIL) death receptor transport to the cell surface in human colon cancer cells selected for resistance to TRAIL-induced apoptosis. *J Biol Chem*. 2004. doi:10.1074/jbc.M405538200

106. LeBlanc HN, Ashkenazi A. Apo2L/TRAIL and its death and decoy receptors. *Cell Death Differ*. 2003. doi:10.1038/sj.cdd.4401187

107. Pai SI, Wu GS, Özören N, et al. Rare loss-of-function mutation of a death receptor gene in head and neck cancer. *Cancer Res*. 1998.

108. Dechant MJ, Fellenberg J, Scheuerpflug CG, Ewerbeck V, Debatin KM. Mutation analysis of the apoptotic “death-receptors” and the adaptors TRADD and FADD/MORT-1 in osteosarcoma tumor samples and osteosarcoma cell lines. *Int J Cancer*. 2004.

doi:10.1002/ijc.20008

109. Fulda S, Meyer E, Debatin KM. Metabolic inhibitors sensitize for CD95 (APO-1/Fas)-induced apoptosis by down-regulating Fas-associated death domain-like interleukin 1-converting enzyme inhibitory protein expression. *Cancer Res*. 2000.

110. Longley DB, Wilson TR, McEwan M, et al. c-FLIP inhibits chemotherapy-induced colorectal cancer cell death. *Oncogene*. 2006. doi:10.1038/sj.onc.1209122

111. Gala JL, Vermylen C, Cornu G, et al. High expression of bcl-2 is the rule in acute lymphoblastic leukemia, except in Burkitt subtype at presentation, and is not correlated with the prognosis. *Ann Hematol*. 1994. doi:10.1007/BF01757343

112. Tsujimoto Y, Finger LR, Yunis J, Nowell PC, Croce CM. Cloning of the chromosome breakpoint of neoplastic B cells with the t(14;18) chromosome translocation. *Science (80-)*. 1984. doi:10.1126/science.6093263

113. Vogler M. Targeting BCL2-Proteins for the Treatment of Solid Tumours. *Adv Med*. 2014. doi:10.1155/2014/943648

114. Rampino N, Yamamoto H, Ionov Y, et al. Somatic frameshift mutations in the BAX gene in colon cancers of the microsatellite mutator phenotype. *Science (80-)*. 1997. doi:10.1126/science.275.5302.967

115. Kitada S, Pedersen IM, Schimmer AD, Reed JC. Dysregulation of apoptosis genes in hematopoietic malignancies. *Oncogene*. 2002. doi:10.1038/sj.onc.1205327

116. Tagawa H, Karnan S, Suzuki R, et al. Genome-wide array-based CGH for mantle cell lymphoma: Identification of homozygous deletions of the proapoptotic gene BIM. *Oncogene*. 2005. doi:10.1038/sj.onc.1208300

117. Choi CH. ABC transporters as multidrug resistance mechanisms and the development of

chemosensitizers for their reversal. *Cancer Cell Int*. 2005. doi:10.1186/1475-2867-5-30

118. Dave SS, Fu K, Wright GW, et al. Molecular diagnosis of Burkitt's lymphoma. *N Engl J Med*. 2006. doi:10.1056/NEJMoa055759

119. Dalla-Favera R, Martinotti S, Gallo RC, Erikson J, Croce CM. Translocation and rearrangements of the c-myc oncogene locus in human undifferentiated B-cell lymphomas. *Science (80-)*. 1983. doi:10.1126/science.6401867

120. Dang C V. MYC, metabolism, cell growth, and tumorigenesis. *Cold Spring Harb Perspect Med*. 2013. doi:10.1101/cshperspect.a014217

121. McKeown MR, Bradner JE. Therapeutic strategies to inhibit MYC. *Cold Spring Harb Perspect Med*. 2014. doi:10.1101/cshperspect.a014266

122. McMahon SB. MYC and the control of apoptosis. *Cold Spring Harb Perspect Med*. 2014. doi:10.1101/cshperspect.a014407

123. Hann SR. MYC cofactors: Molecular switches controlling diverse biological outcomes. *Cold Spring Harb Perspect Med*. 2014. doi:10.1101/cshperspect.a014399

124. Cheung KJJ, Horsman DE, Gascoyne RD. The significance of TP53 in lymphoid malignancies: Mutation prevalence, regulation, prognostic impact and potential as a therapeutic target. *Br J Haematol*. 2009. doi:10.1111/j.1365-2141.2009.07739.x

125. Dunleavy K, Roschewski M, Abramson JS, et al. RISK-ADAPTED THERAPY IN ADULTS WITH BURKITT LYMPHOMA: UPDATED RESULTS OF a MULTICENTER PROSPECTIVE PHASE II STUDY OF DA-EPOCH-R. *Hematol Oncol*. 2017. doi:10.1002/hon.2437_122

126. Psathas JN, Doonan PJ, Raman P, Freedman BD, Minn AJ, Thomas-Tikhonenko A. Lymphoid neoplasia: The Myc-miR-17-92 axis amplifies B-cell receptor signaling via

inhibition of ITIM proteins: A novel lymphomagenic feed-forward loop. *Blood*. 2013. doi:10.1182/blood-2012-12-473090

127. Chung EY, Psathas JN, Yu D, Li Y, Weiss MJ, Thomas-Tikhonenko A. CD19 is a major B cell receptor-independent activator of MYC-driven B-lymphomagenesis. *J Clin Invest*. 2012. doi:10.1172/JCI45851

128. Sander S, Calado DP, Srinivasan L, et al. Synergy between PI3K Signaling and MYC in Burkitt Lymphomagenesis. *Cancer Cell*. 2012. doi:10.1016/j.ccr.2012.06.012

129. Farrell AS, Sears RC. MYC degradation. *Cold Spring Harb Perspect Med*. 2014. doi:10.1101/cshperspect.a014365

130. Amaravadi RK, Yu D, Lum JJ, et al. Autophagy inhibition enhances therapy-induced apoptosis in a Myc-induced model of lymphoma. *J Clin Invest*. 2007. doi:10.1172/JCI28833

131. Yu D, Cozma D, Park A, Thomas-Tikhonenko A. Functional validation of genes implicated in lymphomagenesis: An in vivo selection assay using a Myc-induced B-cell tumor. In: *Annals of the New York Academy of Sciences*. ; 2005. doi:10.1196/annals.1339.047

132. Yu D, Dews M, Park A, Tobias JW, Thomas-Tikhonenko A. Inactivation of Myc in murine two-hit B lymphomas causes dormancy with elevated levels of interleukin 10 receptor and CD20: Implications for adjuvant therapies. *Cancer Res*. 2005. doi:10.1158/0008-5472.CAN-04-4197

133. Yu D, Carroll M, Thomas-Tikhonenko A. p53 status dictates responses of B lymphomas to monotherapy with proteasome inhibitors. *Blood*. 2007. doi:10.1182/blood-2006-10-050294

134. Walter DM, Venancio OS, Buza EL, et al. Systematic in vivo inactivation of chromatin-regulating enzymes identifies Setd2 as a potent tumor suppressor in lung

adenocarcinoma. *Cancer Res*. 2017. doi:10.1158/0008-5472.CAN-16-2159

135. Kim J-S, Lee C, Bonifant CL, Ressom H, Waldman T. Activation of p53-Dependent Growth Suppression in Human Cells by Mutations in PTEN or PIK3CA. *Mol Cell Biol*. 2007. doi:10.1128/mcb.00537-06

136. Sotillo E, Laver T, Mellert H, et al. Myc overexpression brings out unexpected antiapoptotic effects of miR-34a. *Oncogene*. 2011. doi:10.1038/onc.2010.634

137. Wu TD, Nacu S. Fast and SNP-tolerant detection of complex variants and splicing in short reads. *Bioinformatics*. 2010. doi:10.1093/bioinformatics/btq057

138. Anders S, Pyl PT, Huber W. HTSeq-A Python framework to work with high-throughput sequencing data. *Bioinformatics*. 2015. doi:10.1093/bioinformatics/btu638

139. Aken BL, Ayling S, Barrell D, et al. The Ensembl gene annotation system. *Database (Oxford)*. 2016. doi:10.1093/database/baw093

140. Ritchie ME, Phipson B, Wu D, et al. Limma powers differential expression analyses for RNA-sequencing and microarray studies. *Nucleic Acids Res*. 2015. doi:10.1093/nar/gkv007

141. Huber W, Carey VJ, Gentleman R, et al. Orchestrating high-throughput genomic analysis with Bioconductor. *Nat Methods*. 2015. doi:10.1038/nmeth.3252

142. Ogata H, Goto S, Sato K, Fujibuchi W, Bono H, Kanehisa M. KEGG: Kyoto encyclopedia of genes and genomes. *Nucleic Acids Res*. 1999. doi:10.1093/nar/27.1.29

143. Kanehisa M, Sato Y, Kawashima M, Furumichi M, Tanabe M. KEGG as a reference resource for gene and protein annotation. *Nucleic Acids Res*. 2016. doi:10.1093/nar/gkv1070

144. Pajic A, Spitkovsky D, Christoph B, et al. Cell cycle activation by c-myc in a Burkitt lymphoma model cell line. *Int J Cancer*. 2000. doi:10.1002/1097-0215(20000915)87:6<787::AID-IJC4>3.0.CO;2-6

145. O'Brien WT, Klein PS. Validating GSK3 as an in vivo target of lithium action. In: *Biochemical Society Transactions*. ; 2009. doi:10.1042/BST0371133

146. Ring DB, Johnson KW, Henriksen EJ, et al. Selective glycogen synthase kinase 3 inhibitors potentiate insulin activation of glucose transport and utilization in vitro and in vivo. *Diabetes*. 2003. doi:10.2337/diabetes.52.3.588

147. Aberle H, Bauer A, Stappert J, Kispert A, Kemler R. β-catenin is a target for the ubiquitin-proteasome pathway. *EMBO J*. 1997. doi:10.1093/emboj/16.13.3797

148. Dawson MA, Prinjha RK, Dittmann A, et al. Inhibition of BET recruitment to chromatin as an effective treatment for MLL-fusion leukaemia. *Nature*. 2011. doi:10.1038/nature10509

149. Christophorou MA, Martin-Zanca D, Soucek L, et al. Temporal dissection of p53 function in vitro and in vivo. *Nat Genet*. 2005. doi:10.1038/ng1572

150. Yu D, Thomas-Tikhonenko A. A non-transgenic mouse model for B-cell lymphoma: In vivo infection of p53-null bone marrow progenitors by a Myc retrovirus is sufficient for tumorigenesis. *Oncogene*. 2002. doi:10.1038/sj.onc.1205244

151. Fan JS, Zeller K, Chen YC, et al. Time-dependent c-Myc transactomes mapped by array-based nuclear run-on reveal transcriptional modules in human B cells. *PLoS One*. 2010. doi:10.1371/journal.pone.0009691

152. Schütze S, Tchikov V, Schneider-Brachert W. Regulation of TNFR1 and CD95 signalling by receptor compartmentalization. *Nat Rev Mol Cell Biol*. 2008. doi:10.1038/nrm2430

153. Wilson NS, Dixit V, Ashkenazi A. Death receptor signal transducers: Nodes of

coordination in immune signaling networks. *Nat Immunol*. 2009. doi:10.1038/ni.1714

154. Wang H, Sun L, Su L, et al. Mixed Lineage Kinase Domain-like Protein MLKL Causes Necrotic Membrane Disruption upon Phosphorylation by RIP3. *Mol Cell*. 2014. doi:10.1016/j.molcel.2014.03.003

155. Pukae L, Kanakaraj P, Humphreys R, et al. HGS-ETR1, a fully human TRAIL-receptor 1 monoclonal antibody, induces cell death in multiple tumour types in vitro and in vivo. *Br J Cancer*. 2005. doi:10.1038/sj.bjc.6602487

156. Beurel E, Jope RS. The paradoxical pro- and anti-apoptotic actions of GSK3 in the intrinsic and extrinsic apoptosis signaling pathways. *Prog Neurobiol*. 2006. doi:10.1016/j.pneurobio.2006.07.006

157. Sun M, Song L, Li Y, Zhou T, Jope RS. Identification of an antiapoptotic protein complex at death receptors. *Cell Death Differ*. 2008. doi:10.1038/cdd.2008.124

158. Kotliarova S, Pastorino S, Kovell LC, et al. Glycogen synthase kinase-3 inhibition induces glioma cell death through c-MYC, nuclear factor-κB, and glucose regulation. *Cancer Res*. 2008. doi:10.1158/0008-5472.CAN-08-0850

159. Wang Z, Smith KS, Murphy M, Piloto O, Somervaille TCP, Cleary ML. Glycogen synthase kinase 3 in MLL leukaemia maintenance and targeted therapy. *Nature*. 2008. doi:10.1038/nature07284

160. Al-Khouri AM, Ma Y, Togo SH, Williams S, Mustelin T. Cooperative phosphorylation of the tumor suppressor phosphatase and tensin homologue (PTEN) by casein kinases and glycogen synthase kinase 3β. *J Biol Chem*. 2005. doi:10.1074/jbc.M503045200

161. Maccario H, Perera NM, Davidson L, Downes CP, Leslie NR. PTEN is destabilized by phosphorylation on Thr366. *Biochem J*. 2007. doi:10.1042/BJ20061837

162. Jayarama S, Li LC, Ganesh L, et al. MADD is a downstream target of PTEN in triggering apoptosis. *J Cell Biochem*. 2014. doi:10.1002/jcb.24657

163. Yuan XJ, Whang YE. PTEN sensitizes prostate cancer cells to death receptor-mediated and drug-induced apoptosis through a FADD-dependent pathway. *Oncogene*. 2002. doi:10.1038/sj.onc.1205054

164. Klefstrom J, Västrik I, Saksela E, Valle J, Eilers M, Alitalo K. c-Myc induces cellular susceptibility to the cytotoxic action of TNF-alpha. *EMBO J*. 1994. doi:10.1002/j.1460-2075.1994.tb06879.x

165. Mayes PA, Dolloff NG, Daniel CJ, et al. Overcoming hypoxia-induced apoptotic resistance through combinatorial inhibition of GSK-3β and CDK1. *Cancer Res*. 2011. doi:10.1158/0008-5472.CAN-11-1383

166. Ricci MS, Kim SH, Ogi K, et al. Reduction of TRAIL-Induced Mcl-1 and cIAP2 by c-Myc or Sorafenib Sensitizes Resistant Human Cancer Cells to TRAIL-Induced Death. *Cancer Cell*. 2007. doi:10.1016/j.ccr.2007.05.006

167. Sussman RT, Ricci MS, Hart LS, Shi YS, El-Deiry WS. Chemotherapy-resistant side-population of colon cancer cells has a higher sensitivity to TRAIL than the non-SP, a higher expression of c-Myc and TRAIL-receptor DR4. *Cancer Biol Ther*. 2007.

168. Chang DW, Xing Z, Pan Y, et al. C-FLIPL is a dual function regulator for caspase-8 activation and CD95-mediated apoptosis. *EMBO J*. 2002. doi:10.1093/emboj/cdf356

169. Fulda S, Vucic D. Targeting IAP proteins for therapeutic intervention in cancer. *Nat Rev Drug Discov*. 2012. doi:10.1038/nrd3627

170. Löder S, Fakler M, Schoeneberger H, et al. RIP1 is required for IAP inhibitor-mediated sensitization of childhood acute leukemia cells to chemotherapy-induced apoptosis.

Leukemia. 2012. doi:10.1038/leu.2011.353

171. Yip KW, Reed JC. Bcl-2 family proteins and cancer. *Oncogene*. 2008. doi:10.1038/onc.2008.307

172. Roberts AW, Davids MS, Pagel JM, et al. Targeting BCL2 with venetoclax in relapsed chronic lymphocytic leukemia. *N Engl J Med*. 2016. doi:10.1056/NEJMoa1513257

173. Müller M, Wilder S, Bannasch D, et al. p53 activates the CD95 (APO-1/Fas) gene in response to DNA damage by anticancer drugs. *J Exp Med*. 1998. doi:10.1084/jem.188.11.2033

174. Troeger A, Schmitz I, Siepermann M, et al. Up-regulation of c-FLIPS+R upon CD40 stimulation is associated with inhibition of CD95-induced apoptosis in primary precursor B-ALL. *Blood*. 2007. doi:10.1182/blood-2006-08-038398

175. Culjkovic-Kraljacic B, Fernando TM, Marullo R, et al. Combinatorial targeting of nuclear export and translation of RNA inhibits aggressive B-cell lymphomas. *Blood*. 2016. doi:10.1182/blood-2015-05-645069

176. Chatterjee K, Zhang J, Honbo N, Karliner JS. Doxorubicin cardiomyopathy. *Cardiology*. 2010. doi:10.1159/000265166

177. Tamaru JI, Hummel M, Marafioti T, et al. Burkitt's lymphomas express V(H) genes with a moderate number of antigen- selected somatic mutations. *Am J Pathol*. 1995.

178. O'Conor GT. Malignant lymphoma in African children. II. A pathological entity. *Cancer*. 1961. doi:10.1002/1097-0142(196103/04)14:2<270::AID-CNCR2820140207>3.0.CO;2-Q

179. Kalisz K, Alessandrino F, Beck R, et al. An update on Burkitt lymphoma: a review of pathogenesis and multimodality imaging assessment of disease presentation, treatment response, and recurrence. *Insights Imaging*. 2019. doi:10.1186/s13244-019-0733-7

180. Rowe M, Fitzsimmons L, Bell AI. Epstein-Barr virus and Burkitt lymphoma. *Chin J Cancer*. 2014. doi:10.5732/cjc.014.10190

181. López C, Kleinheinz K, Aukema SM, et al. Genomic and transcriptomic changes complement each other in the pathogenesis of sporadic Burkitt lymphoma. *Nat Commun*. 2019. doi:10.1038/s41467-019-08578-3

182. Magrath I, Adde M, Shad A, et al. Adults and children with small non-cleaved-cell lymphoma have a similar excellent outcome when treated with the same chemotherapy regimen. *J Clin Oncol*. 1996. doi:10.1200/JCO.1996.14.3.925

183. Thomas DA, Faderl S, O'Brien S, et al. Chemoimmunotherapy with hyper-CVAD plus rituximab for the treatment of adult Burkitt and Burkitt-type lymphoma or acute lymphoblastic leukemia. *Cancer*. 2006. doi:10.1002/cncr.21776

184. Ribrag V, Koscielny S, Bosq J, et al. Rituximab and dose-dense chemotherapy for adults with Burkitt's lymphoma: a randomised, controlled, open-label, phase 3 trial. *Lancet*. 2016. doi:10.1016/S0140-6736(15)01317-3

185. Kim H, Park ES, Lee SH, et al. Clinical outcome of relapsed or refractory burkitt lymphoma and mature b-cell lymphoblastic leukemia in children and adolescents. *Cancer Res Treat*. 2014. doi:10.4143/crt.2013.047

186. Short NJ, Kantarjian HM, Ko H, et al. Outcomes of adults with relapsed or refractory Burkitt and high-grade B-cell leukemia/lymphoma. *Am J Hematol*. 2017. doi:10.1002/ajh.24720

187. Lovestone S, Boada M, Dubois B, et al. A phase II trial of tideglusib in alzheimer's disease. *J Alzheimer's Dis*. 2015. doi:10.3233/JAD-141959

188. Johnson NA, Savage KJ, Ludkovski O, et al. 4. *Blood*. 2009. doi:10.1182/blood-2009-03-

212191

189. Hu S, Xu-Monette ZY, Tzankov A, et al. MYC/BCL2 protein coexpression contributes to the inferior survival of activated B-cell subtype of diffuse large B-cell lymphoma and demonstrates high-risk gene expression signatures: A report from the International DLBCL Rituximab-CHOP Consortium Program. *Blood*. 2013. doi:10.1182/blood-2012-10-460063

190. Le Gouill S, Talmant P, Touzeau C, et al. The clinical presentation and prognosis of diffuse large B-cell lymphoma with t(14;18) and 8q24/c-MYC rearrangement. *Haematologica*. 2007. doi:10.3324/haematol.11305

191. de Jong D, Voetdijk BM h., Beverstock GC, Van Ommen GJB, Willemze R, Kluin PM. Activation of the c-myc Oncogene in a Precursor-B-Cell Blast Crisis of Follicular Lymphoma, Presenting as Composite Lymphoma. *N Engl J Med*. 1988. doi:10.1056/NEJM198805263182106

192. Huang W, Medeiros LJ, Lin P, et al. MYC/BCL2/BCL6 triple hit lymphoma: a study of 40 patients with a comparison to MYC/BCL2 and MYC/BCL6 double hit lymphomas. *Mod Pathol*. 2018. doi:10.1038/s41379-018-0067-x

193. McPhail ED, Maurer MJ, Macon WR, et al. Inferior survival in high-grade B-cell lymphoma with MYC and BCL2 and/or BCL6 rearrangements is not associated with MYC/IG gene rearrangements. *Haematologica*. 2018. doi:10.3324/haematol.2018.190157

194. Lawrence D, Shahrokh Z, Marsters S, et al. Differential hepatocyte toxicity of recombinant Apo2L/TRAIL versions [2]. *Nat Med*. 2001. doi:10.1038/86397

195. Hague A, Hicks DJ, Hasan F, et al. Increased sensitivity to TRAIL-induced apoptosis occurs during the adenoma to carcinoma transition of colorectal carcinogenesis. *Br J Cancer*. 2005. doi:10.1038/sj.bjc.6602387

196. Lemke J, Von Karstedt S, Zinngrebe J, Walczak H. Getting TRAIL back on track for cancer therapy. *Cell Death Differ*. 2014. doi:10.1038/cdd.2014.81

197. Maddipatla S, Hernandez-Ilizaliturri FJ, Knight J, Czuczman MS. Augmented antitumor activity against B-cell lymphoma by a combination of monoclonal antibodies targeting TRAIL-R1 and CD20. *Clin Cancer Res*. 2007. doi:10.1158/1078-0432.CCR-07-0680

198. Sirota P. Cancer morbidity in psychiatric patients: Influence of lithium carbonate treatment. *Isr J Psychiatry Relat Sci*. 1999.

199. Weinstein IB, Joe AK. Mechanisms of Disease: Oncogene addiction - A rationale for molecular targeting in cancer therapy. *Nat Clin Pract Oncol*. 2006. doi:10.1038/ncponc0558

200. Sharma S V., Settleman J. Oncogene addiction: Setting the stage for molecularly targeted cancer therapy. *Genes Dev*. 2007. doi:10.1101/gad.1609907

201. Daub H, Specht K, Ullrich A. Strategies to overcome resistance to targeted protein kinase inhibitors. *Nat Rev Drug Discov*. 2004. doi:10.1038/nrd1579

202. Engelman JA, Zejnullahu K, Mitsudomi T, et al. MET amplification leads to gefitinib resistance in lung cancer by activating ERBB3 signaling. *Science (80-)*. 2007. doi:10.1126/science.1141478

203. Qin XQ, Livingston DM, Kaelin WG, Adams PD. Deregulated transcription factor E2F-1 expression leads to S-phase entry and p53-mediated apoptosis. *Proc Natl Acad Sci U S A*. 1994. doi:10.1073/pnas.91.23.10918

204. Cox AD, Der CJ. The dark side of Ras: Regulation of apoptosis. *Oncogene*. 2003. doi:10.1038/sj.onc.1207111

205. Alqahtani A, Choucair K, Ashraf M, et al. Bromodomain and extra-terminal motif inhibitors:

A review of preclinical and clinical advances in cancer therapy. *Futur Sci OA*. 2019. doi:10.4155/fsoa-2018-0115

206. Dominguez-Sola D, Ying CY, Grandori C, et al. Non-transcriptional control of DNA replication by c-Myc. *Nature*. 2007. doi:10.1038/nature05953

207. Felsher DW, Bishop JM. Transient excess of MYC activity can elicit genomic instability and tumorigenesis. *Proc Natl Acad Sci U S A*. 1999. doi:10.1073/pnas.96.7.3940

208. Ferrao PT, Bukczynska EP, Johnstone RW, McArthur GA. Efficacy of CHK inhibitors as single agents in MYC-driven lymphoma cells. *Oncogene*. 2012. doi:10.1038/onc.2011.358

209. Cole KA, Huggins J, Laquaglia M, et al. RNAi screen of the protein kinome identifies checkpoint kinase 1 (CHK1) as a therapeutic target in neuroblastoma. *Proc Natl Acad Sci U S A*. 2011. doi:10.1073/pnas.1012351108

210. Goga A, Yang D, Tward AD, Morgan DO, Bishop JM. Inhibition of CDK1 as a potential therapy for tumors over-expressing MYC. *Nat Med*. 2007. doi:10.1038/nm1606

211. Yuneva M, Zamboni N, Oefner P, Sachidanandam R, Lazebnik Y. Deficiency in glutamine but not glucose induces MYC-dependent apoptosis in human cells. *J Cell Biol*. 2007. doi:10.1083/jcb.200703099

212. Gao P, Tchernyshyov I, Chang TC, et al. C-Myc suppression of miR-23a/b enhances mitochondrial glutaminase expression and glutamine metabolism. *Nature*. 2009. doi:10.1038/nature07823

213. Jeremias I, Herr I, Boehler T, Debatin KM. TRAIL/Apo-2-ligand-induced apoptosis in human T cells. *Eur J Immunol*. 1998. doi:10.1002/(SICI)1521-4141(199801)28:01<143::AID-IMMU143>3.0.CO;2-3

214. Zamai L, Ahmad M, Bennett IM, Azzoni L, Alnemri ES, Perussia B. Natural killer (NK) cell-

mediated cytotoxicity: Differential use of TRAIL and Fas ligand by immature and mature primary human NK cells. *J Exp Med*. 1998. doi:10.1084/jem.188.12.2375

215. Seidel JA, Otsuka A, Kabashima K. Anti-PD-1 and anti-CTLA-4 therapies in cancer: Mechanisms of action, efficacy, and limitations. *Front Oncol*. 2018. doi:10.3389/fonc.2018.00086

216. Pesce S, Greppi M, Grossi F, et al. PD/1-PD-Ls Checkpoint: Insight on the Potential Role of NK Cells. *Front Immunol*. 2019. doi:10.3389/fimmu.2019.01242

217. De Bruyn M, Wei Y, Wiersma VR, et al. Cell surface delivery of TRAIL strongly augments the tumoricidal activity of T cells. *Clin Cancer Res*. 2011. doi:10.1158/1078-0432.CCR-11-0303

218. He Y, Hendriks D, van Ginkel R, Samplonius D, Bremer E, Helfrich W. Melanoma-Directed Activation of Apoptosis Using a Bispecific Antibody Directed at MCSP and TRAIL Receptor-2/Death Receptor-5. *J Invest Dermatol*. 2016. doi:10.1016/j.jid.2015.11.009

219. Alexandrov LB, Nik-Zainal S, Wedge DC, et al. Signatures of mutational processes in human cancer. *Nature*. 2013. doi:10.1038/nature12477

220. Maude SL, Teachey DT, Porter DL, Grupp SA. CD19-targeted chimeric antigen receptor T-cell therapy for acute lymphoblastic leukemia. *Blood*. 2015. doi:10.1182/blood-2014-12-580068

221. Singh N, Shestova O, Ravikumar P, et al. Impaired tumor death receptor signaling drives resistance to CAR T cell therapy. *bioRxiv*. 2019. doi:10.1101/627562

222. MacLeod G, Bozek DA, Rajakulendran N, et al. Genome-Wide CRISPR-Cas9 Screens Expose Genetic Vulnerabilities and Mechanisms of Temozolomide Sensitivity in Glioblastoma Stem Cells. *Cell Rep*. 2019. doi:10.1016/j.celrep.2019.03.047

223. Sharma S, Petsalaki E. Application of CRISPR-Cas9 based genome-wide screening approaches to study cellular signalling mechanisms. *Int J Mol Sci*. 2018. doi:10.3390/ijms19040933